Fungal Community Composition Regulates Fine Root Decay: Implications for the Cycling and Storage of Carbon in Terrestrial Ecosystems

by

William A. Argiroff

A dissertation submitted in partial fulfillment
of the requirements for the degree of
Doctor of Philosophy
(Environment and Sustainability)
in the University of Michigan
2022

Doctoral Committee:

Professor Donald R. Zak, Chair
Professor Deborah E. Goldberg
Professor Inés Ibáñez
Professor Timothy Y. James

William. A. Argiroff

argiwill@umich.edu

ORCID iD: 0000-0002-7490-4980

DEDICATION

For Diana and Maggie, whose love and support has helped me learn what is truly important.

ACKNOWLEDGEMENTS

I am deeply grateful to Don Zak for his unwavering support, encouragement, and guidance over the past many years. His knowledge and enthusiasm have helped me grow as a scientist and a person. Thank you to Deborah Goldberg for her encouragement, community ecology insights, and always pushing me to think more deeply. I also thank Inés Ibáñez for her invaluable statistical guidance, patience, and helping me think about ecology in new ways. Finally, I want to thank Tim James for welcoming me into his mycology group and being a consistent intellectual and motivational support. I could not have imagined a committee more generous with their time, wisdom, enthusiasm, and kindness.

I thank Rima Upchurch for her scientific insights, friendship, and patience. None of this work would have been possible without her. Peter Pellitier, Sydney Salley, and Wes Bickford were immensely supportive, and I thank them for their wisdom and friendship. I am grateful to Julia Belke, Beth VanDusen, Kirk Acharya, Samuel Schaffer-Morrison, Jordan Matthews, Edith Juno, and Gwendolen Keller, Stuart Grandy, Christopher Blair, Christina Cartaciano, and many others for field and laboratory assistance. I also thank my PhD cohort for their immense support, as well as Alison Bressler, Jake Hawes, Laís Petri, and the SEAS PhD student community.

Thank you to many past members of the Zak lab. In particular, I am grateful to Zac Freedman for believing in me from the very beginning, and for so consistently offering me honest, thoughtful, and caring advice. I am also grateful to Lauren Cline, Elizabeth Entwistle, Sarah Eisenlord, and Anna Peschel for their support over the years. I also thank Jillian Myers,

Anat Belasen, Rob Powers, Alden Dirks, Rebecca Clemons, and many other current and former members of the James lab for their encouragement and mycological wisdom.

I am very grateful to my family, and especially my grandparents, for their unwavering support. I know Grandpa Chuck and Grandpa Carl would have been very proud. I thank my parents for always believing in me, and for making the decision a long time ago to live somewhere I could spend all my time outside exploring. Finally, thank you to Diana for your wisdom, love, and understanding, and to Maggie for being the most hilarious and amazing person I know. I could not have done this without you.

TABLE OF CONTENTS

LIST OF TABLES

TABLE

LIST OF FIGURES

FIGURE

LIST OF APPENDICES

APPENDIX

ABSTRACT

A central goal in ecology is to understand how the environment modifies the composition of ecological communities and, in turn, the functioning of ecosystems. Fine root litter accounts for half of plant litter production in forest ecosystems and is a primary source of soil organic matter. However, the ecological factors controlling the decay of fine root litter remain a critical gap in our understanding of the terrestrial carbon cycle and its responses to environmental change. Using experimental and observational approaches, I explored how microbial community composition influences the decay of fine root litter into soil organic matter in temperate forest ecosystems. First, I tested whether shifts in fungal and bacterial community composition have slowed fine root litter in a long-term (ca. 20 years) field experiment simulating future rates of anthropogenic atmospheric nitrogen deposition in northern hardwood forests. My work revealed that experimental nitrogen deposition reduced the relative abundance of saprotrophic Agaricomycete fungi that use peroxidase enzymes to fully oxidize lignin. In contrast, experimental nitrogen deposition favored Actinobacteria, which only partially decay lignin. Furthermore, molecular characterization using pyrolysis gas chromatography-mass spectrometry demonstrated that nitrogen deposition increased the abundance of lignin-derived compounds in soil organic matter. Previous studies have shown that anthropogenic nitrogen deposition slows fine root decay and enhances soil carbon storage – plausibly acting as a sink for anthropogenic carbon dioxide emissions – and my findings demonstrate that shifts in microbial community composition that slow the decay of lignin in fine root litter underlie these biogeochemical responses. Second, I explored how turnover in fungal community composition along a natural

soil inorganic nitrogen gradient across northern temperate forests influences fine root decay and the accumulation of soil organic matter. I found that differences in the composition of fungal communities inhabiting decomposing fine root litter did not explain soil organic matter stocks and biochemistry across the soil nitrogen gradient. However, within the soil fungal community, the relative abundance of ectomycorrhizal fungi that have retained genes encoding peroxidase enzymes declined with increasing inorganic nitrogen availability. This response was correlated with an increase in lignin-derived soil organic matter and overall soil carbon storage, suggesting that the decomposition of lignin-derived soil organic matter by certain symbiotic ectomycorrhizal fungi with peroxidase enzymes constrains soil organic matter accumulation across soil nitrogen gradients. Lastly, I used a field decay study with fine root litterbags to quantify the relative importance of environmental and fungal controls over fine root decay rates. I found that ligninolytic saprotrophs, ectomycorrhizal fungi with peroxidases, and their influence on community-level genetic potential for decay, better predict rates of fine root decay than environmental factors. Together, these findings provide evidence that microbial community composition and its responses to the environment regulate the decay of fine roots into soil organic matter. Thus, explicitly accounting for turnover in microbial community composition and its implications for community functioning may improve our ability to accurately predict terrestrial carbon cycling and its responses to environmental change.

CHAPTER 1

Introduction

Mechanisms linking the environment, microbial composition, and ecosystem function

A central goal in ecology is to understand how the environment modifies the composition of ecological communities and, in turn, the functioning of ecosystems (Lavorel & Garnier 2002; Suding *et al.* 2008; de Bello *et al.* 2021). Addressing this knowledge gap is particularly important for microbial communities in soil (Figure 1.1), which mediate key terrestrial ecosystem processes such as plant litter decay, the turnover and persistence of soil organic matter (SOM), and nutrient cycling (Koide *et al.* 2014; Fierer 2017; Liang *et al.* 2017). The composition of soil microbial communities shifts along environmental gradients and in response to anthropogenic environmental change (Tedersoo *et al.* 2014; Sterkenburg *et al.* 2015; Treseder *et al.* 2021). Additionally, soil communities that differ in their composition are also often functionally distinct (Allison & Martiny 2008; Glassman *et al.* 2018; Maynard *et al.* 2018; Smith & Peay 2021). However, it remains challenging to predict which microbial groups respond to a given environmental variable and how these compositional shifts subsequently modify ecosystem functioning (Figure 1.1; Hall *et al.* 2018). Because microbial composition is increasingly incorporated into biogeochemical models, establishing the microbial mechanisms coupling the environment to ecosystem functioning will improve the capacity to predict how terrestrial ecosystems will respond to ongoing environmental change (Wieder *et al.* 2015; Blankinship *et al.* 2018; Bradford *et al.* 2021).

Fine root decay, SOM dynamics, and soil carbon storage

Soil organic matter stores more carbon than the atmosphere and terrestrial vegetation combined (Batjes 1996; Jackson *et al.* 2017), yet it remains unclear whether environmental change will cause soil carbon storage to increase or decline (Sulman *et al.* 2018; Wieder *et al.* 2018). This uncertainty arises, in part, due to our incomplete understanding of how soil microbial communities induce changes in SOM dynamics that cannot be predicted from direct environmental effects alone (Blankinship *et al.* 2018; Sulman *et al.* 2018; Bradford *et al.* 2021). While soil microorganisms form SOM through the production of dead biomass (*i.e.*, "necromass") and other secreted compounds, they also regulate SOM formation by determining the amount of plant-derived compounds remaining from the decay of plant litter (Schimel & Schaeffer 2012; Liang *et al.* 2017; Angst *et al.* 2021). Consequently, understanding the microbial mechanisms coupling the environment to the decay of plant litter and existing SOM is an important step toward predicting how soil carbon storage varies along environmental gradients and in response to environmental change (Schimel & Schaeffer 2012; Bradford *et al.* 2017, 2021).

Although plant litter decay is one of the best studied ecosystem processes, most of our understanding of this process is based on the decay of aboveground litter (*i.e.*, senesced leaves and woody debris; Tenney & Waksman 1929; Berg *et al.* 1993; Bradford *et al.* 2016). However, far less is known about the ecological factors that control the microbial decay of fine root litter (See *et al.* 2019; Berg & McClaugherty 2020; Wambsganss *et al.* 2021). The turnover of the fine roots of trees contribute to plant litter production (Schlesinger & Bernhardt 2013), and first order through third order fine roots – which are the absorptive and most distal branches of the root

network – form ephemeral modules whose senescence accounts for the majority of fine root litter production (Xia *et al.* 2010; McCormack *et al.* 2015). Fine root litter comprises ~50% of litter production in forest ecosystems (Freschet *et al.* 2013), and growing evidence suggests fine root litter is a more important source of SOM than aboveground litter (Rasse *et al.* 2005; Jackson *et al.* 2017; Angst *et al.* 2021). Thus, understanding the microbial mechanisms that control fine root decay is an important step toward resolving key uncertainties in the terrestrial carbon cycle and its responses to the environment.

Fungal community composition is a potential control over fine root decay

The unique biochemical composition of fine roots suggests that composition of saprotrophic fungi could be a particularly important control over fine root decay, but this possibility remains untested. Specifically, fine roots contain much higher concentrations of lignin (35-45%) than leaf litter (Xia *et al.* 2015). Lignin is a complex polyphenolic compound in plant cell walls that is bound to cellulose and hemicellulose and occludes access to these high energy-yielding structural polysaccharides (Talbot *et al.* 2012). Although lignin yields little to no energy for microbial growth, certain species of fungi in the class Agaricomycetes produce class II peroxidases that completely oxidize lignin to CO_2 and enable access to high energy-yielding structural polysaccharides (Kirk & Farrell 1987; Baldrian 2008; del Cerro *et al.* 2021). These enzymes also oxidize lignin-derived polyphenolic compounds in SOM (Kellner *et al.* 2014). Peroxidases arose in the most recent common ancestor of Auriculariales and more recently diverging orders of Agaricomycetes, subsequently undergoing lineage-dependent expansion, diversification, and loss to produce considerable variation in ligninolytic capacity among saprotrophic Agaricomycetes (Floudas *et al.* 2012; Nagy *et al.* 2016; Ruiz-Dueñas *et al.* 2021).

Some fungi outside of Agaricomycetes and certain Actinobacteria can weakly modify lignin using laccases and laccase-like multicopper oxidases (Baldrian 2008; Ahmad *et al.* 2010; Bugg *et al.* 2011), and most other microbes have no capacity for lignin decay whatsoever (Kirk & Farrell 1987). Thus, the decay of lignin-rich fine root litter should be more rapid where ligninolytic saprotrophic fungi in the class Agaricomycetes are more abundant.

The composition of ectomycorrhizal (ECM) fungal communities could also regulate the decay of both fine root litter and root-derived compounds that accumulate as SOM, yet the role of these plant symbionts in fine root decay remains unclear. ECM fungal lineages have retained different numbers and types of peroxidases and other oxidative decay mechanisms due to the repeated evolution of the ECM lifestyle from functionally distinct saprotrophic ancestors, and thereby form a continuum of oxidative decay capacities (Kohler *et al.* 2015; Pellitier & Zak 2018; Miyauchi *et al.* 2020). ECM fungi can slow the decay of plant litter and SOM – a pattern referred to as the "Gadgil effect" – by competing with saprotrophic fungi and inhibiting their activity (Gadgil & Gadgil 1971; Averill & Hawkes 2016; Fernandez & Kennedy 2016). This suppressive effect appears to be strongest for ECM fungi with greater decay capacities, possibly because these taxa can compete more strongly with saprotrophic fungi for the same resources (Fernandez *et al.* 2020). Furthermore, the Gadgil effect may also be stronger for lignin-rich litter due to resource limitation (Smith & Wan 2019; Fernandez *et al.* 2020), suggesting it could be a particularly important control over the decay of fine roots. At the same time, there is some evidence from boreal forests that decay by ECM fungi with peroxidases restricts the accumulation of SOM (Sterkenburg *et al.* 2018; Clemmensen *et al.* 2021; Lindahl *et al.* 2021). While available evidence suggests ECM fungi with peroxidases could slow fine root decay or

accelerate the decay of lignin-derived SOM from fine root litter, the relative importance of these processes is unknown.

Fungal community composition could link fine root decay to soil inorganic N availability

Soil fungi experience different concentrations of inorganic nitrogen (N; *i.e.*, NH_4^+ and NO_3^-) due to both natural and anthropogenic drivers. For example, inorganic N is released during the saprotrophic decay of litter and SOM when microbial growth is energy-limited rather than N-limited (Barnes *et al.* 1998). Soil inorganic N availability varies in space within and among ecosystems due to differences in the net rate at which inorganic N is mineralized from SOM and litter (Vitousek *et al.* 1982; Zak *et al.* 1989; Vitousek & Howarth 1991). Soil inorganic N availability also continues to increase in many terrestrial ecosystems due to enhanced atmospheric N deposition from the burning of fossil fuels (Galloway *et al.* 2004, 2008). Consequently, both natural spatial variation in net N mineralization rates and ongoing anthropogenic N deposition influence the amount of inorganic N to which fungal communities are exposed (Lilleskov *et al.* 2002; Morrison *et al.* 2016).

Inorganic N availability could indirectly regulate fine root decay by determining the abundance of ligninolytic saprotrophic fungi and ECM fungi with peroxidases. For example, field experiments simulating future rates of anthropogenic N deposition reduce the abundance of ligninolytic saprotrophic fungi decomposing lignin-rich substrates (Entwistle *et al.* 2018b). Given the high lignin concentration of fine roots (Xia *et al.* 2015), it is plausible that both anthropogenic N deposition and naturally high inorganic N availability reduce the abundance of ligninolytic fungal saprotrophs in decaying fine root litter, thereby slowing fine root decay and enhancing soil C storage. Additionally, the abundance of ECM fungi with peroxidases generally

declines with increasing soil inorganic N availability (Lilleskov *et al.* 2002; Pellitier *et al.* 2021a; Pellitier & Zak 2021a), suggesting fine root decay could either increase or decrease with increasing N availability depending upon whether ECM with peroxidases accelerate or suppress decay.

Preview of chapters

Using a combination of experimental and observational approaches, I explored how soil inorganic N availability indirectly regulates fine root decay and soil carbon storage by modifying the composition of fungal communities in both soil and decaying fine root litter (Figure 1.1). To evaluate these relationships, I leveraged molecular approaches to characterize both fungal community composition and the biochemical composition of SOM. In Chapter 2, I used a long-term anthropogenic N deposition experiment in northern temperate forests to demonstrate that experimental N deposition has slowed fine root decay and increased soil carbon storage (Zak *et al.* 2008; Xia *et al.* 2018) by reducing the relative abundance of ligninolytic fungi in decaying fine root litter. In Chapter 3, I found evidence consistent with the idea that soil carbon storage increases across a natural gradient of soil inorganic N availability because the abundance of ECM fungi with peroxidases declines, thereby slowing the decay of lignin-derived SOM. However, I show in Chapter 4 that this decline in the abundance of ECM fungi with peroxidases accelerates the early stages of fine root decay, and that fungal composition and its role in shaping community-level genetic decay potential generally overwhelms environmental effects on fine root decay. Together, these findings provide microbial mechanisms through which the environment indirectly modifies ecosystem processes of global significance.

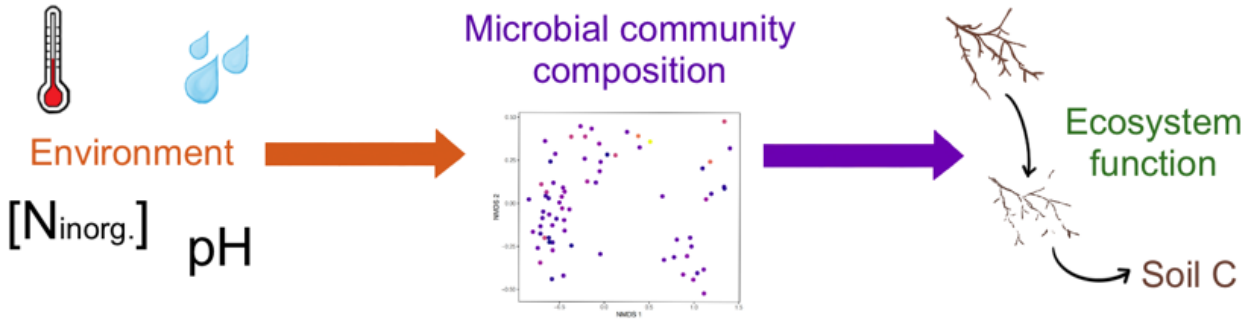

Figure 1.1: Conceptual diagram illustrating the indirect pathway through which the environment (*e.g.*, temperature, water availability, inorganic N availability, and pH influence ecosystem functioning by modifying microbial community composition. Microbial community composition is represented by an ordination of community similarity, and ecosystem functioning is depicted by the decay of fine roots into soil organic matter and the carbon (C) contained therein

CHAPTER 2

Anthropogenic N Deposition Alters Soil Organic Matter Biochemistry and Microbial Communities on Decaying Fine Roots

William A. Argiroff, Donald R. Zak, Rima A. Upchurch, Sydney O. Salley, and A. Stuart Grandy

Abstract

Fine root litter is a primary source of soil organic matter (SOM), which is a globally important pool of C that is responsive to climate change. We previously established that ~20 years of experimental nitrogen (N) deposition has slowed fine root decay and increased the storage of soil carbon (C; +18%) across a widespread northern hardwood forest ecosystem. However, the microbial mechanisms that have directly slowed fine root decay are unknown. Here, we show that experimental N deposition has decreased the relative abundance of Agaricales fungi (-31%) and increased that of partially ligninolytic Actinobacteria (+24%) on decaying fine roots. Moreover, experimental N deposition has increased the relative abundance of lignin-derived compounds residing in SOM (+53%), and this biochemical response is significantly related to shifts in both fungal and bacterial community composition. Specifically, the accumulation of lignin-derived compounds in SOM is negatively related to the relative abundance of ligninolytic *Mycena* and *Kuehneromyces* fungi, and positively related to Microbacteriaceae. Our findings

suggest that by altering the composition of microbial communities on decaying fine roots such that their capacity for lignin degradation is reduced, experimental N deposition has slowed fine root litter decay, and increased the contribution of lignin-derived compounds from fine roots to SOM. The microbial responses we observed may explain widespread findings that anthropogenic N deposition increases soil C storage in terrestrial ecosystems. More broadly, our findings directly link composition to function in soil microbial communities, and implicate compositional shifts in mediating biogeochemical processes of global significance.

Introduction

The microbial decay of fine root litter is a major component of the terrestrial carbon (C) cycle (Schlesinger & Bernhardt 2013), but our understanding of the soil microorganisms mediating this biogeochemically important process is limited (Silver & Miya 2001). Globally, the production of fine root litter accounts for ~22% of terrestrial net primary production (McCormack *et al.* 2015) and ~50% of plant litter entering soil (Freschet *et al.* 2013). Moreover, mounting evidence indicates fine root litter is the primary source of soil organic matter (SOM; Rasse *et al.* 2005; Thomas *et al.* 2012; Jackson *et al.* 2017), which is the largest pool of terrestrial C (Batjes 1996). However, it is presently unclear which ecological factors control the decay of fine roots (Silver & Miya 2001; Hobbie *et al.* 2010; Schimel & Schaeffer 2012; Sun *et al.* 2018), as well as how the microbial metabolism of fine roots into SOM will be impacted by anthropogenic environmental change.

We have established that *ca.* 20 years of experimental nitrogen (N) deposition, which simulates a pervasive driver of global change (Galloway *et al.* 2004, 2008), has slowed fine root decay and increased soil C (+18%) across the geographic extent of a northern hardwood forest

ecosystem in the Upper Great Lakes region (Zak *et al.* 2008; Xia *et al.* 2017, 2018). Although experimental N deposition has not altered the production of leaf (Pregitzer *et al.* 2008) or fine root litter (Burton *et al.* 2004), it has slowed the decay of both (Zak *et al.* 2008; Xia *et al.* 2017, 2018). Previously, we established that fine root litter accounts for 70% of lignified plant material entering soil in our experiment (Xia *et al.* 2015), as well as the majority of lignin-derived monomers in SOM (Thomas *et al.* 2012). Thus, it appears C derived from fine roots, not leaf litter, has increased soil C storage under experimental N deposition. However, we presently do not understand how experimental N deposition has altered the community of microorganisms metabolizing fine root litter into SOM.

We previously obtained evidence that experimental N deposition has slowed lignin decay in fine root litter to a greater extent than leaf litter, a response that has occurred despite no effect of experimental N deposition on the biochemistry of fine root litter (Xia *et al.* 2017, 2018). This difference plausibly arises from the high lignin content of fine roots (45%) relative to leaf litter (14%; Xia *et al.* 2015), and because lignin content controls the long-term rate of plant litter decay (Barnes *et al.* 1998; Berg 2014). Although lignified material was previously quantified as acid insoluble fraction (AIF) in our long-term experiment, which can include other recalcitrant compounds (Xia *et al.* 2015, 2017), AIF was highly predictive of lignin content in fine roots (Xia *et al.* 2017). Importantly, the physiological capacity to metabolize lignin varies among and within fungi and bacteria. For example, some fungal species in the class, Agaricomycetes, deploy class II peroxidase enzymes to completely oxidize lignin to CO_2 (Kirk & Farrell 1987; Floudas *et al.* 2012), whereas some species in the phylum, Actinobacteria, and other bacterial lineages, incompletely degrade lignin into soluble phenolic compounds (Kirk & Farrell 1987; Ahmad *et al.* 2010; Bugg *et al.* 2011). In our long-term study, experimental N deposition has

slowed leaf litter decay by reducing peroxidase gene expression (-73%; Zak *et al.* 2019a), altering expressed peroxidase composition (Entwistle *et al.* 2018a), and increasing the potential for incomplete lignin decay by bacteria (Eisenlord *et al.* 2013; Freedman & Zak 2014), but it has not altered the abundance of ligninolytic fungi on this substrate (Hassett *et al.* 2009; Freedman *et al.* 2016; Entwistle *et al.* 2018b). However, the concentration of lignin in fine root litter is three times greater than in leaf litter (Xia *et al.* 2015), and we previously found that experimental N deposition decreases the abundance of ligninolytic fungi on lignin-rich artificial substrates decaying in the field (Entwistle *et al.* 2018b). If experimental N deposition has also decreased the abundance of ligninolytic fungi on fine root litter, this response could explain why fine root decay has slowed to a greater extent than leaf litter. If this expectation is correct, then reduced fine root decay under experimental N deposition should be the primary source of C accumulating in soil due to experimental N deposition, which should alter SOM biochemistry by increasing the contribution of lignin-derived compounds to SOM formation.

Here, our objective was to determine if anthropogenic N deposition has altered the composition of soil microorganisms decaying fine root litter. To accomplish this, we compared the composition of fungal and bacterial communities colonizing decaying fine root litter exposed to ambient N and experimental N deposition. We also investigated the biochemical composition of SOM under ambient and experimental N deposition to determine if, by slowing the decay of fine roots, experimental N deposition has increased the concentration of lignin-derived compounds in SOM.

Materials and Methods

Description of study sites

We tested the effects of experimental N deposition on the composition of microbial communities decomposing fine root litter and the biochemical composition of both fine root litter and SOM in four replicate northern hardwood forest stands in upper and lower Michigan, USA (Figure A.1). Each stand contains six 30-m x 30-m plots; half receive ambient N deposition (n = 3) and half have received experimental N deposition since 1994 (n = 3; ambient N + 30 kg N ha^{-1} yr^{-1} as $NaNO_3$ pellets in 6 equal applications during the growing season). To reduce edge effects, each plot is surrounded by a 10-m wide buffer zone that receives the same treatment as its respective plot. The forest stands are dominated by sugar maple (*Acer saccharum* Marsh., >80% basal area) on sandy spodosols that are Typic Haplorthods of the Kalkaska series (>85% sand). The forest floor consists of a thick Oe/Oa horizon that contains a mat of fine roots at its boundary with the A horizon. The forest stands are matched in both vegetation and soil characteristics (Burton *et al.* 1991) and encompass the full latitudinal range of the northern hardwood ecosystem in the Upper Great Lakes region; this ~500 km distance spans gradients of ambient N deposition, mean annual temperature, and precipitation (Table A.1). Thus, our experimental design allows us to generalize our findings across this important and widespread ecosystem.

Field-based decomposition experiment

To obtain fine roots for our field decomposition experiment, we collected 60 soil cores (5-cm diameter) to a depth of 10 cm in each plot, which included both Oe/Oa and A horizons (Xia *et al.* 2018). Although these soil cores contain fine root material from both the O and A horizons, the vast majority are derived from the dense mat of fine roots that sits at the O/A horizon boundary

(Zak *et al.* 2017; Xia *et al.* 2018). We transported the cores on ice to the University of Michigan and stored them at -20 °C. Sample collection was carried out in September and October 2013. We thawed the soil cores, passed them through a 2-mm sieve, retrieved first through third order fine roots (Pregitzer *et al.* 2002; Xia *et al.* 2015), and pooled the roots by plot. We rinsed soil from the roots and dried them at 60 °C for 24 hrs. We collected the three distal root orders because, as the ephemeral absorptive modules of the root network, they are morphologically similar and exhibit the highest turnover (Guo *et al.* 2008; McCormack *et al.* 2015; Xia *et al.* 2018), thus comprising the largest input of fine root C to soil.

We placed three mesh litter bags of fine roots (~2 g dry mass in each bag) at three separate positions in the same plot from which the roots originated, in their original location in the soil profile at the boundary of the Oe/Oa and A horizons (3 litter bags x 24 plots = 72 litter bags total). While it could be argued that fine roots may have decayed differently had they been incubated at the surface of the O horizon or deeper in the mineral soil, one of the few studies to test the effects of vertical location in the soil profile on fine root decay found that fine roots located in the O and A horizons of a red pine (*Pinus resinosa*) plantation did not decay at different rates (Li *et al.* 2015). Moreover, the vast majority of fine roots in these northern hardwood forest stands are located at the boundary of the O and A horizons (Zak *et al.* 2017; Xia *et al.* 2018). Thus, we are confident the abiotic and biotic conditions experienced by the fine roots we deployed reflected those experienced by the majority of fine root litter in these forests. We constructed each 15-cm x 15-cm litter bag with 300 µm polyester mesh on top and 20 µm polyester mesh on the bottom, which allowed microfauna and fungal hyphae to enter the bags, respectively (Hobbie 2005; Xia *et al.* 2018). Litter bags were placed in the field in June 2014, collected after 12 months of decomposition, and immediately stored on ice. Each bag was

weighed, and its contents were homogenized by hand. A subsample was removed for physical and chemical analyses, dried at 60 °C for 24 hrs, and the remaining material was stored at -80 °C prior to microbial community analyses.

DNA isolation

To determine if experimental N deposition altered the composition of fungal and bacterial communities, we characterized these communities using ribosomal DNA (rDNA) sequence abundances. We isolated total genomic DNA from three replicate subsamples taken from each root litter bag (0.05 g fine root material per subsample) using the DNeasy Plant Mini Kit (Qiagen, Valencia, CA, USA) following a modified manufacturer's protocol. Specifically, following chemical lysis as specified, we performed physical lysis by bead beating with four 2.38-mm stainless steel beads at 1,200 rpm for 45 s using the PowerLyzer 24 Bench Top Bead-Based Homogenizer (MoBio Laboratories, Carlsbad, CA, USA). Debris was pelleted by centrifugation at 16,000 x *g* for 5 min. After DNA extractions were completed, we verified the quality of extracted DNA with a NanoDrop 8000 Spectrophotometer (Thermo Scientific, Waltham, MA, USA) and gel electrophoresis. We pooled replicate extractions from each litter bag and stored DNA at -80 °C prior to PCR amplification.

PCR amplification, amplicon sequencing, and sequence quality control

We performed PCR amplification of fungal rDNA using the primers LROR and LR3 (Vilgalys & Hester 1990) that target the D1-D2 region of the 28S rRNA gene, which is suitable for both taxonomic and phylogenetic analyses (Liu *et al.* 2012; Porter & Golding 2012). The V1-V3 regions of the bacterial 16S rRNA gene were targeted using the primers 27f and 519r (Lane

1991). For each gene, we performed triplicate PCR reactions for each sample using the Expand High Fidelity PCR System (Roche, Indianapolis, IN, USA) and a Mastercycler ProS thermocycler (Eppendorf, Hauppauge, NY, USA). PCR reaction conditions are described in Table A.2. Primers contained an additional 16 bp barcode for sample multiplexing for sequencing (described below; for barcode sequences, see Table A.3).

We pooled triplicate reactions and purified PCR products using the MinElute PCR Purification Kit (Qiagen). The quality of purified PCR products was assessed as described above, and we quantified DNA mass with the Quant-iT PicoGreen dsDNA Assay Kit (LifeTechnologies, Carlsbad, CA, USA) and a BioTek SynergyHT Multi-Detection Microplate Reader (BioTek Instruments, Winooski, VT, USA). Sequencing was performed at the University of Michigan DNA Sequencing Core on 16 SMRT chips with a PacBio RS II system (Pacific Biosciences, Menlo Park, CA, USA) utilizing circular consensus sequencing, which achieves error rates comparable to other high-throughput sequencing platforms (Travers *et al.* 2010; Fichot & Norman 2013). PCR products were pooled in equal masses per sample per SMRT chip prior to sequencing. Mean amplicon lengths were 688 bp and 525 bp for fungal 28S and bacterial 16S, respectively. Only sequences with at least five-fold circular consensus coverage were retained.

We processed sequences using mothur v1.40.5 (Schloss *et al.* 2009). We removed sequences containing homopolymers >8 nucleotides in length, with average quality scores <30 using a 50-nt sliding window, an ambiguous base call, or >1 mismatch in either the barcode or primer sequence. Fungal sequences were aligned against a 28S reference alignment from the RDP LSU training set (Mueller *et al.* 2014) and bacterial 16S sequences were aligned against the SILVA v132 reference alignment (Quast *et al.* 2013). Chimeric sequences were identified using

UCHIME (Edgar *et al.* 2011) and removed. We clustered fungal sequences and bacterial sequences into operational taxonomic units (OTUs) at 99% and 97% sequence similarity, respectively. The most abundant sequence for each OTU was used as the representative for that OTU, and taxonomic assignments were made using the RDP classifier with the LSU training set v11 for fungi (Cole *et al.* 2014) and the SILVA v132 reference alignment with the naive Bayesian classifier (Wang *et al.* 2007) in mothur for bacteria. Raw sequences are available in fastq format in GenBank under the accession numbers SRR8591550 (16S) and SRR8591551 (28S).

Microbial community composition

Some fungi in the class Agaricomycetes, and some bacteria in the phylum Actinobacteria, can metabolize lignin (Kirk & Farrell 1987; Floudas *et al.* 2012); thus, we tested if experimental N deposition altered the relative abundances of these two groups. We further summed sequence abundances in fungal orders and bacterial families, and compared relative abundances between the ambient and experimental N deposition treatments for orders and families that accounted for at least 1% of fungal and bacterial sequences, respectively, and exhibited a change in relative abundance of at least 20%. Further, species of Agaricomycete fungi and Actinobacteria span a diverse range of autecologies (Kirk & Farrell 1987; Hibbett *et al.* 2014), and it is difficult to directly interpret the functional consequences of changes in the relative abundance of these broad groups. Thus, we assessed the effect of experimental N deposition on fungal and bacterial community composition (*i.e.*, β-diversity), using multivariate analyses at the genus and family levels, respectively. First, abundances were Hellinger-transformed to avoid subsampling biases (McMurdie & Holmes 2013, 2014). We then performed distance-based redundancy analysis (db-

RDA) on Bray-Curtis dissimilarity calculated from these abundances to visualize differences in community composition due to site and experimental N deposition. We plotted the scores for abundant (>1%) classified fungal genera and bacterial families to determine which taxa drove differences in community composition in response to experimental N deposition.

Biochemical analyses and relationships with microbial community composition

We characterized the biochemical composition of undecomposed fine roots, decayed fine roots, and SOM using pyrolysis gas chromatography-mass spectrometry (py-GC/MS). Mineral soil (0-10 cm) was obtained from each plot receiving ambient N and experimental N for biochemical analysis of SOM. We elected to characterize the biochemistry of SOM in mineral soil for four reasons. First, organic matter has rapidly accumulated (+18%) in the mineral soil of our experiment (Zak *et al.* 2008). Second, the lignin-derived compounds remaining in mineral soil appear to be derived primarily from fine root litter (Thomas *et al.* 2012), emphasizing the importance of relating microbial composition on fine root litter to the biochemistry of SOM in mineral soil. Third, we recently obtained evidence that experimental N deposition has caused an accumulation of occluded particulate organic matter in our experiment, which was hypothesized to be an accumulation of fine-root derived C (Zak *et al.* 2017). Finally, previous biochemical characterizations of mineral soil SOM have not detected the expected accumulation of lignin-derived compounds in response to experimental N deposition (Thomas *et al.* 2012; Zak *et al.* 2017); thus, we employed a high-resolution method (*i.e.*, py-GC/MS) to definitively test this alternative. Dried fine root and soil samples (~1 g per sample type per plot) were ground for 6 minutes using a ball mill. Samples were then pyrolyzed at 600 °C in quartz tubes for 20 s using a DS Pyroprobe 5150 pyrolyzer, and analyzed using a ThermoTrace GC Ultra gas chromatograph

(Thermo Fisher Scientific, Austin, TX, USA) and ITQ 900 mass spectrometer (Thermo Fisher Scientific; *sensu* Pold *et al.* 2017). Mass spectrometry peaks were assigned to compounds using AMDIS software and a previously-compiled compound library, and relative abundances for each compound were determined by dividing by the largest peak present in that sample (Grandy *et al.* 2007, 2009; Wickings *et al.* 2011). Individual compounds were summed by their origins to determine the relative abundances of broad compound classes (*i.e.*, aromatic, lignin, lipids, N-bearing, phenols, polysaccharides, proteins, and compounds of unknown origin). To evaluate if SOM biochemistry was related to microbial community composition on decaying fine roots, we fit vectors of compound abundances in SOM to db-RDA ordinations and overlaid vectors with a significant fit (see *Statistical analyses*).

Although compounds other than lignin, such as suberin, are also important biochemical constituents of fine roots (McCormack *et al.* 2015), we elected to focus our study on lignin for four reasons. First, lignin dominated fine root litter biochemistry (35-45%) in our long-term experiment based on previous findings (Xia *et al.* 2015, 2017) and the results we have obtained in our present study (see Figure 2.1). Second, the biochemical composition of lignin-derived monomers in SOM in our experiment was biochemically more similar to fine root-derived lignin than to leaf litter-derived lignin (Thomas *et al.* 2012), a finding that specifically implicates fine root-derived lignin as an important source of SOM. Third, the decay of AIF in fine roots (which is dominated by lignin in our long-term experiment) was reduced under experimental N deposition (Xia *et al.* 2017, 2018), leading us to address the mechanism by which this reduction of decay has occurred in the present study. Finally, suberin is relatively more abundant in higher order (e.g., 4th and 5th order) transport fine roots, as opposed to the ephemeral absorptive fine root modules (orders 1-3; McCormack *et al.* 2015) that are the focus of our present study due to

their dominance of fine root turnover (Xia *et al.* 2010, 2015). Taken together, these lines of evidence support our focus on the microbial degradation of fine root lignin in response to experimental N deposition.

Statistical analyses

We used two-way ANOVA to test the effect of experimental N deposition, site, and their interaction on Hellinger-transformed taxon abundances (*e.g.*, Agaricales) and $\log_2$-transformed compound abundances. Among-group means were compared using protected Fisher's least significant difference (LSD) test in the agricolae package (de Mendiburu 2017) in R. We tested the effects of experimental N deposition, site, and their interaction on community composition using two-way permutational multivariate analysis of variance (PERMANOVA; Anderson 2001) and Bray-Curtis dissimilarity matrices calculated from Hellinger-transformed fungal genus and bacterial family abundances. PERMANOVA was implemented in the vegan package v2.5-3 (Oksanen *et al.* 2018) in R. PERMANOVA cannot distinguish differences in composition from heterogeneous variance; thus, we tested the homogeneity of multivariate dispersion using PERMDISP (Anderson 2004) in vegan ('betadisper' function). A non-significant PERMDISP result confirms that a significant PERMANOVA test has detected a true difference in composition. Vectors for compound abundances were fit to db-RDA ordinations using the 'envfit' function in vegan. Due to the broad geographic expanse of our experiment and inherent heterogeneity of the soil environment, we accepted statistical significance at $\alpha = 0.1$. Data processing and visualization were performed using the collection of packages comprising the tidyverse v1.2.1 (Wickham 2017) in R. Statistical analyses were performed in R v3.5.1 (R Core

Team 2018) and RStudio v1.1.453 (RStudio Team 2018), and code for sequence processing and statistical analyses is available at https://github.com/ZakLab-Soils/N-deposition_roots.

Results

Fine root and SOM biochemistry

Experimental N deposition did not affect the relative abundance of any compound class in undecayed or decaying fine root litter (ANOVA, $P > 0.1$; Figure 2.1). However, we found that experimental N deposition increased the relative abundance of lignin-derived compounds in SOM by 53% (5.2% under ambient N to 7.9% under experimental N; $P = 0.092$; Figure 2.1). Although this response was not highly statistically significant, it was ecologically significant due to its magnitude (>50% change), its uniformity across a large geographic expanse (site by treatment interaction, $P > 0.1$), and the rapidity with which it occurred (~20 years).

Sequence processing, OTU clustering, and taxonomic distribution

Our sequencing effort yielded 126,159 high-quality (*i.e.*, passed filtering steps described in *Materials and Methods*) fungal sequences (5,257 ± 1,656 per sample; mean ± SD) and 154,135 high-quality bacterial sequences (6,422 ± 1,058 per sample). We obtained 2,071 non-singleton fungal OTUs and 5,957 non-singleton bacterial OTUs across all samples. Basidiomycota (63%) and Ascomycota (35%) represented the majority of fungal sequences. The fungal classes Agaricomycetes (57%), Sordariomycetes (11%), unclassified Ascomycota (8%), Leotiomycetes (6%), Tremellomycetes (5%), and Eurotiomycetes (5%) were most abundant. Dominant bacterial phyla included Proteobacteria (55%), Bacteroidetes (15%), Acidobacteria (10%), and Actinobacteria (7%).

Effects of experimental N deposition on microbial community composition

The abundance of Agaricomycetes declined (-22%, from 62.3 ± 4.8% to 48.8 ± 7.5%, mean ± SE) in response to experimental N deposition (ANOVA, $P = 0.085$; Figure A.2). Similarly, experimental N deposition reduced the abundance of Agaricales (-31%; $P = 0.059$; Figure 2.2), the most abundant order of Agaricomycetes colonizing fine root litter. Fungal orders that responded positively to experimental N deposition did not belong to the class, Agaricomycetes. For example, experimental N deposition increased the abundance of fungal orders Chaetothyriales (+566%; $P = 0.011$), Hypocreales (+37%; $P = 0.033$), and Tremellales (+291%; $P = 0.009$; Figure 2.2). The responses of Hypocreales (site by treatment; $P = 0.017$) and Tremellales ($P = 0.042$) varied in magnitude, but not direction by site (Figure A.3). Additionally, the relative abundance of Actinobacteria increased (+24%, from 6.5 ± 0.5% to 8.1 ± 0.7%) in response to experimental N deposition (ANOVA; treatment; $P = 0.025$), driven primarily by sites B and C (site by treatment interaction; $P = 0.024$; Figure A.2). Among bacterial families, Microbacteriaceae were favored by experimental N deposition (+81%; $P = 0.005$); this response varied in magnitude by site, but not in direction (site by treatment; $P = 0.053$; Figure A.3).

Experimental N deposition significantly altered the genus-level composition of fungal communities on decaying fine roots (PERMANOVA; $P = 0.001$; Figure 2.3a), without altering dispersion (PERMDISP; $P = 0.17$). The shift in community composition due to experimental N deposition (denoted by the "*Exp. N*" vector in Figure 2.3b) was associated with a lower abundance of the ligninolytic fungal genera *Mycena* and *Kuehneromyces* (Figure 2.3b). Specifically, the points labeled "*Myc"* and "*Kue"* in Figure 2.3b represent the loadings for these genera in the site by treatment ordination in Figure 2.3a; if an arrow were drawn from the origin in the ordination to a genus loading, it would represent the direction in which the abundance of

that genus increases. Thus, the relative abundance of *Mycena* and *Kuehneromyces* increase in the opposite direction of the vectors representing the shift in fungal community composition due to experimental N deposition ("*Exp. N").* In other words, the experimental N deposition treatment is associated with a lower abundance of these two genera. This pattern indicates that a decline in the abundance of these genera drove the significant change in fungal community composition on decaying fine roots in response to experimental N deposition.

Similarly, experimental N deposition significantly altered bacterial community composition on decaying fine roots (PERMANOVA; $P = 0.014$; PERMDISP; $P = 0.39$; Figure 2.3c). The Actinobacterial family, Microbacteriaceae, was among the bacterial families positively associated with the change in community composition due to experimental N deposition (Figure 2.3d). This family contains ligninolytic species (Taylor *et al.* 2012), which incompletely metabolize lignocellulose into soluble phenolic compounds. The effects of experimental N deposition on other bacterial families putatively involved in lignin degradation (Wilhelm *et al.* 2019) were idiosyncratic. The community composition of fungal and bacterial communities differed among sites (PERMANOVA, site; $P < 0.001$). The effect of experimental N deposition was not uniform across sites for fungi or bacteria (site by treatment; $P < 0.05$). However, the significant site by treatment interaction was apparent in db-RDA ordinations (Figure 2.3a,c), in which clear separation occurred between communities under ambient and experimental N deposition at all sites, except site D.

Relationships between SOM biochemistry and microbial community composition

To directly link changes in SOM biochemistry with changes in bacterial and fungal community composition elicited by experimental N deposition, we fit a vector for the relative abundance of

each compound class in SOM to fungal and bacterial db-RDA ordinations. We found that the shift in fungal community composition driven by experimental N deposition was significantly associated with greater relative abundances of lignin-derived compounds ($r^2 = 0.39$; $P = 0.011$) and N-bearing compounds ($r^2 = 0.33$; $P = 0.022$) in SOM (Figure 2.3b). Similarly, the change in bacterial community composition elicited by experimental N deposition was significantly related to a greater relative abundance of lignin-derived compounds ($r^2 = 0.29$; $P = 0.032$; Figure 2.3d), although the relationship was less direct than that with fungal community composition (Figure 2.3b). In contrast, a lower abundance of lipids was associated with changes in bacterial community composition under experimental N deposition ($r^2 = 0.21$; $P = 0.072$; Figure 2.3d).

Discussion

Anthropogenic N deposition has slowed the accumulation of CO_2 in the atmosphere by increasing C storage in northern forests (Pan *et al.* 2011; Keenan *et al.* 2016). Nitrogen deposition fosters this terrestrial C sink by slowing microbial litter decay and increasing SOM (Pregitzer *et al.* 2008; Zak *et al.* 2008; Janssens *et al.* 2010; Frey *et al.* 2014; Chen *et al.* 2018). Here, we provide evidence that anthropogenic N deposition has altered the composition of fungal and bacterial communities on decaying fine root litter by suppressing the relative abundance of ligninolytic fungi and favoring bacteria with weaker ligninolytic capacity, which plausibly explains why the decay of fine root litter has declined and soil C storage has increased in our long-term N deposition experiment (Zak *et al.* 2008; Xia *et al.* 2017, 2018). Moreover, we demonstrate that shifts in microbial community composition are significantly related to an increase in the relative abundance of lignin-derived compounds in SOM, which suggests that changes in the microbial decay of fine root litter have caused the end products of this process to

accumulate as SOM to a greater extent under experimental N deposition. A recent modeling study estimated that up to 51% of C accumulating in surface soil (O and A horizons to a depth of 10 cm) in this experiment could be explained by reduced decay of fine root litter (Xia *et al.* 2018), and our findings shed light onto the compositional changes in microbial communities eliciting this response. Furthermore, mounting evidence suggests that anthropogenic N deposition slows fine root decay in other ecosystems (Sun *et al.* 2016; Kou *et al.* 2018), and that fine root C is a primary source of SOM in general (Rasse *et al.* 2005; Thomas *et al.* 2012; Jackson *et al.* 2017). Thus, the microbial responses we observed here may underlie widespread findings that anthropogenic N deposition increases soil C storage in terrestrial ecosystems, including those contributing to the increasing C sink in the Northern Hemisphere that has slowed the rate at which anthropogenic CO_2 has accumulated in the atmosphere (Janssens *et al.* 2010; Pan *et al.* 2011; Frey *et al.* 2014; Maaroufi *et al.* 2015; Keenan *et al.* 2016).

Our findings suggest that declines in the relative abundance of ligninolytic fungi have reduced fine root decay in our experiment, as well as the others detailed above. Specifically, experimental N deposition decreased the relative abundance of Agaricomycetes (-22%) and its most abundant order, Agaricales (-31%; Figure 2.2). Agaricomycetes contains the "white-rot" fungi, which decay lignin using class II peroxidases (Kirk & Farrell 1987; Baldrian 2008; Floudas *et al.* 2012). However, there is considerable functional diversity within the Agaricomycetes (Hibbett *et al.* 2014); thus, the lower relative abundance of the genera *Mycena* and *Kuehneromyces* associated with experimental N deposition (Figure 2.3b) is a particularly important piece of evidence we obtained. Specifically, *Kuehneromyces* and *Mycena* are genera of white-rot fungi that decay lignin using class II peroxidases (Miyamoto *et al.* 2000; Hofrichter 2002; Ghosh *et al.* 2003; Kellner *et al.* 2014). *Mycena* were the most abundant fungi on decaying

fine roots (~22% of fungal sequences overall) in our study, and were also dominant saprotrophs on decaying fine roots in other forest ecosystems (Kohout *et al.* 2018; Philpott *et al.* 2018); thus, this genus may be important for how fine root decay responds to anthropogenic N deposition more generally. Taken together, our results clearly demonstrate that experimental N deposition is associated with a lower relative abundance of ligninolytic fungi on decaying fine roots.

In contrast, experimental N deposition favored ligninolytic bacteria and non-ligninolytic fungi. The relative abundance of Actinobacteria increased under experimental N deposition (+24%), including the family, Microbacteriaceae (+81%; Figures 2.2 and 2.3d). Experimental N deposition also increased the abundance of Saccharibacteria (+46%) and the fungal orders Chaetothyriales (+566%), Hypocreales (+37%), and Tremellales (+291%; Figure 2.2). These responses are likely ecologically important because ligninolytic Actinobacteria, including some Microbacteriaceae, degrade lignin to soluble phenolic compounds rather than oxidizing the polymer to CO_2 (Ahmad *et al.* 2010; Bugg *et al.* 2011; Taylor *et al.* 2012); this is consistent with greater phenolic dissolved organic C production in our experiment (Pregitzer *et al.* 2004). Some Saccharibacteria can modify aromatic compounds, but there is no evidence to indicate they degrade lignin (Luo *et al.* 2009). Other bacterial lineages have been implicated in lignin decay, including some that have responded to experimental N deposition (Figure 2.3d; Janusz *et al.* 2017); however, the cumulative effect of these changes in composition on bacterial lignin degradation remains to be tested. Some Hypocreales and Chaetothyriales also possess oxidases that could modify lignin (Assavanig *et al.* 1992; Hölker *et al.* 2002; Martinez *et al.* 2008; Teixeira *et al.* 2017), and yeasts in Tremellales dominate the late, lignin-rich stages of oak leaf litter decomposition (Voříšková & Baldrian 2013). However, these fungal lineages lack peroxidases capable of complete lignin oxidation (Floudas *et al.* 2012). Together, these

responses suggest that experimental N deposition has favored a microbial community with a lower capacity to degrade lignin in fine root litter.

In combination with a higher relative abundance of lignin-derived compounds in SOM, our observations specifically link changes in microbial community composition on fine root litter to the accumulation of SOM (Pregitzer *et al.* 2008; Zak *et al.* 2008). Foremost, experimental N deposition significantly altered fungal community composition by decreasing the relative abundance of ligninolytic *Mycena* and *Kuehneromcyes*, and these shifts in composition were significantly associated with a greater relative abundance of lignin-derived compounds in SOM (Figure 2.3a,b). Similarly, the relative abundance of lignin-derived compounds in SOM was positively related to the shift in bacterial community composition elicited by experimental N deposition (Figure 2.3c,d). The substantial declines in the relative abundance of ligninolytic fungi and increases in the relative abundance of bacteria with weaker ligninolytic capacity we observed (Figures 2.2 and 2.3) likely account for the reduction in fine root lignin decay (Xia *et al.* 2017) and mass loss (Xia *et al.* 2018) previously reported from our experiment, wherein fine root litter was allowed to decay in the field in an identical manner as our current study. Moreover, our findings suggest that by substantially altering the composition of microbial communities on fine roots, experimental N deposition has slowed the decay of lignin-rich fine root litter, thereby increasing the contribution of lignin-derived compounds from fine roots to SOM formation.

It is unclear why experimental N deposition decreased the abundance of ligninolytic fungi on fine root litter, whereas this response has not occurred on leaf litter in the same long-term experiment or others (Morrison *et al.* 2016, 2018; Whalen *et al.* 2018). A reduction in the competitive ability of ligninolytic fungi on lignin-rich substrates has been proposed to explain

the negative effects of experimental N deposition on ligninolytic enzyme activity and litter decay (DeForest *et al.* 2004; Waldrop *et al.* 2004; Janssens *et al.* 2010; Talbot & Treseder 2012; Entwistle *et al.* 2018b; Morrison *et al.* 2018), but the mechanisms underlying putative changes in competitive ability on lignin-rich substrates are not understood. Our observation that the relative abundance of ligninolytic fungi was reduced to a greater extent on fine root litter than leaf litter could be consistent with this hypothesis, although the role of competition and its specific mechanisms are unknown. A trade-off between stress tolerance and competitive ability has recently been proposed to explain the effects of experimental N deposition on ligninolytic fungi (Morrison *et al.* 2018), and numerous other mechanisms involving niche differentiation and an increased efficiency of non-ligninolytic fungi have also been suggested (*e.g.*, Talbot & Treseder 2012). Our findings, including the relationships between microbial composition and other components of SOM (*e.g.*, N-bearing compounds and lipids; Figure 2.3), emphasize the need to understand whether biotic interactions influence how experimental N deposition alters microbial community composition. For example, the distinction between these putative competition-mediated changes in composition and physiological responses (*i.e.*, down-regulated peroxidase transcription) would be represented differently in mechanistic ecosystem models (Allison 2012; Treseder *et al.* 2012; Hawkes & Keitt 2015). At present, these competitive processes are speculative and their mechanisms are not understood; a mechanistic understanding of these interactions will facilitate their extension to the effects of anthropogenic N deposition on fine root decay and soil C storage in other ecosystems.

The fact that experimental N deposition did not alter the biochemical composition of fine roots after one year of decay (Figures 2.2 and 2.3), and that it did increase the lignin content of SOM (Figures 2.1 and 2.3), indicates that the changes in microbial community composition we

documented have functional implications during the later stages of fine root decay (*i.e.*, beyond one year). Several pieces of evidence from our long-term experiment are consistent with this expectation. For example, based on the decay of identical fine root litter in identical litter bags, there was no effect of experimental N deposition on the mass loss (Xia *et al.* 2018) or biochemistry (Xia *et al.* 2017) of fine root litter after one year of decay. However, experimental N deposition significantly increased the mass of fine root litter remaining after three years of decay (Xia *et al.* 2018) due to a reduction in the decay of lignin (Xia *et al.* 2017). These reductions in the later stages of fine root decay align with the accumulation of lignin-derived compounds in SOM revealed in our current study (Figures 2.1 and 2.3). An important assumption is that the changes in microbial community composition we observed after one year persist to later stages of decay, thereby decreasing the loss of lignin and overall mass loss of fine root litter. Although this assumption remains to be tested, our findings clearly suggest that changes in microbial community composition (Figures 2.2 and 2.3) have slowed the decay of lignin in fine root litter (Xia *et al.* 2017, 2018), thereby increasing the amount of lignin-derived compounds from fine root litter in SOM (Figures 2.1 and 2.3).

The biochemical changes in SOM we observed may explain how experimental N deposition has increased the physical protection of SOM by mineral occlusion, as we have previously reported (Zak *et al.* 2017). Although relatively unmodified lignin is not thought to remain in long-term pools of SOM (Grandy *et al.* 2007), it can be stabilized through the adsorption of dissolved organic matter to mineral surfaces, or the physical occlusion of particulate litter by clay and silt particles in microaggregates (Cotrufo *et al.* 2015; Lehmann & Kleber 2015). In our experiment, experimental N deposition has not altered the amount of C in the highest density soil fraction (>1.8 g cm^{-1}) that represents mineral-adsorbed SOM; however, it

has increased mineral-occluded particulate SOM, which indicates greater physical protection of litter fragments in microaggregates (Zak *et al.* 2017). Previous analyses have revealed no effect of experimental N deposition on SOM biochemistry or other factors involved in aggregate formation (Thomas *et al.* 2012; Zak *et al.* 2017). However, it is plausible that a reduction in the microbial decay of fine root litter has increased the amount of time a given mass of fine root fragments remain in contact with soil particles, thereby fostering their occlusion (Cotrufo *et al.* 2015). Although this mechanism remains to be directly tested, our results suggest that reduced microbial decay of fine root litter may increase the physical stabilization of fine root material in microaggregates, which could influence the longevity of the terrestrial C sink.

A reduction in soil pH has recently been proposed as the primary mechanism by which experimental N deposition decreases the microbial decay of plant litter and increases soil C storage (Averill & Waring 2018); however, our findings provide a distinct and novel mechanism that is independent of soil pH. For example, experimental N deposition induced Mn-limitation in soils receiving experimental N deposition in an oak-dominated forest in New England, likely due to enhanced leaching of Mn from soils at low pH (Whalen *et al.* 2018). Since the late stages of litter decay (dominated by lignin degradation) occur more rapidly when Mn concentrations are high (Berg 2014), likely due to the role of Mn as a diffusible redox mediator for ligninolytic manganese peroxidase enzymes (Hofrichter 2002), pH-induced Mn-limitation was thought to explain reduced rates of litter decay (Whalen *et al.* 2018). Additionally, experimental N deposition could reduce microbial activity due to the direct negative effects of low pH on microbial physiology (Averill & Waring 2018). However, soil pH does not differ among sites in our long-term experiment (Table A.1), nor has experimental N deposition decreased soil pH (Eisenlord & Zak 2010). Thus, neither Mn-limitation nor the direct negative effects of low soil

pH on microbial activity explain reductions in fine root decay in our experiment. Instead, our findings suggest a pH-independent mechanism, in which the decreased abundance of highly ligninolytic fungi and increased role for less complete bacterial lignin degradation has slowed the decay of fine root litter.

In summary, we demonstrated that over 20 years of experimental N deposition has reduced the relative abundance of ligninolytic fungi and increased that of ligninolytic bacteria on decaying fine roots, which plausibly explains how fine root decay has slowed and SOM has accumulated in our study (Zak *et al.* 2008; Xia *et al.* 2017, 2018). Furthermore, we found that an accumulation of lignin-derived compounds in SOM was significantly related to changes in microbial community composition on decaying fine root litter, particularly a decline in the relative abundance of ligninolytic fungi. Together, this evidence suggests that by altering microbial community composition on fine root litter, which is the dominant source of lignified plant material to soil, experimental N deposition has caused an accumulation of root-derived C as SOM. It is important to point out that fine root litter may account for a smaller proportion of lignin-derived compounds that enter soil in forest ecosystems dominated by species with higher leaf litter lignin concentrations (*e.g.*, *Quercus*, *Pinus*) than sugar maple. Nonetheless, our findings unite a growing body of evidence that experimental N deposition enriches SOM in compounds that are abundant in fine roots (Grandy *et al.* 2008; Frey *et al.* 2014; vandenEnden *et al.* 2018; Wang *et al.* 2019) with the changes in microbial composition that are responsible for their accumulation. To better understand how experimental N will modify terrestrial C storage and mediate climate under future rates of anthropogenic N deposition (Galloway *et al.* 2004, 2008), we must explicitly test ecological mechanisms (*e.g.*, putative competitive interactions) that may alter microbial community composition and slow fine root decay, as well as better

understand how the altered products of fine root decomposition are stabilized into SOM. Taken together, our findings link the composition and function of microbial communities, as well as highlight the role of compositional shifts in mediating biogeochemical processes of global significance.

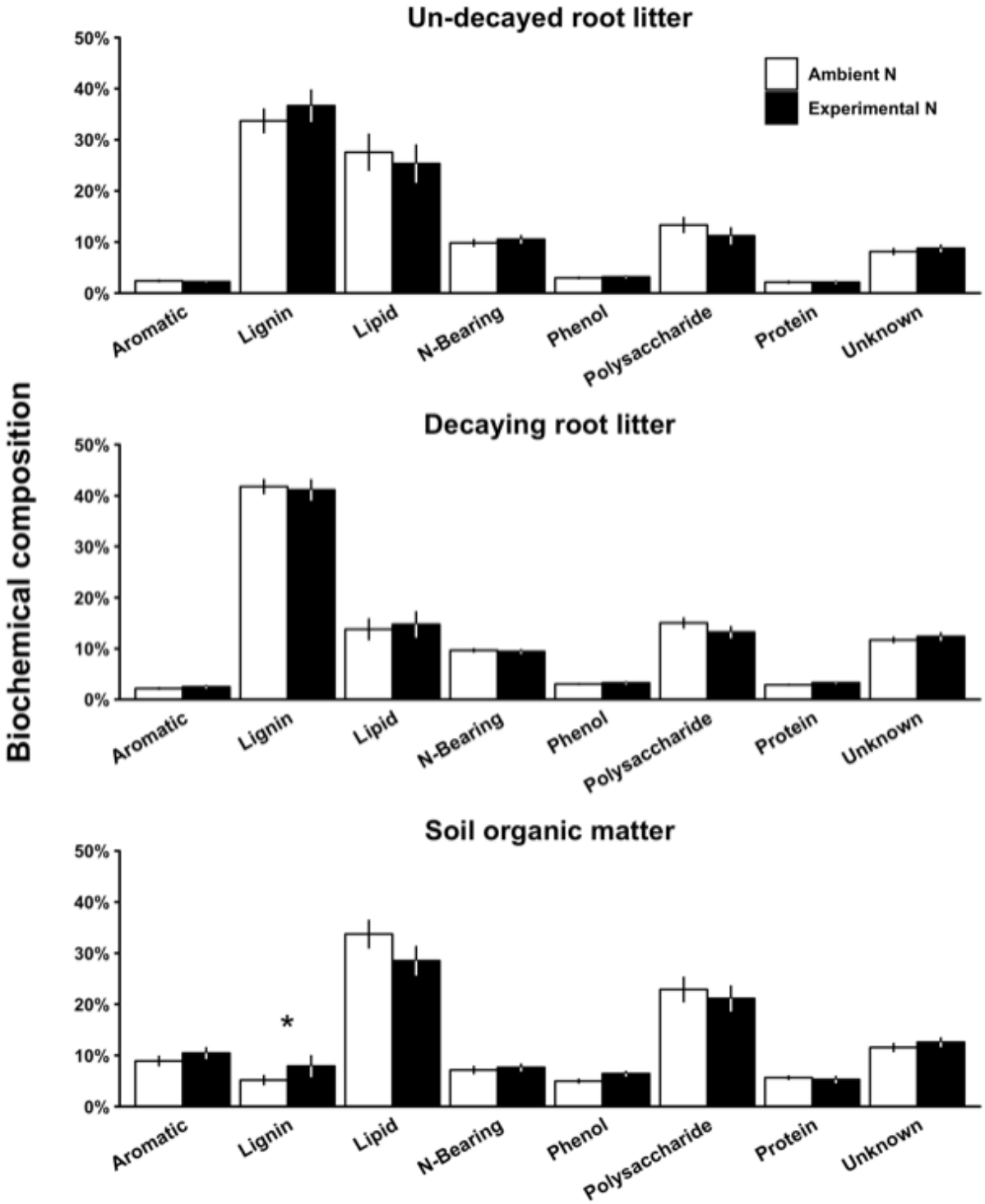

Figure 2.1: Biochemical composition of fine root litter and soil organic matter based on the relative abundance (%) of compound classes. Bars represent mean relative abundances and error

bars are 1 standard error of the mean (n = 12). * P < 0.1 for effect of experimental N deposition by two-way ANOVA.

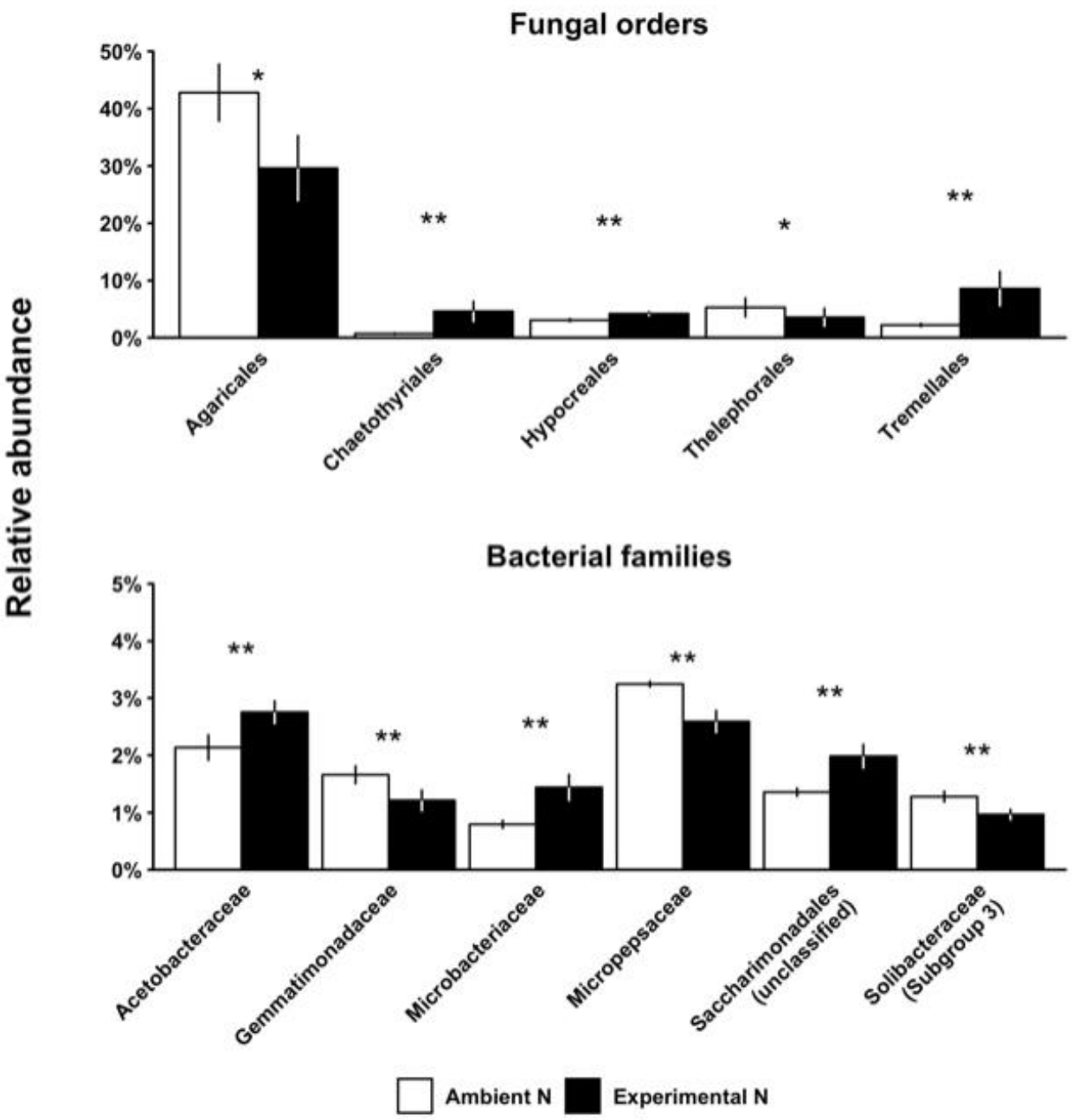

Figure 2.2: Relative abundance of fungal orders and bacterial families exhibiting significant

responses to experimental N deposition after 12 months. Bars represent mean relative abundances and error bars are one standard error (n = 12). * $P < 0.1$, ** $P < 0.05$, for effect of experimental N deposition by two-way ANOVA

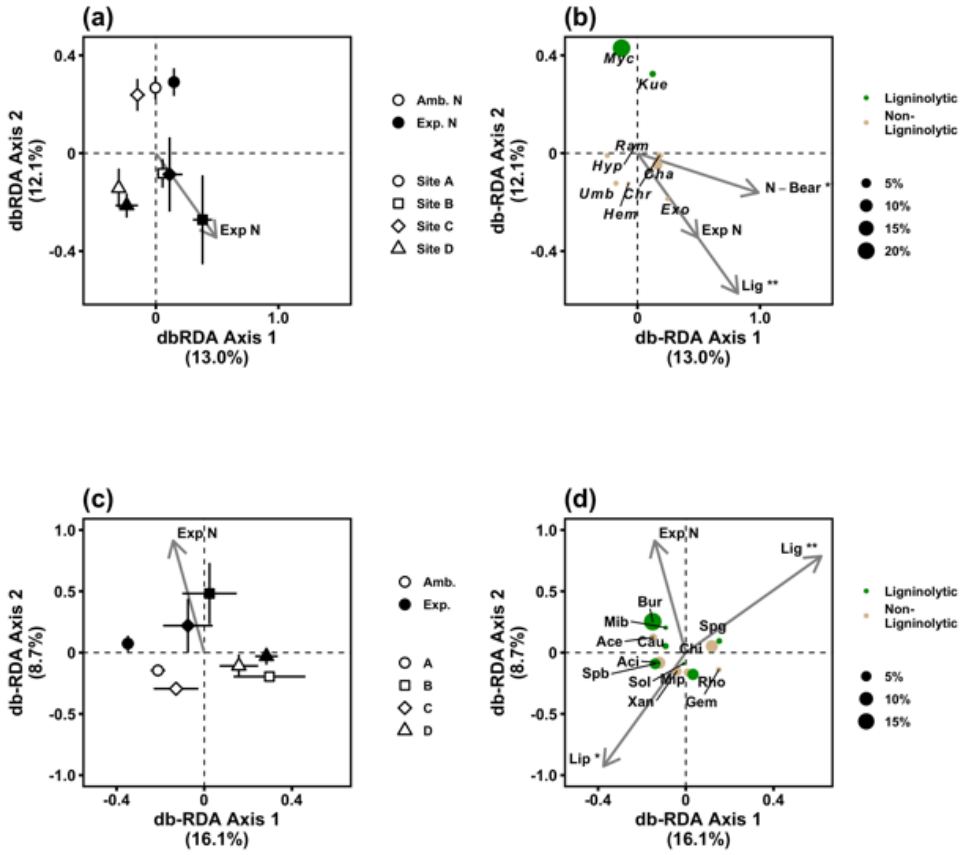

Figure 2.3: db-RDA ordinations determined from Bray-Curtis dissimilarity calculated using Hellinger-transformed abundances of fungal genera (a, b) and bacterial families (c, d). Ordinations were constrained to include variation due to experimental N deposition and site, which together accounted for 37.7% of variation in Bray-Curtis dissimilarity for fungi and 33.2% for bacteria. Panels (a) (fungi) and (c) (bacteria) display site by treatment mean loadings (error bars are one standard error). Panels (b) (fungi) and (d) (bacteria) include taxon loadings (which represent the direction from the origin in which a genus increases in relative abundance) and compound class vectors from SOM. Classified taxa that accounted for >1% of sequences were included. Involvement of non-Actinobacterial families in lignin degradation was based on (Wilhelm *et al.* 2019). * $P < 0.1$, ** $P < 0.05$ for vector fit. *Cha, Chaetomium*; *Chr*,

Christiansenia; *Exo*, *Exophiala*; *Hyp*, *Hypocrea*; *Hem*, *Hemimycena*; *Kue*, *Kuehneromyces*; *Myc*, *Mycena*; *Ram*, *Ramariopsis*; *Umb*, *Umbelopsis*; Lig, lignin-derived compounds; N-Bear, N-bearing compounds (b). Ace, Acetobacteraceae; Aci, Acidobacteriaceae Subgroup 1, Bur, Burkholderiaceae; Cau, Caulobacteraceae, Chi, Chitinophagaceae; Gem, Gemmatimonadaceae; Mib, Microbacteriaceae; Mip, Micromonosporaceae; Rho, Rhodanobacteraceae; Sol, Solibacteraceae Subgroup 3; Spb, Sphingobacteriaceae; Spg, Sphingomonadaceae; Xan, Xanthobacteraceae, Lig, lignin-derived compounds; Lip, lipid (d).

CHAPTER 3

Decay by Ectomycorrhizal Fungi Couples Soil Organic Matter to Nitrogen Availability

William A. Argiroff, Donald R. Zak, Peter T. Pellitier, Rima A. Upchurch, and Julia P. Belke

Abstract

Interactions between soil nitrogen (N) availability, fungal community composition, and soil organic matter (SOM) regulate soil carbon (C) dynamics in many forest ecosystems, but context dependency in these relationships has precluded general predictive theory. We found that ectomycorrhizal (ECM) fungi with peroxidases decreased with increasing inorganic N availability across a natural inorganic N gradient in northern temperate forests, whereas ligninolytic fungal saprotrophs exhibited no response. Lignin-derived SOM and soil C were negatively correlated with ECM fungi with peroxidases and were positively correlated with inorganic N availability, suggesting decay of lignin-derived SOM by these ECM fungi reduced soil C storage. The correlations we observed link SOM decay in temperate forests to tradeoffs in tree N nutrition and ECM composition, and we propose SOM varies along a single continuum across temperate and boreal ecosystems depending upon how tree allocation to functionally distinct ECM taxa and environmental stress covary with soil N availability.

Introduction

Interactions between inorganic nitrogen (N) availability and fungal community composition are important controls over soil organic matter (SOM) dynamics in temperate and boreal forests (Kyaschenko *et al.* 2017; Averill & Waring 2018), yet the context dependency of these relationships has precluded general theory to predict how SOM varies due to fungal responses to N availability. For example, SOM in many boreal and sub-alpine forests is negatively correlated with the abundance of ectomycorrhizal (ECM) fungi that decay SOM using class II peroxidases (hereafter, "peroxidases"; Lindahl *et al.* 2021), and SOM either increases or decreases with soil N availability depending upon whether these ECM taxa decline or increase (Clemmensen *et al.* 2015, 2021). In contrast, SOM stocks decline with increasing N availability in fertile boreal forests because of an increase in ligninolytic saprotrophic fungi (Kyaschenko *et al.* 2017), which also decay lignified compounds in plant litter and SOM using peroxidases (Floudas *et al.* 2012). In a high fertility temperate forest, SOM declined with increasing N availability due greater decay by non-ligninolytic saprotrophic Ascomycete fungi (Mayer *et al.* 2021). However, relationships between soil inorganic N availability, fungal composition, and SOM remain poorly understood in temperate forests spanning low to intermediate fertility. Addressing this gap may provide a unified framework for predicting how fungal composition and inorganic N availability regulate SOM and the vast amounts of carbon (C) it stores across boreal and temperate forests (Jackson *et al.* 2017).

Nitrogen deposition experiments in temperate forests suggest increasing inorganic N availability across natural gradients could enhance the accumulation of SOM by modifying the composition of saprotrophic fungi in decaying fine roots (Figure 3.1). Senesced fine roots comprise ~50% of plant litter entering forest soils (Freschet *et al.* 2013) and, due to high lignin

concentrations (Xia *et al.* 2015; Sun *et al.* 2018), are the major source of lignin-derived polyphenolic SOM in many temperate forests (Thomas *et al.* 2012; Xia *et al.* 2015). Experimental N additions in these ecosystems reduce the abundance of ligninolytic saprotrophic fungi inhabiting decaying fine roots – possibly by decreasing their competitive ability – thereby slowing fine root decay, causing lignin-derived compounds to accumulate as SOM (Xia *et al.* 2018; Argiroff *et al.* 2019), and enhancing soil C storage (Zak *et al.* 2008; Chen *et al.* 2018). If this fungal mechanism operates across natural soil N gradients in temperate forests, it could cause SOM to increase with increasing inorganic N availability (Figure 3.1, *Saprotroph Mechanism*).

Increasing inorganic N availability could also promote soil C storage in temperate forests by altering the composition of ectomycorrhizal (ECM) fungal communities (Figure 3.1). Certain ECM lineages have retained peroxidases in their evolution from ligninolytic saprotrophic ancestors, which these ECM fungi likely use to obtain N organically bound in complex polyphenolic SOM (Pellitier & Zak 2018; Miyauchi *et al.* 2020). Recent evidence revealed that the relative abundance of ECM fungi with peroxidases in root tips of temperate forest trees declined across a natural gradient of soil inorganic N availability (Pellitier *et al.* 2021b; Pellitier & Zak 2021a), suggesting high inorganic N availability could enhance soil C storage by reducing the decay of existing lignin-derived SOM by ECM fungi with peroxidases (Figure 3.1, *ECM Mechanism*). While ECM with peroxidases likely restrict SOM accumulation in boreal forests (Baskaran *et al.* 2017; Clemmensen *et al.* 2021; Lindahl *et al.* 2021), studies in temperate forests have not addressed the regulatory role of compositional variation within the ECM fungal community because they have primarily focused on how SOM varies between ecosystems

dominated by either ECM or arbuscular mycorrhizal fungi (Phillips *et al.* 2013; Averill *et al.* 2018).

Here, we tested the hypothesis that soil C storage increases with soil inorganic N availability and that this response is linked to declines in saprotrophic as well as ECM fungi with the genetic potential to decay lignin and lignin-derived SOM (Figure 3.1). We characterized fungal community composition, lignin-derived SOM, and soil C storage across a natural gradient of soil inorganic N availability in northern broadleaf temperate forests (Zak *et al.* 1989; Pellitier *et al.* 2021b, a; Pellitier & Zak 2021a), in which microsite differences in topography create an inorganic N availability gradient by influencing water availability and nutrient retention (Zak *et al.* 1989; Zak & Pregitzer 1990). We predicted that the relative abundance of ligninolytic fungi in decaying fine root litter and ECM fungi with peroxidases in soil would decline with increasing soil inorganic N availability. We further reasoned that lignin-derived SOM and soil C storage would be negatively correlated with the relative abundance of ligninolytic fungi in decaying fine roots (Figure 3.1; *Saprotroph Mechanism*) or ECM fungi with peroxidases in soil (Figure 3.1; *ECM Mechanism*). These fungal responses should cause lignin-derived SOM – and overall soil C – to be positively correlated with inorganic N availability (Figure 3.1). We focused on ligninolytic fungi in decaying fine root litter because these fungi regulate the amount of lignin-derived fine root material entering SOM (Thomas *et al.* 2012; Argiroff *et al.* 2019), and we targeted ECM fungi with peroxidases in soil because ECM fungi primarily decay compounds in existing SOM (Figure 3.1; Pellitier & Zak 2018; Sterkenburg *et al.* 2018). By addressing this knowledge gap and comparing our findings to studies from contrasting ecosystems, we aimed to generate a unified framework for predicting how fungal composition regulates the relationship between N availability and SOM across boreal and temperate forests.

Materials and Methods

Site descriptions and study design

We established 72 circular plots (2-m diameter) randomly in 12 forest sites (6 plots per site) in northern Lower Michigan, USA (Figure B.1). All plots were located in even-aged (~100 year-old) second-growth northern hardwood forests on uniformly sandy soils (~85% sand), and do not vary in climate due to close geographic proximity (separated by <50 km; Zak *et al.* 1989; Zak & Pregitzer 1990). Plots were in mixed stands of *Quercus rubra* (red oak) and *Acer rubrum* (red maple), which co-occur across the inorganic N availability gradient, to minimize differences in the biochemistry of litter inputs. Plots were adjacent to previously studied ECM communities in *Q. rubra* root tips (Pellitier *et al.* 2021b, a; Pellitier & Zak 2021a). Our plots ranged in mineralization rates from 0.08 to 1.19 μg N $g^{-1} \cdot d^{-1}$ (Figure B.4). These values captured the full gradient of inorganic N availability in the upper Lake States region and have remained seasonally and interannually stable since the 1980s (Zak *et al.* 1989; Zak & Pregitzer 1990; Pellitier *et al.* 2021a).

Soil and SOM characteristics

In May of 2019, we obtained 6 soil cores (2.5 cm diameter x 10 cm depth) within each plot (Oe and A horizons, excluding Oi) evenly spaced around a 1-m radius from the plot center. We transported cores on ice to the University of Michigan, sieved field-moist soil through 2-mm mesh, removed fine roots, and homogenized the sieved soil by plot (6 cores homogenized per plot x 6 plots x 12 sites = 72 samples). We froze a subsample of fresh soil at -80 °C for DNA isolation, and immediately used two 30 g subsamples of sieved field-moist soil for 28-day

laboratory net N mineralization assays to quantify inorganic N availability (Vitousek *et al.* 1982; Zak *et al.* 1989). We measured extractable inorganic N (NO_3^- and NH_4^+) pre- and post-incubation with an AQ2 Discrete Analyzer (SEAL Analytical). Laboratory N mineralization measurements are strongly correlated with *in situ* net N mineralization across the forest ecosystems in this study system (Zak *et al.* 1989; Zak & Pregitzer 1990) and are therefore a robust representation of inorganic N availability. Inorganic N availability is also correlated with fine root C/N and SOM C/N (Figure B.2), and therefore reflects N availability more broadly.

We used a subsample of oven-dried ground soil to determine the relative abundance of lignin-derived SOM by pyrolysis gas chromatography-mass spectrometry (py-GC/MS) following previously described methods (Supporting Methods B.1; Grandy *et al.* 2007, 2009; Pold *et al.* 2017; Argiroff *et al.* 2019). We determined soil C and N from ground soil using a CN analyzer (LECO). The remaining field-moist soil was air-dried at room temperature and used to determine soil pH with 30 g of air-dried soil in 1:1 slurries in deionized water. We interpolated hourly soil temperature and volumetric water content from May to October of 2019 at each plot by regressing handheld probe measurements against nearest hourly values from a Micro Station data logger (ONSET) at each site.

Decaying fine root litter

We used litterbags to characterize fungal communities in decaying fine root litter (Sun *et al.* 2018; Argiroff *et al.* 2019). In May of 2018, we collected soil at each site around 5 mature *Q. rubra* individuals, which occur in the overstory at all sites and therefore represent a large fraction of fine root litter in these forest ecosystems. We collected, rinsed, and dried fine roots ≤0.5 mm in diameter and composited them by site. We chose the diameter cutoff of ≤0.5 mm because this

retained approximately first- through third-order fine roots, which comprise the absorptive fine root modules that turn over rapidly and produce the majority of fine root litter (Xia *et al.* 2010; McCormack *et al.* 2015). For each site, we placed ~3 g of fine root litter into each of twelve 12-cm x 12-cm nylon mesh bags (opening size 53 μm), which admit fungal hyphae but prevent fine root ingrowth (Hobbie *et al.* 2010; Li *et al.* 2015; Sun *et al.* 2018). We sterilized litterbags and roots using ethylene oxide (Steris Corporation; Cline & Zak 2015) to eliminate fungi without altering root biochemistry, and thus assumed any fungi in fine root litter colonized from adjacent soil after deployment. In May of 2019 (during soil collection), we placed two litterbags horizontally near the center of each plot and replaced overlying soil without disturbing its vertical distribution. Bags were located at the interface of the O and A horizons (depth of ~ 3 cm) within the dense mat of fine roots (Figure B.3). After 13 months of decay (July of 2020), we retrieved the litter bags, transported them on ice to the laboratory, and homogenized roots by plot. Roots were weighed, a subsample was stored at -80 °C for DNA isolation, an additional subsample was oven-dried to constant mass at 60 °C and ashed at 500 °C for 6 hours to determine moisture content and mineral content, respectively, and mass loss was calculated to determine decay rates.

Fungal community composition

We characterized fungal communities inhabiting soil and decaying fine roots using the ITS2 region of the fungal nuclear ribosomal internal transcribed spacer (ITS) region, which is the universal fungal DNA barcode (Schoch *et al.* 2012; Nilsson *et al.* 2019a). We isolated DNA from 0.15 g decaying fine roots and 1 g soil from each plot (Supporting Methods B.1). We targeted the ITS2 region using PCR amplification with ITS4-Fun/5.8S-Fun primers following

previously published protocols (Supporting Methods B.1; Taylor *et al.* 2016; Pellitier *et al.* 2019). PCR libraries were normalized, purified, and sequenced using MiSeq 2x250 bp with v2 chemistry (Illumina). We obtained high quality sequences and calculated amplicon sequence variants (ASVs; Callahan *et al.* 2017; Pauvert *et al.* 2019) from forward reads using 'DADA2' (Rosen *et al.* 2012; Callahan *et al.* 2016) with 'cutadapt' (Martin 2011). Additionally, we used quantitative real-time PCR (qPCR) of the ITS region with ITS1F and 5.8S primers to determine absolute fungal abundance in soil and decaying roots (Entwistle *et al.* 2018b).

We classified sequences using the naïve Bayesian classifier (Wang *et al.* 2007) and the UNITE database (Kõljalg *et al.* 2013; Nilsson *et al.* 2019b). We removed genera present in fewer than 5 plots and accounting for <0.1% of sequences separately for the soil and fine roots datasets, leaving 72% of fungal reads from soil and 70% from decaying roots that were assigned to functional groups (Table B.1). Ligninolytic saprotrophs were identified with FUNGuild (Nguyen *et al.* 2016) and literature (Entwistle *et al.* 2018b; Ruiz-Dueñas *et al.* 2021). We used literature to identify ECM genera containing species with class II peroxidases ("AA2" CAZymes; Levasseur *et al.* 2013; Lombard *et al.* 2014) in their genomes (Bödeker *et al.* 2009; Kohler *et al.* 2015; Nagy *et al.* 2016; De Crop *et al.* 2017; Miyauchi *et al.* 2020). We assumed all species in an ECM genus have peroxidases if these genes have been detected in the species with sequenced genomes belonging to that genus, which may change as more ECM genomes are sequenced. Class II peroxidases are confined to Auriculariales and more recently diverging orders of Agaricomycetes (Floudas *et al.* 2012; Nagy *et al.* 2016). Thus, we assumed ECM and saprotrophic genera outside these lineages do not have peroxidases or strong ligninolytic capacity (hereafter "ECM without peroxidases" and "non-ligninolytic saprotrophs"). Remaining ECM genera were identified using FUNGuild. We acknowledge dichotomizing ECM genera into

those with and without peroxidases is a coarse approximation of oxidative decay capacity since there is considerable variation within genera in peroxidase gene copies (Miyauchi *et al.* 2020). However, it is currently unclear how variation in peroxidase gene copy number corresponds to *in situ* ECM decay activity (Pellitier & Zak 2018), and we believe our current classification is an acceptable initial approximation of function pending experimental verification. We identified "other mycorrhizas" and "fungi with other or uncertain ecology" using FUNGuild and the literature (Smith & Read 2010; Seitzman *et al.* 2011; Martino *et al.* 2018). Functional group abundances are relative to the total fungal community unless otherwise specified.

Statistical analyses

We used generalized additive mixed models (GAMM) in the package 'mgcv', which accommodate complex nonlinear patterns (Wood 2011), to test three sets of relationships. First, we evaluated the relationship between each fungal functional group and inorganic N availability for soil and decaying fine root litter. We corrected *P*-values for false discovery rate using the Benjamini-Hochberg false discovery rate correction (Benjamini & Hochberg 1995) for these 12 individual GAMMs. In a complementary test of these patterns, we used the package 'TITAN2' (Baker & King 2010) to test for fungal genera that significantly responded to the inorganic N supply gradient, based on Hellinger-transformed abundances (Legendre & Legendre 2012). Genera with both purity and reliability $\geq$0.95 were considered significantly related to inorganic N availability (Baker & King 2010). Second, we used multiple GAMM to understand if lignin-derived SOM and soil C were correlated with fungal functional groups. Each model had lignin-derived SOM or soil C as the independent variable, and the six fungal functional groups in soil or

in decaying fine root litter as the predictor variables. Finally, we used separate GAMM to test whether lignin-derived SOM and soil C were correlated with inorganic N availability.

We performed all analyses using fungal genera present in ≥5 plots and accounting for ≥0.1% of sequences and elected not to subsample sequence counts to limit uncertainty and data loss (McMurdie & Holmes 2013, 2014). We $\log_{10}$-transformed soil C to obtain normally distributed residuals. Plots within each site varied considerably in inorganic N availability, and there was substantial overlap in inorganic N among plots from different sites (Figure B.4). Given this within-site variation and strong heterogeneity in SOM and fungal community composition at fine spatial scales (Taylor *et al.* 2014; Bogar *et al.* 2019), we quantified all variables at the plot level and treated these values separately. Because plots within the same site may be similar due to spatial proximity and unmeasured ecological processes, we accounted for spatial autocorrelation using a spatial correlation structure in all GAMM. Four plots had ecologically unrealistic values for net N mineralization or SOM biochemistry, likely from sampling error (Figure B.4). We removed these plots from all analyses. We accepted statistical significance at $\alpha = 0.05$. All analyses were performed in R version 4.0.2 (R Core Team 2020) with RStudio version 1.4.869 (RStudio Team 2020), using the packages 'ShortRead' (Morgan *et al.* 2009), 'Biostrings' (Pagès *et al.* 2020), 'phyloseq' (McMurdie & Holmes 2013), and the 'tidyverse' (Wickham *et al.* 2019).

Results

Fungal responses to inorganic N availability

ECM fungi with peroxidases (26% of sequences) were the most abundant functional group in soil (Figure B.5), and were dominated by *Russula*, *Piloderma*, and *Cortinarius* (Figure B.6).

Ligninolytic saprotrophs (32%) were most abundant in decaying fine root litter (Figure B.5) and were dominated by *Mycena*, *Gymnopus*, and *Trechispora* (Figure B.6). The abundance of ECM with peroxidases decreased as soil inorganic N availability increased in both soil ($R^2_{adj.}$ = 0.455, $P_{adj.}$ < 0.001; Figure 3.2a) and decaying fine root litter ($R^2_{adj.}$ = 0.516, $P_{adj.}$ < 0.001; Figure 3.2b; Table B.2). ECM root tips (Pellitier *et al.* 2021a), fine root biomass (Figure B.7), and ITS copy number also declined with increasing inorganic N availability (Figure B.8). Thus, the absolute abundance of ECM fungi with peroxidases clearly declined with inorganic N availability. The proportion of taxa with peroxidases within the ECM fungal community also declined with increasing inorganic N availability, although this response was not significant after accounting for spatial autocorrelation (P = 0.101; Figure B.9). The relative abundance of ligninolytic saprotrophs in soil increased as inorganic N availability increased ($R^2_{adj.}$ = 0.064, $P_{adj.}$ = 0.034; Figure 3.2a), whereas ligninolytic saprotrophs in decaying fine root litter were not influenced by inorganic N availability ($P_{adj.}$ = 0.34; Figure 3.2b). The relative abundance of ECM fungi without peroxidases in soil also declined with increasing inorganic N availability ($R^2_{adj.}$ = 0.079, $P_{adj.}$ = 0.025; Figure 3.2a), whereas this functional group in decaying fine root litter did not respond to inorganic N availability ($P_{adj.}$ = 0.12; Figure 3.2b). The relative abundance of non-ligninolytic saprotrophic fungi increased with increasing inorganic N availability in soil ($R^2_{adj.}$ = 0.284, $P_{adj.}$ < 0.001; Figure 3.2a) and decaying fine roots ($R^2_{adj.}$ = 0.189, $P_{adj.}$ < 0.001; Figure 3.2b). The relationship between ECM fungi with peroxidases and inorganic N availability was robust to inclusion of soil pH, volumetric water content, and temperature in the GAMM (Table B.3). Sequencing yield and taxonomic distributions are described in Tables B.4-B.7.

We found that 7 of 8 ECM genera in soil that possess peroxidases significantly declined in relative abundance as inorganic N availability increased (Figure 3.3a). Similarly, most ECM

genera with peroxidases in decaying fine root litter significantly declined as inorganic N supply increased (Figure 3.3b). ECM genera without peroxidases exhibited mixed responses to the inorganic N availability gradient in both soil and decaying fine root litter (Figure 3.3). Non-ligninolytic saprotrophic genera in soil generally increased as inorganic N availability increased (Figure 3.3a), but few ligninolytic saprotrophs responded significantly to inorganic N availability (Figure 3.3).

Links between fungal communities, SOM, and soil C

Lignin-derived SOM (P = 0.039; Figure 3.4a) and soil C (P = 0.019; Figure 3.4b) were significantly negatively related to ECM fungi with peroxidases in soil (Table B.8). Lignin-derived SOM was positively related to the relative abundance of non-ligninolytic saprotrophic fungi in decaying fine root litter (P = 0.013; Figure 3.4c), as well as the relative abundance of fungi with other or uncertain ecology (P = 0.034; Figure B.10); however, the latter relationship was driven by two large outliers and was likely spurious. Lignin-derived SOM and soil C were not significantly related to the relative abundance of ligninolytic saprotrophs ($P > 0.05$; Figure 3.4 and Table B.8).

Response of SOM biochemistry and soil C storage to inorganic N availability

The relative abundance of lignin-derived SOM, which accounted for 13% of SOM on average (Figure B.11), increased as inorganic N availability increased ($R^2_{adj.}$ = 0.085, $P_{adj.}$ = 0.045; Figure 3.5a). Soil C was strongly positively correlated with lignin-derived SOM ($R^2_{adj.}$ = 0.407, $P_{adj.} <$ 0.001; Figure 3.5b; Table B.9). Consequently, soil C increased with increasing inorganic N availability ($R^2_{adj.}$ = 0.069, $P_{adj.}$ = 0.016; Figure 3.5c). These relationships were robust to the

inclusion of soil pH, volumetric water content, and temperature in the GAMM (Table B.3). Furthermore, fine root mass loss was not correlated with inorganic N availability, lignin-derived SOM, or soil C storage (Figure B.12).

Discussion

Turnover in ECM composition constrains SOM accumulation

Our findings suggest the accumulation of SOM in ECM-dominated temperate forests is restricted by the decay activity of ECM fungi with peroxidases (Figures 3.4-3.5). Although ligninolytic genera (*e.g.*, *Mycena*) were abundant in root litter (Figures 3.2b and B.5-B6; Tables B.1 and B.7), which is common for fungal communities decaying fine roots (Kohout *et al.* 2018; Philpott *et al.* 2018; Argiroff *et al.* 2019), we found no evidence that these fungi responded to inorganic N availability (Figures 3.2-3.3). Furthermore, lignin-derived SOM and soil C storage were not significantly related to the relative abundance of ligninolytic saprotrophic fungi (Figures 3.4) or fine root mass loss (Figure B.12). These observations were inconsistent with the *Saprotroph Mechanism* (Figure 3.1), plausibly because natural inorganic N gradients are more subtle than N deposition experiments. In contrast, the relative abundance of ECM fungi with peroxidases declined with increasing inorganic N availability (Figures 3.2-3.3). This response was nearly uniform across ECM genera with peroxidases, including *Cortinarius*, *Piloderma,* and *Russula* (Figure 3.3, Tables B.1 and B.7; Miyauchi *et al.* 2020). Importantly, lignin-derived SOM and soil C storage were negatively related to the relative abundance of ECM fungi with peroxidases in soil, which is consistent with the prediction that naturally high inorganic N availability promotes soil C storage by reducing the decay of existing lignin-derived SOM by ECM fungi with peroxidases (Figure 3.1; *ECM Mechanism*). We caution that these relationships have

relatively low explanatory power ($R^2 < 0.1$), suggesting other processes also contribute to differences in SOM in our study. Nonetheless, our findings highlight a surprising similarity between SOM in the mineral soil of temperate broadleaf forests and low fertility boreal ecosystems with large organic horizons, whereby soil C storage is reduced where ECM fungi that have retained greater oxidative decay capacities are more abundant (Clemmensen *et al.* 2015, 2021; Lindahl *et al.* 2021).

Studies of mycorrhizae and SOM in temperate forests have primarily focused on how soil C storage differs between ecosystems dominated by ECM or arbuscular mycorrhizae (Phillips *et al.* 2013; Averill *et al.* 2018), yet our observations suggest compositional turnover *within* ECM-dominated fungal communities is also an important control over SOM dynamics. Because ECM fungi do not assimilate or respire the organic C compounds they decay while acquiring organic N (Treseder *et al.* 2006; Baldrian 2009; Lindahl & Tunlid 2015), many conceptualizations assume ECM fungi selectively liberate N from SOM (Orwin *et al.* 2011; Smith & Wan 2019; Fernandez *et al.* 2020). However, ECM lineages that have retained peroxidases from ligninolytic saprotrophic ancestors are unlikely to liberate N from SOM without also extensively decaying lignin-derived SOM, because peroxidases and ancillary enzymes fully and extracellularly oxidize lignin-derived compounds to CO_2 (Kirk & Farrell 1987; Hofrichter 2002; Pellitier & Zak 2018). This prediction is consistent with our observation that lignin-derived SOM and soil C storage were negatively correlated with the relative abundance of ECM fungi with peroxidases (Figure 3.4a-b). By contrast, ECM fungi that have evolved within Ascomycota or other non-ligninolytic saprotrophic lineages either have minimal decay capacity or use non-enzymatic Fenton chemistry to selectively acquire organic N (Rineau *et al.* 2012; Shah *et al.* 2016; Pellitier & Zak 2018). Accordingly, we observed no correlation between soil C and ECM fungi without

peroxidases (Figure 3.4). Thus, the effect of ECM fungi on soil C storage appears to depend on the decay traits of dominant ECM taxa.

The results of our study have important implications for how soil C storage in temperate forests may respond to environmental change. For example, rising atmospheric CO_2 stimulates plant growth (Campbell *et al.* 2017), and ectomycorrhizal plants may increase their investment in organic N acquisition by ECM mutualists to maintain this growth (Terrer *et al.* 2016). Our observation that certain ECM fungi may decrease soil C when acquiring N from SOM (Figure 3.4a,b) suggests elevated CO_2 could decrease soil C storage in temperate forests by increasing organic N acquisition. This prediction is consistent with recent evidence that elevated CO_2 decreases soil C in ecosystems dominated by plants associated with ECM fungi (Terrer *et al.* 2021), and our study provides a plausible mechanism to explain this pattern. However, just as functional variation among ECM communities alters the capacity for trees to obtain N from SOM under elevated CO_2 (Pellitier *et al.* 2021a), our study suggests that not all ECM communities will similarly impact SOM as atmospheric CO_2 continues to increase. Assuming elevated CO_2 does not modify ECM composition, we propose that increased plant allocation to organic N acquisition in response to rising atmospheric CO_2 will reduce soil C storage where ECM communities are dominated by taxa with peroxidases but will not decrease soil C storage where ECM have selective or minimal decay capacity.

A unified framework linking ECM fungi, N availability, and SOM

We propose apparent context dependency in relationships between SOM, fungi, and N availability can be resolved into general predictive understanding if we consider how plant allocation to “expensive” ECM decay capacities and environmental stress vary with N

availability (Figure 3.6). Plants associate with ECM mutualists that optimize the organic N acquisition return of their photosynthate investment (Hortal *et al.* 2017; Bogar *et al.* 2019). Specifically, investment in ECM symbionts with energetically costly organic N acquisition capacities is beneficial to plant hosts when inorganic N is scarce, favoring ECM taxa with a greater genetic potential to obtain N from SOM using peroxidases and other oxidative enzymes (Baskaran *et al.* 2017; Defrenne *et al.* 2019; Pellitier & Zak 2021a). These decay traits enable ECM communities in soils with low inorganic N availability to more substantially supplement tree N nutrition with N from SOM across the ecosystems in our study (Pellitier *et al.* 2021b, a), and our current findings suggest this enhanced decay, in turn, reduces lignin-derived SOM and soil C storage (Figure 3.6). We propose that this nutritional tradeoff continues to operate in relatively fertile boreal forests, in which ECM fungi with peroxidases decline with increasing N availability and plausibly enable greater SOM decay by ligninolytic saprotrophs (Figure 3.6; Kyaschenko *et al.* 2017).

However, as N availability continues to decline from relatively fertile to low fertility boreal ecosystems, the relationship between ECM with peroxidases and fertility reverses (Figure 3.6; Clemmensen *et al.* 2015). This occurs because declines in tree productivity and pH favor stress tolerant mycorrhizae belonging to Ascomycota over ECM fungi with peroxidases that require greater photosynthate allocation (Sterkenburg *et al.* 2015), causing soil C storage to increase with declining fertility (Clemmensen *et al.* 2015). Thus, we propose that the abundance of ECM with peroxidases restricts SOM accumulation across gradients of soil inorganic N availability, but that the direction of this relationship depends on the location along a broader continuum of N availability and photosynthate allocation that connects boreal and temperate ecosystems (Figure 3.6). Exceptions to this pattern could occur where narrower ranges of soil N

availability in fertile temperate forests cause less variation in ECM abundance (Mayer *et al.* 2021) or where dramatic transitions in boreal and subarctic ecosystem types reverse the relationships between environmental stress, host allocation to ECM with greater decay potential, and N availability (Clemmensen *et al.* 2021).

Important considerations and conclusions

Aboveground productivity in the forests we studied is positively correlated with inorganic N availability (Zak *et al.* 1989), suggesting higher aboveground litter production could cause greater soil C storage where inorganic N availability is also high. However, this explanation is unlikely because fine root biomass declined with inorganic N availability (Figure B.7). Thus, total litter production (above- plus belowground) may be relatively even across the inorganic N availability gradient. Additionally, because fine root litter is the primary source of lignin-derived SOM in forest soils (Thomas *et al.* 2012; Xia *et al.* 2015), the amount of lignified plant material entering soil should be greatest at the low end of the inorganic N availability gradient. Because we observed the lowest amount of lignin-derived SOM in low inorganic N soils (Figure 3.5a), these putative differences in fine root litter inputs strengthen our conclusion that decay by ECM fungi with peroxidases regulate SOM.

Although our results are based on correlations between fungal community composition and SOM, we used these approaches to test specific *a priori* hypotheses (Figure 3.1; Prosser 2020; Lindahl *et al.* 2021). Nonetheless, experimental approaches will be required to verify the *ECM Mechanism* (Figure 3.1). For example, trenching experimentally excludes ECM fungi to isolate their role in SOM dynamics (Gadgil & Gadgil 1971; Averill & Hawkes 2016; Sterkenburg *et al.* 2018). However, given the long-term limitations of this approach (Fernandez

& Kennedy 2016), a combination of laboratory manipulations, field observations, and modeling will be required to verify the quantitative importance of ECM fungi for SOM dynamics across inorganic N availability gradients (Zak *et al.* 2019b; Bradford *et al.* 2021). An additional mechanism through which anthropogenic N deposition slows lignin decay is by reducing the expression of saprotrophic peroxidase genes (Entwistle *et al.* 2018a; Zak *et al.* 2019a), a response also observed in some ECM fungi (Bödeker *et al.* 2014). Accounting for this possibility across natural gradients of inorganic N availability should be another objective of future studies.

Together, our observations support the idea that soil C increases across a natural soil inorganic N availability gradient due to a decline in decay by ECM fungi with peroxidases (Figure 3.1, *ECM Mechanism*). Our study suggests ECM community composition and its turnover across soil N availability gradients is one control over SOM in temperate forests, and we propose that shifts in plant allocation to certain ECM fungi and environmental stress across these gradients place temperate and boreal ecosystems along a single continuum of soil N availability, ECM fungi, and SOM (Figure 3.6). We emphasize that decay by ECM fungi and its effect on soil C vary with ECM community composition and cannot be universally ascribed to all ECM communities (Figure 3.6). In addition to rising atmospheric CO_2, numerous additional drivers of environmental change alter the composition and activity of ECM communities, including anthropogenic N deposition (Lilleskov *et al.* 2002; Bödeker *et al.* 2014) and climatic shifts (Steidinger *et al.* 2020). Explicitly considering the direct decay of SOM by ECM fungi and the contingency of this process on ECM community composition may improve our ability to predict how ongoing environmental change impacts soil C storage.

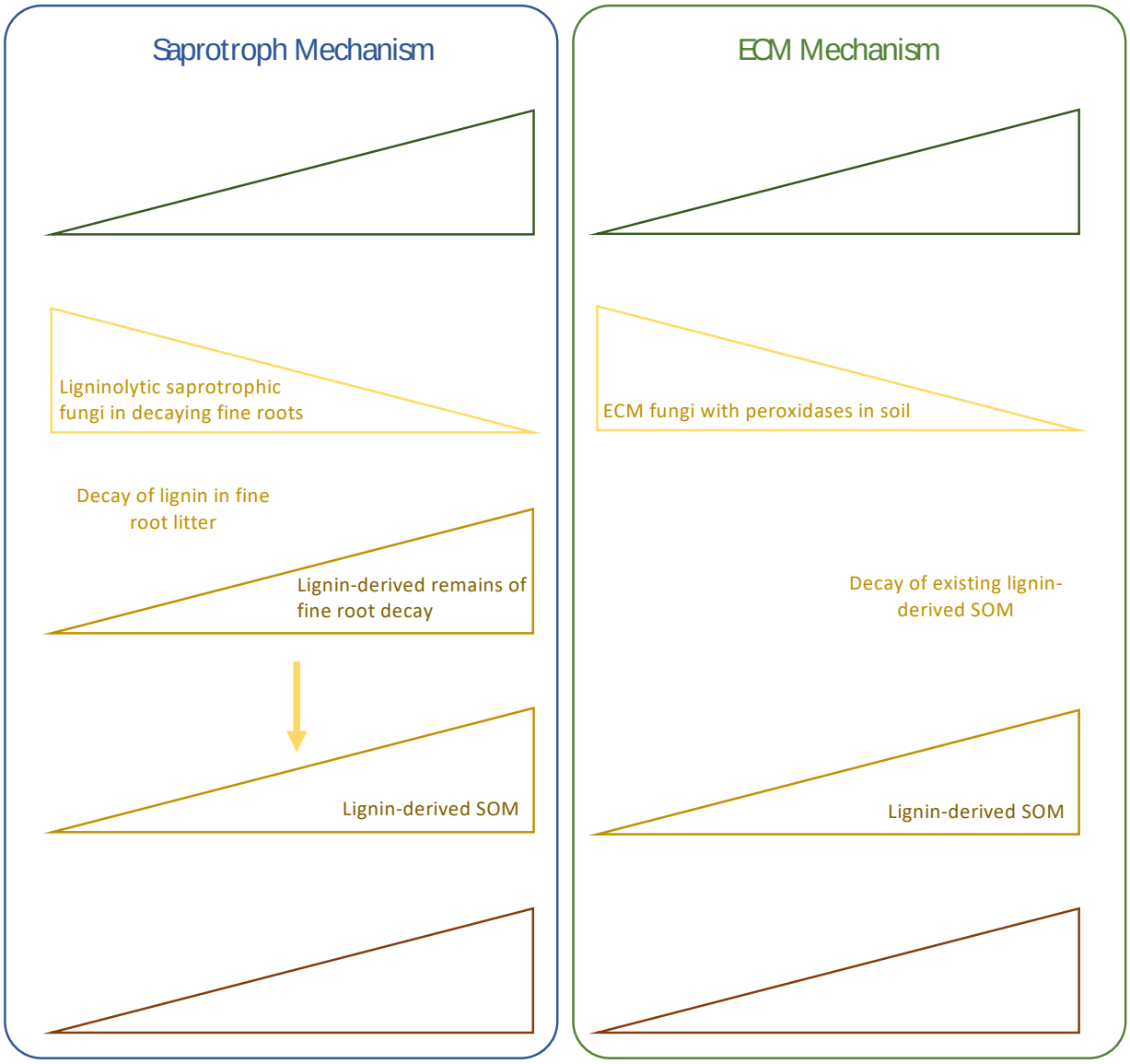

Figure 3.1: Two fungal mechanisms (*Saprotroph Mechanism* and *ECM Mechanism*) could cause naturally high inorganic N availability to suppress the decay of lignin and its derivatives, thereby promoting the accumulation of lignin-derived SOM and increasing soil C storage.

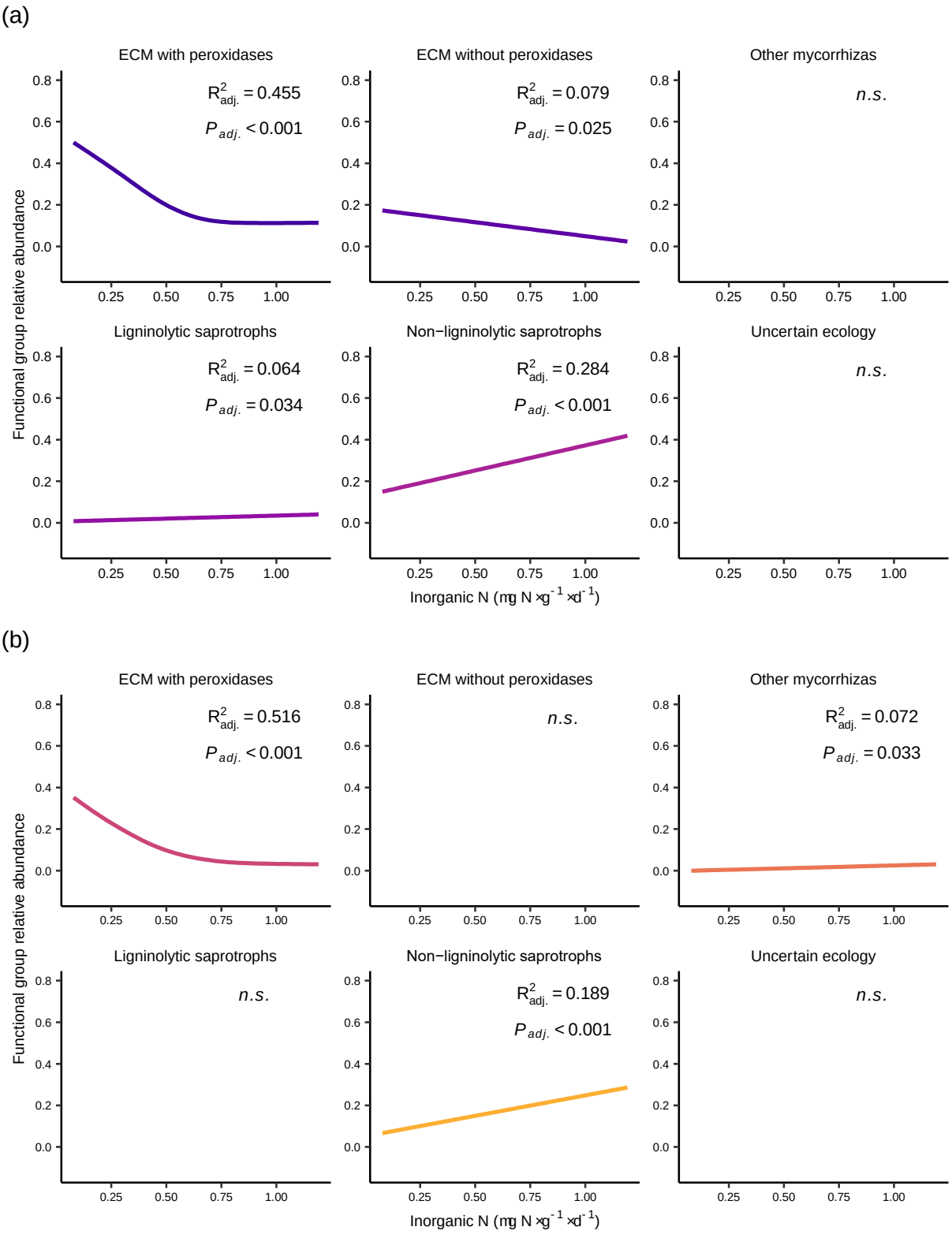

Figure 3.2: Fungal functional group responses in soil (a) and decaying fine root litter (b) across the soil inorganic N availability gradient. Each plot (and each color) represents a separate

GAMM with the relative abundance of a functional group as the dependent variable and soil inorganic N availability as the independent variable, from which trend lines, 95% confidence intervals, and R^2 were calculated. We corrected *P*-values for multiple tests using the Benjamini-Hochberg false discovery rate correction. We explicitly accounted for spatial autocorrelation in GAMM models with a spatial correlation structure based on the geographic coordinates of each plot (n = 68). *n.s.*, not significant.

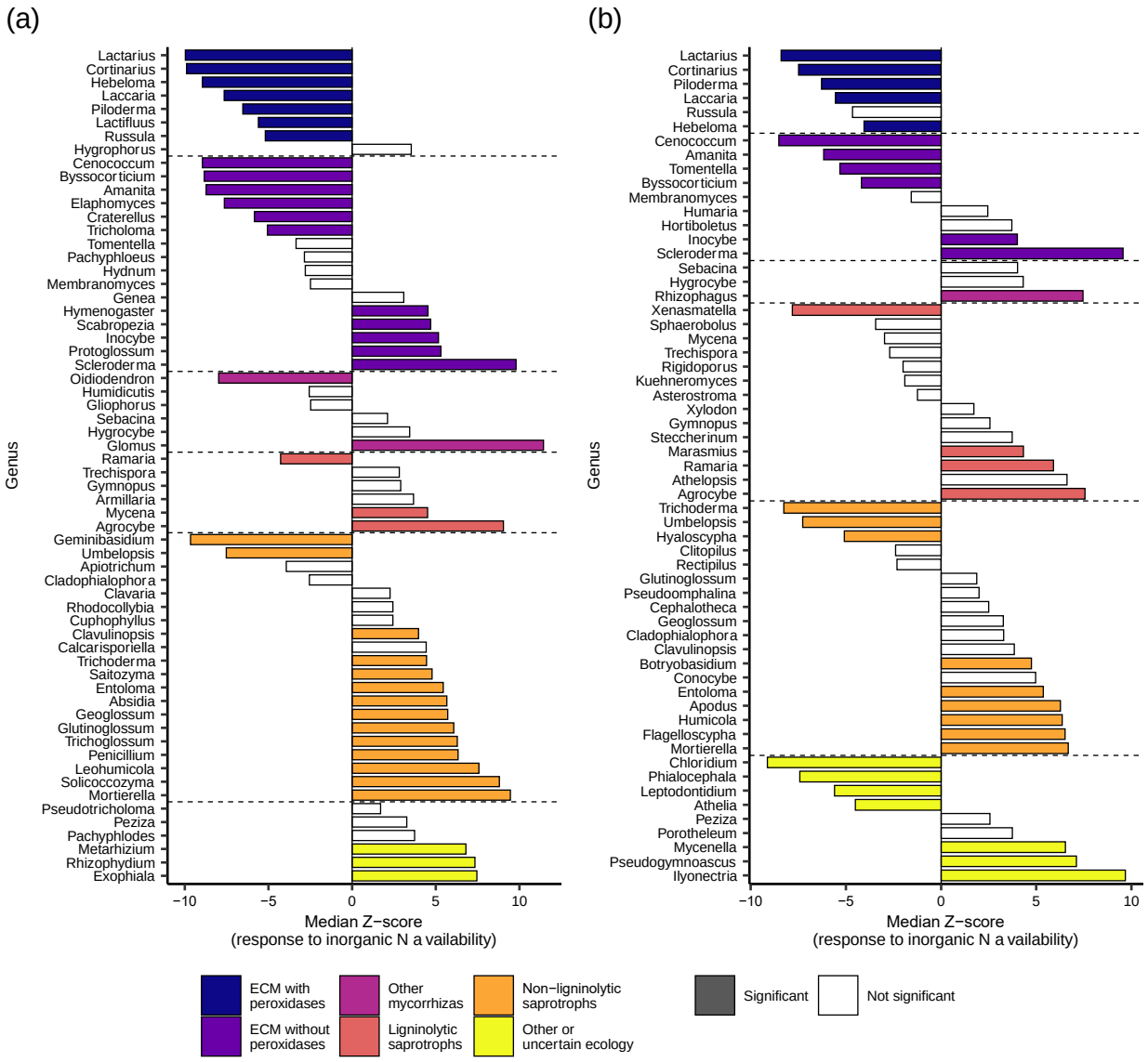

Figure 3.3: Responses to inorganic N availability for individual genera in soil (a) and fine root litter (b) determined by TITAN analysis. ECM fungal genera with peroxidases nearly universally declined in relative abundance with increasing inorganic N availability. Bars display median Z-scores (across 1000 bootstrap replicates), which represent the magnitude of the change in genus relative abundance across the gradient of inorganic N availability. Positive Z-scores indicate genera that increased with increasing inorganic N availability, whereas negative Z-scores indicate genera that decreased in relative abundance with increasing inorganic N availability. We

considered responses with booth purity and reliability ≥0.95 as statistically significant (solid bars), and < 0.95 for either purity or reliability as not significant (faded bars). Genus abundances were Hellinger-transformed prior to TITAN analysis.

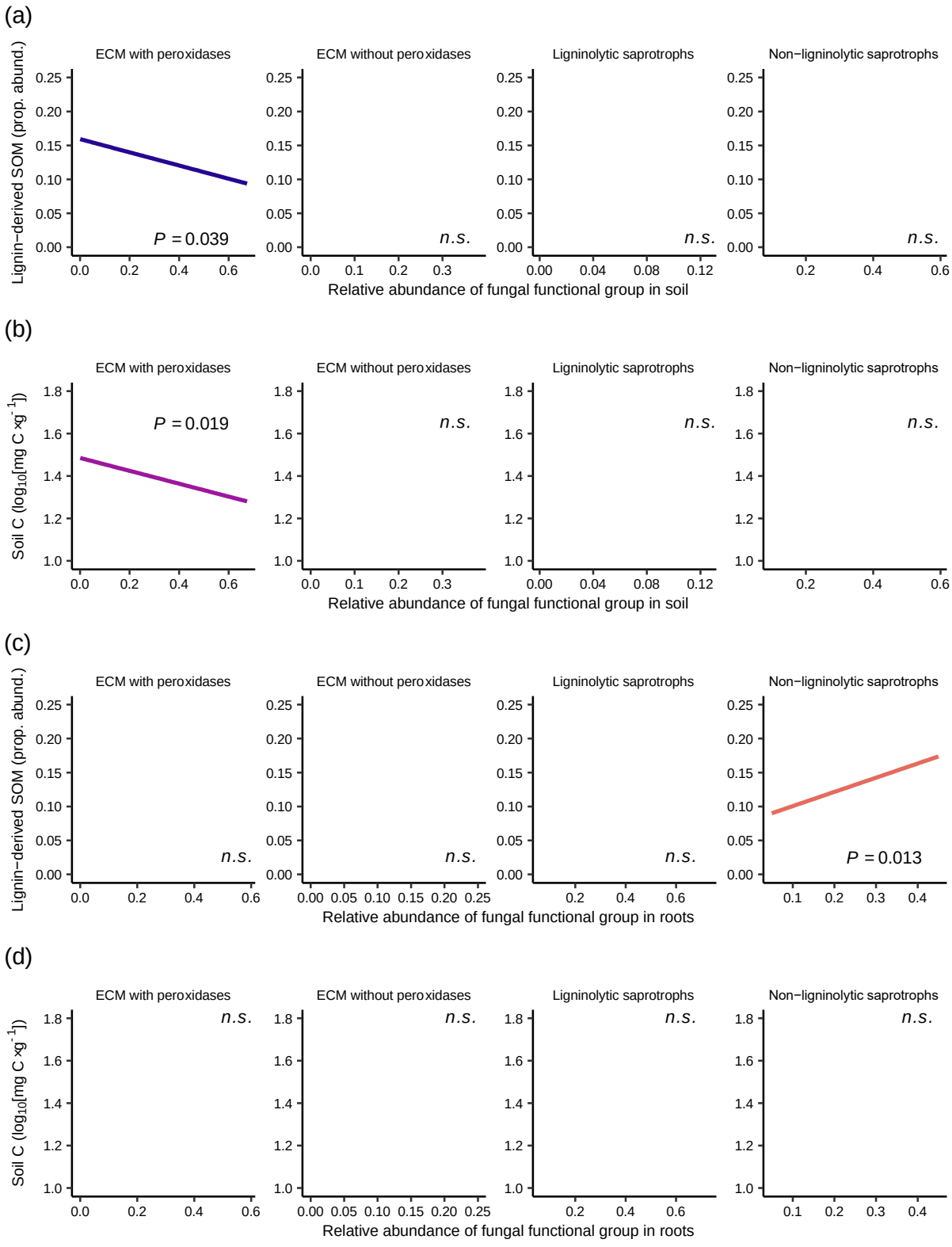

Figure 3.4: Partial plots from multiple GAMM showing relationship between lignin-derived SOM and fungal functional groups in soil (a), soil C and fungal functional groups in soil (b),

lignin-derived SOM and fungal functional groups in decaying fine roots (c), and soil C and fungal functional groups in soil (d). Each lettered panel represents a separate multiple GAMM with all functional groups as predictor variables, from which *P*-values and $R^2_{adj.}$ were calculated. Other mycorrhizas and fungi with uncertain ecology were included in the four models but are not shown (see Figure B.7). We explicitly accounted for spatial autocorrelation in GAMM models with a spatial correlation structure based on the geographic coordinates of each plot (n = 68). Trend lines and confidence intervals are for visualization purposes only.

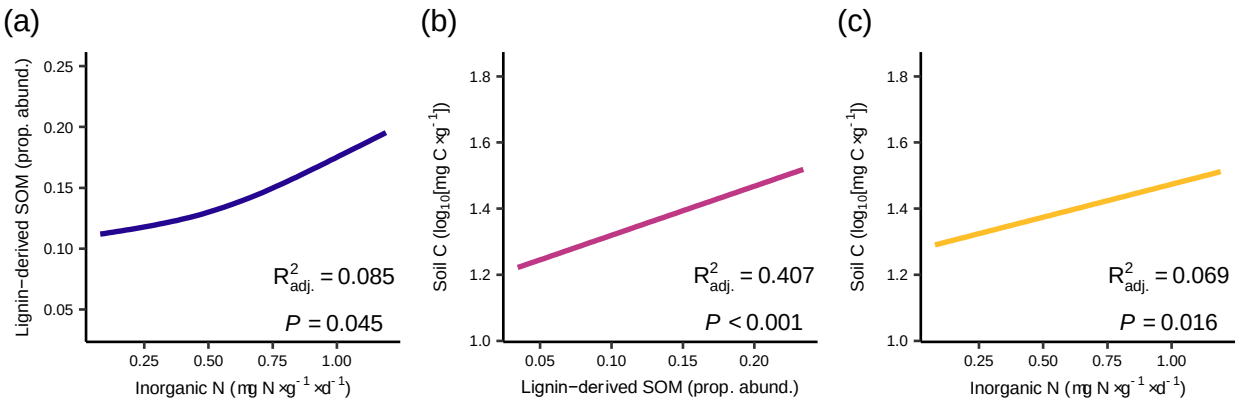

Figure 3.5: Relationships between lignin-derived SOM and inorganic N availability (a), soil C and lignin-derived SOM (b), and soil C storage and inorganic N availability (c). Each plot (and each color) represents a separate GAMM with the relative abundance of a functional group as the dependent variable and soil inorganic N availability as the independent variable, from which trend lines, 95% confidence intervals, and R^2 were calculated. We explicitly accounted for spatial autocorrelation in GAMM models among plots (n = 68) using a spatial correlation structure.

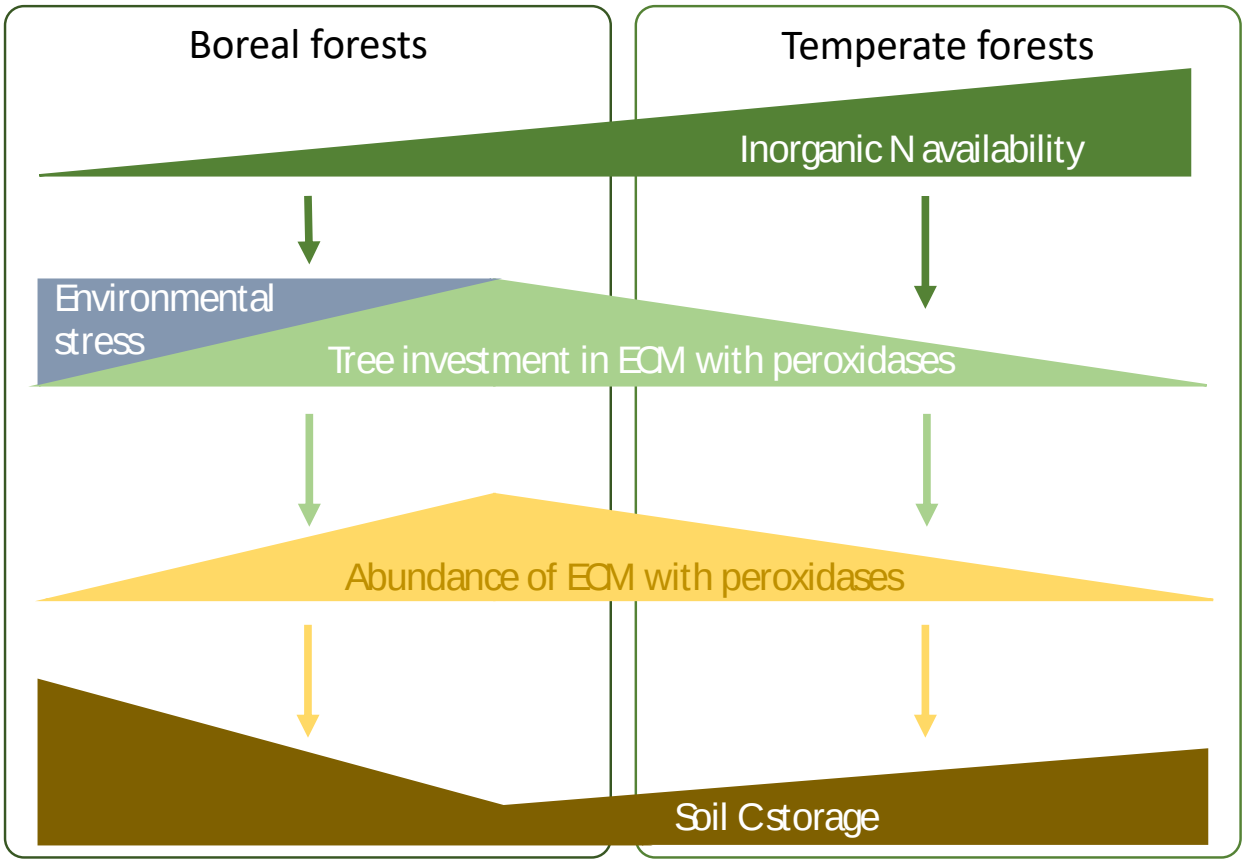

Figure 3.6: Illustration of our proposed framework unifying relationships between N availability, ECM composition, and SOM across temperate and boreal ecosystems. As inorganic N availability decreases from high fertility to low fertility temperate forests, the abundance of ECM with peroxidases increases due to increased photosynthate allocation to ECM with greater decay capacity. This shift in fungal composition increases the decay of lignin-derived SOM, thereby causing soil C storage to decline with decreasing inorganic N availability. This pattern continues into high-fertility boreal forests, until reduced productivity and increased environmental stress favor stress-tolerant ericoid mycorrhizae over ECM taxa with peroxidases. Consequently, SOM increases as inorganic N declines after this point.

CHAPTER 4

Fungal Community Composition and Genetic Potential Regulate Fine Root Decay in Northern Temperate Forests

William A. Argiroff, Donald R. Zak, Rima A. Upchurch, Peter T. Pellitier, and Julia P. Belke

Abstract

Understanding how differences in genetic potential among soil microorganisms regulates spatial patterns in litter decay remains a persistent challenge in ecology. Furthermore, despite fine root litter accounting for ~50% of total litter production in forest ecosystems, far less is known about the microbial decay of fine roots relative to aboveground litter. Here, we evaluated whether fine root decay occurred more rapidly when fungal communities in fine root litter have a greater genetic potential for litter decay. Additionally, we tested the idea that these linkages between decay and fungal genes can be adequately captured by delineating saprotrophic and ectomycorrhizal fungal functional groups based on whether they have genes encoding peroxidase enzymes, which oxidize lignin and polyphenolic compounds. We used a litterbag study paired with fungal DNA barcoding to characterize fine root decay rates and fungal community composition at the landscape scale in northern temperate forests, and we estimated the genetic potential of fungal communities for litter decay using publicly available genomes. Fine root decay occurred more rapidly where fungal communities had a greater genetic potential for decay,

especially of cellulose and hemicellulose. Fine root decay was positively correlated with ligninolytic saprotrophic fungi and negatively correlated with ECM fungi with peroxidases, likely because ligninolytic saprotrophs and ECM fungi had the highest and lowest genetic potentials for plant cell wall degradation, respectively. These fungal variables overwhelmed direct environmental controls, suggesting fungal community composition and genetic variation are primary controls over fine root decay in temperate forests.

Introduction

An important goal in ecology is to understand how genetic differences among microorganisms determine the functioning of communities and ecosystems (Zak *et al.* 2006; Fierer 2017; Hall *et al.* 2018). For example, variation in the functional genes of ectomycorrhizal (ECM) fungi modifies tree growth, coupling turnover in fungal community composition to the functioning of terrestrial ecosystems (Pellitier *et al.* 2021a; Anthony *et al.* 2022). Fungi also differ substantially in their genetic potential for the decay of plant litter (Riley *et al.* 2014; Miyauchi *et al.* 2020; Ruiz-Dueñas *et al.* 2021), an ecosystem process that broadly controls the balance of carbon between soil and the atmosphere (Schlesinger & Bernhardt 2013). However, it remains unclear whether differences in the genetic potential of soil microorganisms regulate patterns in plant litter decay across broad spatial scales (Jansson & Hofmockel 2018; Bradford *et al.* 2021).

Fungal species are often categorized into functional groups (*e.g.*, saprotrophic vs. ECM) based upon their ecological roles and functional capabilities (Nguyen *et al.* 2016; Zanne *et al.* 2020; Tanunchai *et al.* 2022). Whereas ECM fungi generally have a reduced complement of genes encoding extracellular decay enzymes relative to free-living saprotrophic fungi (Kohler *et al.* 2015; Lindahl & Tunlid 2015; Martino *et al.* 2018), both saprotrophic and ECM fungal

species span broad continuums of genetic potentials for decay (Riley *et al.* 2014; Pellitier & Zak 2018). Consequently, it remains an open question how to assign functional groups to capture fungal genetic variation that operates at ecosystem scales (Talbot *et al.* 2015; Romero-Olivares *et al.* 2021; Treseder *et al.* 2021). Because process-based ecosystem models of carbon cycling increasingly incorporate microbial functional groups (Wieder *et al.* 2018; Sulman *et al.* 2019; Bradford *et al.* 2021), delineating fungal functional groups that adequately represent links between fungal genes and spatial patterns in litter decay has important implications for our understanding of the terrestrial carbon cycle.

The presence of genes encoding class II fungal peroxidases, which fully oxidize lignin and other complex polyphenolic compounds (Kirk & Farrell 1987; Hofrichter 2002; Bödeker *et al.* 2014), could distinguish ecologically relevant groups within the broader classifications of saprotrophic and ECM fungi. "Ligninolytic" saprotrophic fungi extensively decay lignocellulose because they have large suites of genes coding for peroxidases, as well as hemicellulolytic and cellulolytic enzymes, whereas non-ligninolytic saprotrophs lack peroxidase genes required to fully decay lignified compounds (Baldrian 2008; Floudas *et al.* 2012; Riley *et al.* 2014). Similarly, only certain lineages of ECM fungi have retained peroxidases and other oxidative decay mechanisms during their evolution from saprotrophic ancestors (Bödeker *et al.* 2009; Pellitier & Zak 2018; Miyauchi *et al.* 2020). Nonetheless, genetic differences among saprotrophic and ECM fungal functional groups with and without peroxidases have not been directly linked to landscape-level patterns in plant litter decay.

Fine root litter is produced by the senescence of the smallest absorptive roots of trees (Xia *et al.* 2010; McCormack *et al.* 2015). Approximately 50% of total plant litter production in forest ecosystems is comprised of fine root litter (Freschet *et al.* 2013), and compounds derived

from the decay of fine root litter are a primary source of soil organic matter (Rasse *et al.* 2005; Jackson *et al.* 2017; Angst *et al.* 2021). Furthermore, fine root litter contains high concentrations of lignin (Xia *et al.* 2015), suggesting its decay should be particularly sensitive to whether fungi have the genetic capacity for extensive lignocellulose degradation. However, our understanding of plant litter decay and its controlling factors is based almost exclusively on the decay of aboveground litter (*i.e.*, senesced leaves and coarse woody debris; Berg *et al.* 1993; Bradford *et al.* 2016; Berg & McClaugherty 2020). Consequently, the ecological factors controlling fine root decay are an important gap in our understanding of the terrestrial carbon cycle (Berg & McClaugherty 2020).

In this study, we evaluated whether the genetic decay potential of fungal communities regulates fine root decay at the landscape scale. We measured rates of fine root decay across 12 northern temperate forest ecosystems that span environmental gradients of inorganic nitrogen (N) availability, water content, temperature, and pH (Zak *et al.* 1989; Pellitier *et al.* 2021a; Argiroff *et al.* 2022). We characterized fungal community composition in decaying fine root litter using DNA barcoding, and we used publicly available genomes to estimate the genetic potential of fungal communities for litter decay by calculating community-weighted gene abundances for plant cell wall-degrading enzymes (PCWDE; Anthony *et al.* 2022). We reasoned that fungal communities with greater genetic potential for plant litter decay should decay fine root litter more rapidly, and that higher genetic decay potential should be conferred primarily by lignin-degrading saprotrophs. ECM fungi can accelerate (Lindahl *et al.* 2021; Argiroff *et al.* 2022) or slow organic matter decay (Sterkenburg *et al.* 2018; Fernandez *et al.* 2020), and an additional objective of our study was to determine how ECM fungi with and without peroxidases specifically influenced community-level genetic decay potential and the decay of fine root litter.

Finally, because environmental conditions can alter decay by modifying microbial physiology and community composition (Bradford *et al.* 2021), we evaluated the relative importance of environmental effects versus fungal controls. Collectively, our results provide evidence that the composition and genetic potential of fungal communities are primary controls over fine root decay, which is a poorly understood component of the terrestrial carbon cycle.

Materials and Methods

Site descriptions

Our study was conducted in 72 plots distributed across 12 forest sites (6 plots per site) in northern Lower Michigan, USA (Figure C.1; Argiroff *et al.* 2022). Plots were 2-m diameter circles randomly located in even-aged (~100 year-old) second-growth northern hardwood forests that contained both *Quercus rubra* and *Acer rubrum*, and were near previously-described ECM fungal communities in *Q. rubra* root tips (Pellitier *et al.* 2021a, b; Pellitier & Zak 2021a). Climatic and certain edaphic characteristics were similar among sites due to relatively close proximity (separated by <50 km) and uniform soil texture (>85% sand; Zak *et al.* 1989; Zak & Pregitzer 1990). However, microsite differences in topography have produced variation in nutrient retention and microclimates among and within sites, which have resulted in seasonally and interannually consistent differences in soil inorganic N availability, water content, temperature, and pH within and among sites (Figure C.2; Zak *et al.* 1989; Zak & Pregitzer 1990; Pellitier *et al.* 2021a; Argiroff *et al.* 2022).

Fine root decay

In May 2018, we collected five soil cores with a rectangular corer (12-cm × 12-cm) to a depth of 10 cm around five *Q. rubra* individuals at each site. We transported cores to the University of Michigan on ice and stored them at -20 °C. We thawed the cores, rinsed roots free of adhering soil particles, and obtained fine roots ≤0.5 mm in diameter. We dried the roots at 65 °C for 48 hours, combined them at the site level, and ground a subsample with a ball mill for the determination of un-decayed fine root biochemistry. The diameter cutoff of ≤0.5 mm retained primarily first- through third-order fine roots, which belong to absorptive fine root modules that undergo rapid turnover and comprise most fine root litter produced by trees (Xia *et al.* 2010; McCormack *et al.* 2015). Furthermore, because *Q. rubra* occurs as dominant overstory trees in all sites, the roots we collected represent a large portion of fine root litter in these ecosystems.

We placed ~3 g fine root litter from the appropriate site into 12-cm × 12-cm nylon mesh litterbags (12 sites × 6 plots × 2 bags = 144 total litterbags) with 53 μm openings, which permit the ingrowth of fungal hyphae but exclude new fine roots (Hobbie *et al.* 2010; Li *et al.* 2015; Sun *et al.* 2018). We sterilized the litterbags using ethylene oxide (Cline & Zak 2015), and placed two litterbags per plot within the zone of greatest fine root density (~3 cm depth; Figure C.3; See *et al.* 2019). We collected the litterbags after 13 months (May 2019 – July 2020), transported them on ice to the University of Michigan, homogenized the roots by plot, and weighed them. We obtained a subsample of the decaying roots for the immediate measurement of extracellular enzyme activities, and we stored a subsample at -80 °C for characterization of fungal community composition. A subsample was oven-dried at 60 °C to determine moisture content for mass loss measurements, a portion of which was ashed at 500 °C for 6 hours to measure mineral content.

We calculated fine root decay as the proportion of initial ash-free dry mass lost over the 13-month field incubation.

Fungal DNA barcoding

We isolated and purified DNA from 0.15 g (three 0.05 g subsamples) of decaying fine roots from each plot (n = 72) using the DNeasy Plant Mini Kit and DNeasy PowerClean CleanUp kit (Qiagen) following modified manufacturer's protocols (Supporting Methods C.1; Argiroff *et al.* 2022). We amplified the ITS2 region of the universal fungal DNA barcode (*i.e.*, the ribosomal internal transcribed spacer; Schoch *et al.* 2012; Nilsson *et al.* 2019a) using PCR with ITS4-Fun/5.8S-Fun primers (Table C.1 and Supporting Methods C.1; Taylor *et al.* 2016; Pellitier *et al.* 2019). sequenced using MiSeq 2 × 250 bp with v2 chemistry (Illumina) by the University of Michigan Microbiome Core. We determined the copy number of fungal ITS amplicons in decaying fine root litter using quantitative PCR (qPCR) and the ITS1F/5.8S primers following Entwistle *et al.* (2018b).

We obtained high quality fungal sequences and determined amplicon sequence variants (ASVs; Callahan *et al.* 2017; Pauvert *et al.* 2019) from forward reads using DADA2 (Rosen *et al.* 2012; Callahan *et al.* 2016) paired with ‘cutadapt’ (Martin 2011). We assigned taxonomic classifications to sequences with the UNITE database (Kõljalg *et al.* 2013; Nilsson *et al.* 2019b) using the naïve Bayesian classifier (Wang *et al.* 2007) implemented in DADA2. We did not subsample sequence counts to avoid data loss and uncertainty (McMurdie & Holmes 2013, 2014).

Genetic potential for decay

To understand if fine root decay was related to the genetic decay potential of fungal communities, we first estimated genomic decay traits for abundant genera assigned to functional groups (see below) in decaying fine root litter using sequenced genomes in the MycoCosm genome portal (Grigoriev *et al.* 2014) following Anthony *et al.* (2022). For each genome, we obtained gene copy numbers for 58 plant cell wall degrading enzyme (PCWDE) gene families (Ruiz-Dueñas *et al.* 2021) annotated using the CAZy database (Table C.2; Levasseur *et al.* 2013; Lombard *et al.* 2014). We then calculated copy numbers of each PCWDE family per 10,000 genes in the genome to correct for differences in genome size (Treseder & Lennon 2015; Romero-Olivares *et al.* 2021; Anthony *et al.* 2022). 27 of 50 abundant genera belonging to the four focal functional groups (ligninolytic saprotrophs, non-ligninolytic saprotrophs, ECM with peroxidases, and ECM fungi without peroxidases) matched at least one sequenced genome and were assigned decay traits, which accounted for 81% of sequences assigned to the four focal functional groups and 56% of sequences overall (Table C.3). We inferred the community-level genetic potential for plant litter decay in each plot by averaging the genes for each PCWDE per genome at the genus level, and subsequently calculating community-weighted mean gene copies for each PCWDE based on the relative abundance of each genus (Anthony *et al.* 2022).

Fungal functional groups

We assigned functional groups to all classified genera present in ≥5 plots and representing ≥0.1% of sequences (Table C.4) using the approach described by Argiroff *et al.* (2022). Specifically, we identified ECM fungal genera with peroxidases by using the literature to determine if species within each genus possess verified class II peroxidase genes (Bödeker *et al.*

2009; Kohler *et al.* 2015; Nagy *et al.* 2016; Miyauchi *et al.* 2020). We identified ligninolytic saprotrophic fungal genera using FUNGuild (Nguyen *et al.* 2016) and literature (Entwistle *et al.* 2018b; Ruiz-Dueñas *et al.* 2021). Because class II peroxidases evolved in the most recent common ancestor of Auriculariales and more recently diverging Agaricomycetes (Floudas *et al.* 2012; Nagy *et al.* 2016; Ruiz-Dueñas *et al.* 2021), we designated all ECM and saprotrophic fungi outside of these lineages as "ECM fungi without peroxidases" and "non-ligninolytic saprotrophs". "Other mycorrhizas" and "fungi with other or uncertain ecology" were identified with FUNGuild and literature (Smith & Read 2010; Seitzman *et al.* 2011; Martino *et al.* 2018), but were excluded from analyses because they together comprised a much smaller proportion of fungal sequences (<4%). Absolute abundances of these functional groups were calculated by multiplying relative abundances (*i.e.*, the proportion of fungal sequences) by ITS copy number as quantified by qPCR (*sensu* Clemmensen *et al.* 2015) and subsequently used in all analyses.

Enzymatic potential for decay

We used ~0.5 g of decaying root litter and previously described methods (Saiya-Cork *et al.* 2002; Cline & Zak 2015) to measure the potential activity of five extracellular enzymes involved in litter decay. We assayed β-1,4-glucosidase and cellobiohydrolase to determine the enzymatic potential for cellulose decay, phenol oxidase and peroxidase to determine the potential for lignin decay, and N-acetyl-β-glucosaminidase, which is involved in the turnover and remodeling of fungal biomass (Baldrian 2008). We used 200 μM methylumbelliferyl-linked substrates to fluorometrically determine potential activities of β-1,4-glucosidase, cellobiohydrolase, and N-acetyl-β-glucosaminidase. We used 25-mM L-dihydroxy-phenylalanine to measure phenol oxidase and peroxidase activities based on absorbance.

Environmental variables

We collected 6 2.5-cm diameter soil cores at each plot to a depth of 10 cm in May, 2019 at litterbag deployment, and transported the cores on ice to the University of Michigan. We passed the soil through a 2-mm sieve, removed visible fine roots by hand, and homogenized the soil by plot, resulting in 72 soil samples. Two 30 g subsamples were used for 28-day net N mineralization assays (Vitousek *et al.* 1982; Zak *et al.* 1989) to determine soil inorganic N availability, which reflects *in situ* inorganic N availability (Zak *et al.* 1989; Zak & Pregitzer 1990) and N in root litter and soil organic matter (Figure C.4). A subsample was oven-dried at 105 °C for 24 hours, ground to a fine powder in a ball mill, and used to determine soil C and N with a CN analyzer (LECO). Sieved soil was air-dried for the determination of soil pH in slurries of 30 g of soil and 30 mL deionized water. We characterized the biochemistry of un-decayed fine root litter using pyrolysis gas chromatography-mass spectrometry (py-GC/MS; Supporting Methods C.1; Pold *et al.* 2017) to determine the relative abundance of aromatics, lignin, lipids, N-bearing, phenols, polysaccharides, proteins, and unknown origin.

We measured the mean of hourly soil volumetric water content and temperature during the growing season (May 1 to October 31, 2019, and May 1 to June 31, 2020) using a Micro Station data logger (ONSET) at each site. We interpolated values for each plot by regressing plot-level measurements (n = 4) taken through the period of decay with hand-held probes against nearest logger values. Water content was calculated as the number of days the daily mean volumetric water content was ≥80% of field capacity, the threshold above which soil microbial activity is at its maximum in these ecosystems (Zak *et al.* 1999).

Statistical analyses

We used the 'TITAN2' package (Baker & King 2010) to identify PCWDE gene families whose estimated community-weighted mean abundances were associated with more rapid fine root decay. We treated PCWDE gene families as species abundances and fine root decay rates as an environmental gradient. PCWDE gene families were considered significantly associated with rapid fine root decay if they had purity and reliability values ≥0.95 and positive Z-scores (Baker & King 2010). We used one-way ANOVA and Tukey's HSD to test differences in the summed gene counts of PWDEs among fungal functional groups. We used generalized additive mixed models (GAMMs) to test the relationships between continuous variables. GAMMs, which accommodate complex nonlinear relationships that may arise in ecological datasets, were implemented in the R package 'mgcv' (Wood 2011). We included a spatial correlation structure to account for the fact that plots within a site are closer together than plots between sites. We elected to keep plots separate in all analyses to avoid data loss and mean inference fallacies caused by data aggregation at the site level (Bradford *et al.* 2021), and because fine root decay rates and environmental conditions varied considerably both within and among sites (Figures C.2 and C.5). We removed 2 plots from all analyses, one in which mass loss was over 4 standard deviations greater than the mean root decay rate and one for which the net N mineralization assay failed, for a total $n = 70$ plots. Response variables for GAMMs were $\log_{10}$-transformed to ensure residuals were normally distributed. Fungal and environmental variables were standardized to mean = 0 and standard deviation = 1 before inclusion as predictors in GAMMs (Maynard *et al.* 2018). We accepted statistical significance at $\alpha = 0.05$, and we performed all statistical analyses using R version 4.1.2 (R Core Team 2018) and RStudio version 2021.9.0+351

(RStudio Team 2018), with the 'phyloseq' (McMurdie & Holmes 2013), 'ShortRead' (Morgan *et al.* 2009), 'biostrings' (Pagès *et al.* 2020), and 'tidyverse' (Wickham *et al.* 2019) packages.

Results

Genetic decay capacity and fine root decay

Twenty-four gene families were significantly related to fine root decay based on TITAN2 analysis, 23 of which were associated with more rapid decay rates (Figure 4.1a). We used a multiple GAMM to determine if fine root decay was predicted by the community-level abundance of PCWDEs, using this estimate of genetic decay potential and four soil environmental conditions (inorganic N availability, water content, temperature, and pH) as independent variables. Fine root decay increased with an increasing community-level abundance of PCWDEs ($R^2_{adj.} = 0.138$, $P = 0.032$; Figure 4.1b), and was unrelated to any environmental variable ($P > 0.05$; Figure C.6a and Table C.5). In a second GAMM using PCWDEs specifically associated with rapid root decay, fine root decay was positively correlated with the community-level abundance of these rapid decay PCWDEs ($R^2_{adj.} = 0.179$, $P = 0.005$; Figure 4.1c) and was unrelated to the environment ($P > 0.05$; Figure C.6b and Table C.5).

Genetic decay capacity and fungal functional groups

Fungal communities in decaying fine root litter consisted primarily of ligninolytic saprotrophic genera (33% of fungal sequences) such as *Mycena* and other Basidiomycota, followed by non-ligninolytic saprotrophs (15%), ECM with peroxidases (14%), and ECM without peroxidases (6%; Figures C.7-C.8 and Tables C.6-C.7; see Table C.8 for a summary of sequencing effort). We used ANOVA to compare genome-level differences in genetic potential for litter decay

between fungal functional groups (Figure 4.2a). Gene copies belonging to PCWDEs were most abundant in genomes of lignin-degrading saprotrophic fungi, followed by non-ligninolytic fungal saprotrophs, and both ECM functional groups ($P < 0.05$; Figure 4.2a). Gene copies belonging to PCWDEs associated with rapid fine root decay were also most abundant in genomes of lignin-degrading saprotrophic fungi, followed by non-ligninolytic fungal saprotrophs, and both ECM functional groups ($P < 0.05$; Figure 4.2a).

We then used two multiple GAMMs to understand the fungal and environmental determinants of community-level genetic decay potential (Figure 4.2b-c). The summed community-weighted mean abundance of all PCWDEs was positively correlated with the abundance of lignin-degrading fungi and negatively correlated with the abundance of ECM fungi with peroxidases, together accounting for 52% of the variance in genetic decay capacity ($R^2_{adj.} = 0.516$, $P < 0.001$; Figure 4.2b). Similarly, the summed abundance of PCWDEs associated with rapid fine root decay was positively correlated with lignin-degrading fungi and negatively correlated with ECM fungi with peroxidases, accounting for 60% of the variance in genetic decay capacity ($R^2_{adj.} = 0.601$, $P < 0.001$; Figure 4.2c). Neither community-level estimate of genetic decay potential was related to non-ligninolytic saprotrophs, ECM fungi without peroxidases, or environmental conditions ($P > 0.05$; Figures 4.2b-c, Figure C.9, and Table C.9).

Enzyme activities and fungal functional groups

We assayed the potential activity of cellulolytic and ligninolytic enzymes, as well as N-acetyl-β-glucosaminidase, to understand whether shifts in fungal composition corresponded to differences in the activity of these decay enzymes (Figures C.10-C.12, Table C.10). Although cellulolytic enzymes were not related to the abundance of ligninolytic saprotrophic fungi (Figures C.10a),

ligninolytic enzyme activity and N-acetyl-β-glucosaminidase were positively correlated with the abundance of ligninolytic saprotrophs (Figures C.11 and C.12a, Table C.10).

Fine root decay and fungal functional groups

We used one GAMM with fine root decay as the response variable and four fungal functional groups and four environmental variables as predictors to understand how fine root decay was related to fungal community composition and the environment (Figure 4.3). Fine root decay was significantly positively correlated with the abundance of ligninolytic fungi and negatively correlated with the abundance of ECM fungi with peroxidases ($R^2_{adj.} = 0.365$, $P < 0.01$; Figure 4.3a and Table C.11). Although fine root decay was negatively correlated with non-ligninolytic saprotrophic fungi ($P = 0.015$; Figure 4.3a) and soil water content ($P = 0.037$; Figure 4.3b), these relationships were driven by a small number of plots and were likely spurious. Fine root decay was unrelated to ECM fungi without peroxidases ($P = 0.29$; Figure 4.3a and Table C.11), as well as to soil inorganic N availability, temperature, and pH ($P > 0.05$; Figure 4.3b and Table C.11).

Relationships between fungal functional groups and the environment

To understand how environmental conditions may indirectly influence fine root decay by modifying fungal community composition, we used a separate multiple GAMM to predict the abundance of each fungal functional group from four environmental variables (Figure 4.4). The abundance of lignin-degrading saprotrophs declined with increasing soil pH and exhibited a weak unimodal relationship with soil water content ($R^2_{adj.} = 0.260$, $P < 0.05$; Figure 4.4 and Table C.12). Similarly, non-ligninolytic saprotrophs were weakly unimodally related to water content ($R^2_{adj.} = 0.130$, $P < 0.05$; Figure 4.4 and Table C.12). ECM fungi with peroxidases

declined as soil inorganic N availability and soil pH increased ($R^2_{adj.}$ = 585, $P < 0.05$; Figure 4.4 and Table C.12). ECM fungi without peroxidases were positively correlated with soil temperature ($R^2_{adj.}$ = 0.107, $P < 0.05$; Figure 4.4 and Table C.12).

Discussion

Our study addresses a long-standing goal in microbial ecology, which is to understand how the composition of microbial communities and their genetic differences regulate ecosystem functioning (Fierer 2017; Hall *et al.* 2018). Traditional ecological theory assumes environmental conditions and litter biochemistry control litter decay rates across broad spatial scales by uniformly regulating the physiology of microbial communities, irrespective of differences in microbial traits and interactions (Berg *et al.* 1993; Bradford *et al.* 2016; Berg & McClaugherty 2020). This paradigm has been challenged by growing evidence that the decay of leaf litter and woody debris can respond to differences in microbial community composition in ways that are not predicted by the environment alone (Glassman *et al.* 2018; Maynard *et al.* 2018; Smith & Peay 2021). However, the mechanisms through which microbial composition regulates litter decay have remained unclear, limiting our ability to accurately structure and parameterize biogeochemical models that predict how the terrestrial carbon cycle will respond to ongoing environmental change (Bradford *et al.* 2021). Our findings begin to address this knowledge gap by demonstrating that landscape-level patterns in fine root decay are correlated with the abundance of ligninolytic saprotrophic fungi and ECM fungi with peroxidases (Figure 4.3), and that these links between composition and function are underpinned by differences in the community-level genetic potential for litter decay (Figures 4.1-4.2).

Fine root decay was related to the genetic potential of fungal communities for plant cell wall degradation, occurring more rapidly where the community weighted mean abundance was greater for all PCWDE genes and rapid decay associated PCWDE genes (Figure 4.1b-c). Somewhat surprisingly – given the lignin-rich biochemistry of fine root litter (Figure C.13; Xia *et al.* 2015) – the gene families associated with rapid root decay did not include peroxidases (CAZyme family "AA2") and were instead primarily involved in the decay of cellulose and hemicellulose (Figure 4.1a). Cellulose and hemicellulose metabolism occurs more extensively than the oxidation of lignin in earlier stages of litter decay (Talbot & Treseder 2012; Berg 2014; Berg & McClaugherty 2020), plausibly explaining why genes involved in the depolymerization of these compounds regulated the relatively early stages of fine root decay (~13 months) we observed. However, peroxidases likely still enabled ligninolytic saprotrophic fungi to access cellulose and hemicelluloses occluded by lignin polymers (Baldrian 2008; Talbot *et al.* 2012), which could have contributed to the positive correlation between decay and ligninolytic saprotrophs (Figure 4.3a). Predicting community level phenotypes of soil microbes from functional gene abundances has remained a persistent challenge (Jansson & Hofmockel 2018). While it is important to recognize that our findings are based on estimates of functional gene abundances from genomes matching only a portion of fungal sequences (56%) at the genus level, sour study provides new evidence that fine root decay is coupled to the abundance of key cellulolytic and hemicellulolytic PCWDE genes in fungal communities.

Links between fine root decay and genetic potential (Figure 4.1) corresponded to shifts in the abundance of fungal functional groups (Figures 4.2-4.3). We found that ligninolytic saprotrophic fungi, which are abundant members of fungal communities in decaying roots (Figures C.7-C.8; Kohout *et al.* 2018; Philpott *et al.* 2018; Argiroff *et al.* 2019), had the most

gene copies of all PCWDEs and those associated with rapid fine root decay in their genomes (Figure 4.2a). Although this finding aligns with previous genomic evidence (Floudas *et al.* 2012; Riley *et al.* 2014; Nagy *et al.* 2016), our results provide new insights into the consequences of these genomic differences at the community and ecosystem levels. Specifically, the community-level genetic potential for fine root decay was greater where ligninolytic fungi were more abundant (Figure 4.2b-c), plausibly explaining the positive correlation between fine root decay and ligninolytic fungi we observed (Figure 4.3a). Similarly, ECM fungi with peroxidases had the fewest copies of PCWDEs associated with rapid root decay in their genomes (Figure 4.2a), which is consistent with the large contractions in hydrolytic enzyme-encoding genes revealed by previous genomic analyses (Kohler *et al.* 2015; Martino *et al.* 2018; Miyauchi *et al.* 2020). We found that both the genetic potential for litter decay and rates of fine root decay were negatively correlated with the abundance of ECM fungi with peroxidases (Figures 4.2-4.3), suggesting genomic characteristics of ECM fungi also operate at community and ecosystem scales to influence landscape-level patterns in fine root decay.

The composition of ECM fungal communities may influence soil organic matter dynamics (Frey 2019; Zak *et al.* 2019b), and our findings suggest functional differences among ECM lineages are particularly important for fine root decay. ECM fungi can slow the decay of plant litter by competing with free-living saprotrophic fungi (Fernandez & Kennedy 2016), which mediate the majority of litter decay (Lindahl & Tunlid 2015; Starke *et al.* 2021). ECM fungi with greater decay capacity are thought to more extensively compete with saprotrophic fungi (Fernandez *et al.* 2020), which may explain why fine root decay was negatively correlated with ECM fungi with peroxidases (Figure 4.3a) but was unrelated to ECM fungi without peroxidases (Figure 4.3a). Interestingly, we previously found that ECM fungi with peroxidases

directly accelerated the decay of soil organic matter in these ecosystems (Argiroff *et al.* 2022). Consequently, ECM fungi with peroxidases appear to slow the early stages of root litter decay (Figure 4.3a) but accelerate the decay of older soil organic matter (Argiroff *et al.* 2022). These stage-dependent effects of ECM fungi on decay have been observed in boreal forests (Sterkenburg *et al.* 2018), and our results suggest they control spatial variation in soil organic matter dynamics within temperate forest ecosystems.

The presence of peroxidases distinguished ecologically relevant groups within the broader classifications of saprotrophic and ECM fungi (Figures 4.2-4.3), which has important implications for incorporating gene-to-ecosystem mechanisms into process-based models of carbon cycling. Microbe-explicit processes can improve ecosystem carbon models, but distilling the immense taxonomic and functional diversity of soil microbial communities to support these models remains an important challenge (Wieder *et al.* 2015, 2018; Bradford *et al.* 2021). We found that the division of fungal genera into ligninolytic saprotrophs, non-ligninolytic saprotrophs, ECM fungi with peroxidases, and ECM fungi without peroxidases, accounted for 44-47% of the variation in genome-level PCWDE abundance (Figure 4.2a), 52-60% of the community-level abundance of these PCWDEs (Figure 4.2b-c), and 37% of the variation in fine root decay (Figure 4.3). Moreover, community-level genetic variation and fine root decay were primarily correlated with ligninolytic saprotrophs and ECM with peroxidases, but weakly related to or uncorrelated with non-ligninolytic saprotroph and ECM fungi without peroxidases (Figures 4.2-4.3). Consequently, the abundances of these four functional groups can be adequate proxies for mechanistic links between fungal genetic potential and the decay of fine root litter as fine root decay is incorporated into ecosystem carbon models.

Extracellular enzyme activities provided complementary evidence that shifts in the abundance of fungal functional groups regulated fine root decay (Figures C.10-C.12 and Table C.10). Cellulolytic enzyme activity was not related to the abundance of ligninolytic saprotrophs (Figure C.10a). However, ligninolytic enzyme activity was positively correlated with the abundance of ligninolytic saprotrophic fungi (Figure C.11a), indicating lignin degradation by this functional group could contribute to more rapid root decay. N-acetyl-β-glucosaminidase activity was positively correlated with the relative abundance of ligninolytic saprotrophic fungi (Figure C.12a). This chitin-depolymerizing enzyme is involved in the remodeling and recycling of fungal cell walls (Baldrian 2008), and its correlation with ligninolytic saprotrophic fungi could reflect that this fungal functional group was undergoing more rapid growth and turnover than others in our study. Enzyme activities are sometimes related to rates of decomposition and soil carbon cycling (Chen *et al.* 2018), but this is not always the case (Sorouri & Allison 2022). Our findings suggest that the genetic potential for litter decay can be a better predictor of links between fungal composition and fine root decay rates in temperate forests (Figures 4.1-4.3), but that extracellular enzyme activities also captured certain dynamics that genetic data did not (*e.g.*, lignin degradation; Figures C.11a and C.12a).

Environmental controls over fine root decay are often weaker and more variable than for the decay of aboveground litter (Beidler & Pritchard 2017; See *et al.* 2019; Wambsganss *et al.* 2021), and our results suggest these patterns may arise because fungal community composition and genetic variation overwhelm the direct effects of the environment on fine root decay. Unlike the abundance of fungal functional groups and genetic decay potential, which accounted for 14-37% of the variation in decay rates we observed (Figures 4.1 and 4.3), the environmental variables we measured did not directly predict fine root decay (Figure 4.4). Fine root decay was

likely positively correlated with the abundance of ligninolytic fungi (Figure 4.3a) because they are the only microbes with the genetic capacity to simultaneously and completely decaying lignin, cellulose, and hemicelluloses (Kirk & Farrell 1987; Hofrichter 2002; Baldrian 2008). Similarly, fine root decay likely decreased with increasing abundances of ECM fungi with peroxidases (Figure 4.3a) because resource limitation of saprotrophic growth is greater for lignin-rich litter and competitive suppression by ECM is stronger (Smith & Wan 2019; Fernandez *et al.* 2020). We propose that the uniquely high lignin concentrations of fine roots (Figure C.13; Xia *et al.* 2015) cause their decay to depend more heavily on the composition of fungal communities than environmental effects on overall community activity. Consequently, environmental effects on decay appear to be indirectly propagated through their influence on fungal composition, such as the negative effect of soil pH on ECM fungi with peroxidases and ligninolytic saprotrophs and the negative effect of inorganic N availability on ECM fungi with peroxidases (Figure 4.4).

An important limitation of this study is that our results are based on correlations between fine root decay, genetic potentials, fungal community composition, and the environment. Although we tempered this limitation by addressing specific hypotheses (Prosser 2020; Lindahl *et al.* 2021), it will be important to experimentally manipulate the composition of fungal communities to explicitly test its role in regulating fine root decay (Glassman *et al.* 2018; Sterkenburg *et al.* 2018; Smith & Peay 2021). Additionally, although it is nearly impossible to estimate fine root mass loss without using a litterbag approach, this method inherently removes endophytic taxa that are important initial inhabitants of decaying fine root litter (Kohout *et al.* 2018, 2021). The presence of fungal endophytes can modify community assembly and litter decay through priority effects (Cline *et al.* 2018). Because the composition of root endophytes

varies among our study sites (Pellitier & Zak 2021b), it is possible that we did not capture the full extent to which fungal community composition and genetic decay potential influences fine root decay. Finally, although we found that fungal genes and functional group abundances were the primary determinants of fine root decay, these fungal variables accounted for <40% of variation in decay rates (Figures 4.1-4.3). Differential expression of peroxidases and other genes encoding PCWDEs can also control decay rates (Entwistle *et al.* 2018a; Zak *et al.* 2019a), and it is possible that accounting for gene expression along with genetic potential and functional group abundances will increase explanatory power.

Together, our findings revealed that variation in the abundance of ligninolytic saprotrophs and ECM fungi with peroxidases regulated spatial patterns in fine root decay by modifying the genetic potential of fungal communities for plant cell wall degradation (Figures 4.1-4.3). These results improve our understanding of a poorly resolved component of the terrestrial carbon cycle (Berg & McClaugherty 2020) by demonstrating the fungal community composition and genetic variation are primary controls over fine root decay in northern temperate forests. An important goal in microbial ecology is to understand the mechanisms that couple microbial community composition to soil biogeochemistry (Fierer 2017), and our work addresses this knowledge gap by demonstrating that shifts in fungal community composition control fine root decay by determining the abundance of key genes encoding cellulolytic and hemicellulolytic enzymes (Figures 4.1-4.3). Finally, models of soil carbon cycling increasingly include microbial functional groups, traits, and interactions (Bradford *et al.* 2021). We found that fungal composition and genetic variation overwhelmed the direct effects of the environment on fine root decay (Figures 4.3, C.6, and C.9), and instead indirectly coupled environmental conditions to the decay of fine root litter (Figure 4.4). Thus, models based on fungal functional

groups will be essential to understanding how ongoing environmental change modifies fine root decay, a globally important process that is central to the cycling and storage of carbon in soil.

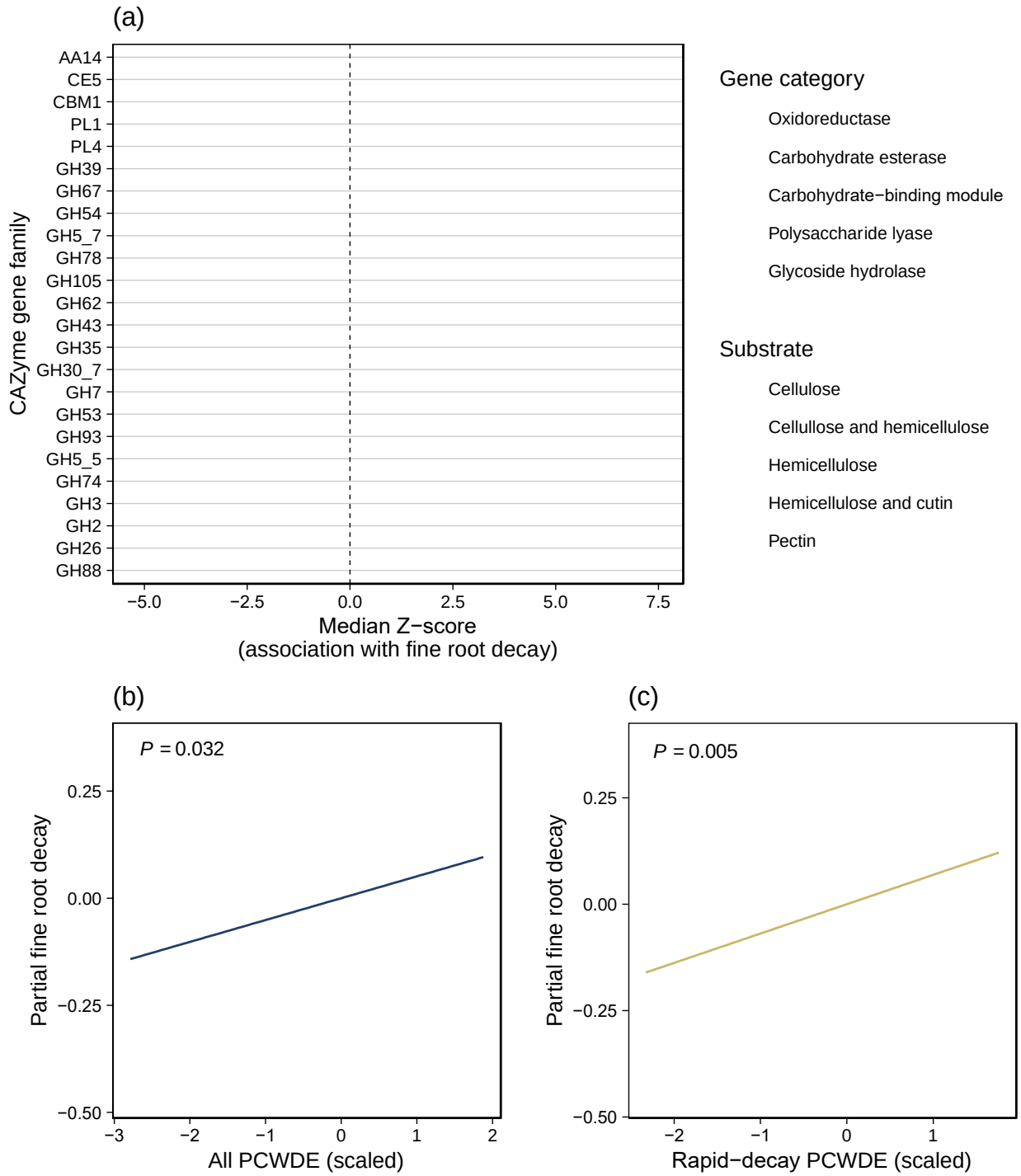

Figure 4.1: Association between the community-weighted mean values of plant cell wall degrading enzyme (PCWDE) gene families and fine root decay determined by TITAN analysis (a). 23 of 24 statistically significant gene families were associated with more rapid fine root decay. Points indicate median Z-scores (across 1000 bootstrap replicates), which represent the

magnitude of the change in the community-weighted mean of a gene family across a gradient of slow- to rapid fine root decay. Positive Z-scores indicate associations with rapid decay, and negative Z-scores indicate associations with slower decay. We considered responses statistically significant if both purity and reliability were ≥0.95. Partial regression plots showing the relationships between fine root decay and the summed abundance of all 58 PCWDE community-weighted mean abundances (b) and the summed abundance of PCWDE gene families associated with rapid decay (c). These relationships were evaluated using multiple GAMMs with the four environmental variables and either all or rapid decay associated PCWDEs and as predictors. The models explained 14% (all PCWDEs) and 18% (rapid decay PCWDEs) of the variance in gene families ($R^2_{adj.}$ = 0.138 and $R^2_{adj.}$ = 0.179; Figure C.6 and Table C.5). The abundance of each predictor was scaled to a mean of 0 and SD of 1 to accurately estimate effect sizes. We accounted for potential spatial autocorrelation using a spatial correlation structure in GAMM models that incorporates the geographic coordinates of each plot (n = 70).

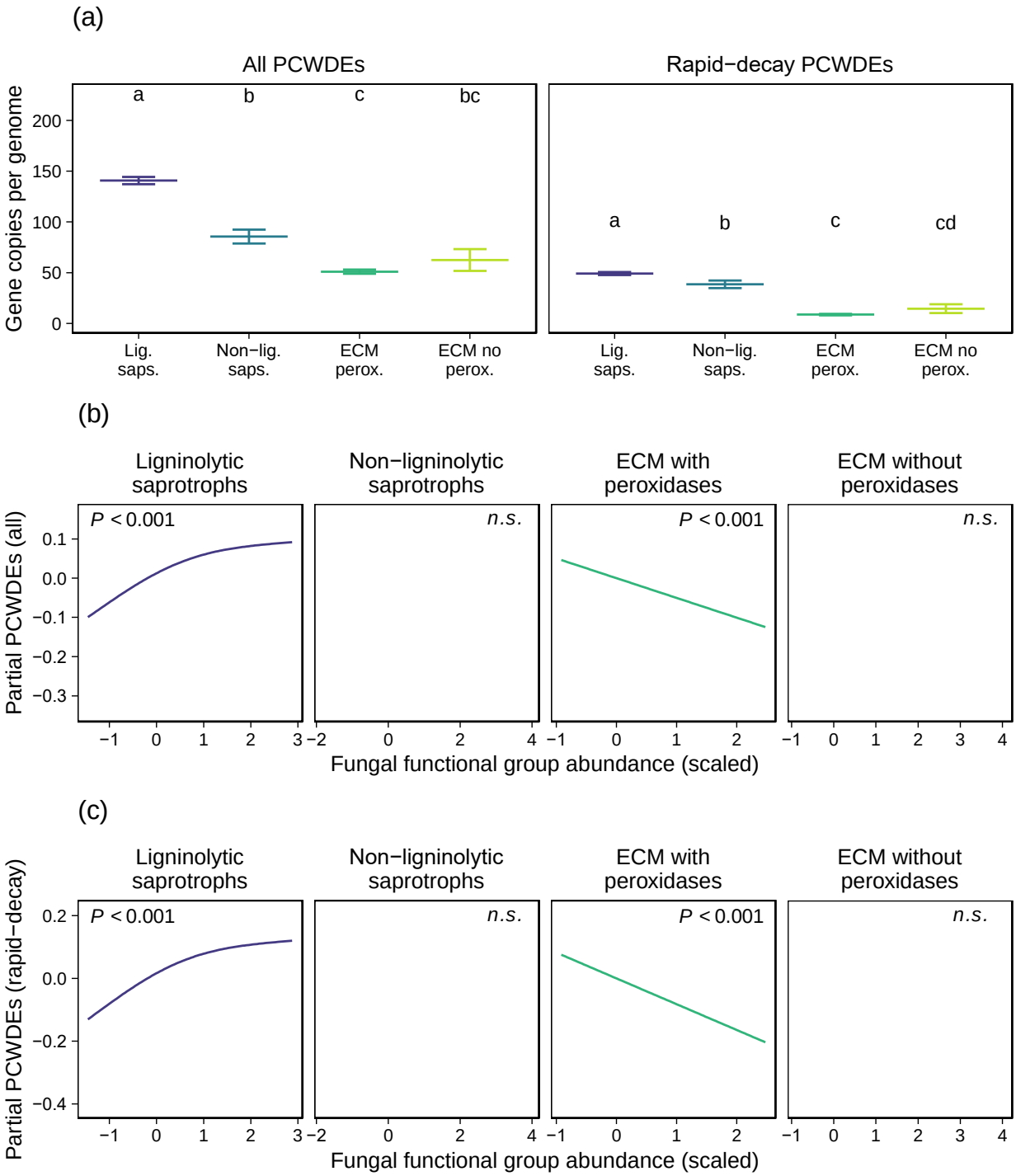

Figure 4.2: Total number of genes in all 58 PCWDEs or rapid root decay PCWDEs in the genomes of fungi belonging to different functional groups (a). Horizontal lines are means, and error bars represent ± 1 SE; different lowercase letters represent different means based on Tukey's HSD ($P < 0.05$). Partial regression plots showing the relationships between fungal

functional groups and the community-weighted mean abundance all PCWDEs (b) and rapid decay associated PCWDE gene families (c). These relationships were evaluated using a multiple GAMM with four functional groups and four environmental variables as predictors. The models explained 52% of the variance in all PCWDE gene families ($R^2_{adj.}$ = 0516) and 60% of the variance in PCWDE gene families associated with rapid decay ($R^2_{adj.}$ = 0.601). Each functional group and environmental variable was scaled to a mean of 0 and SD of 1 to accurately estimate effect sizes. Environmental variables included in each model were not significant predictors of PCWDE abundances (Figure C.9). We accounted for potential spatial autocorrelation using a spatial correlation structure in GAMM models that incorporates the geographic coordinates of each plot (n = 69). *n.s.*, not significant.

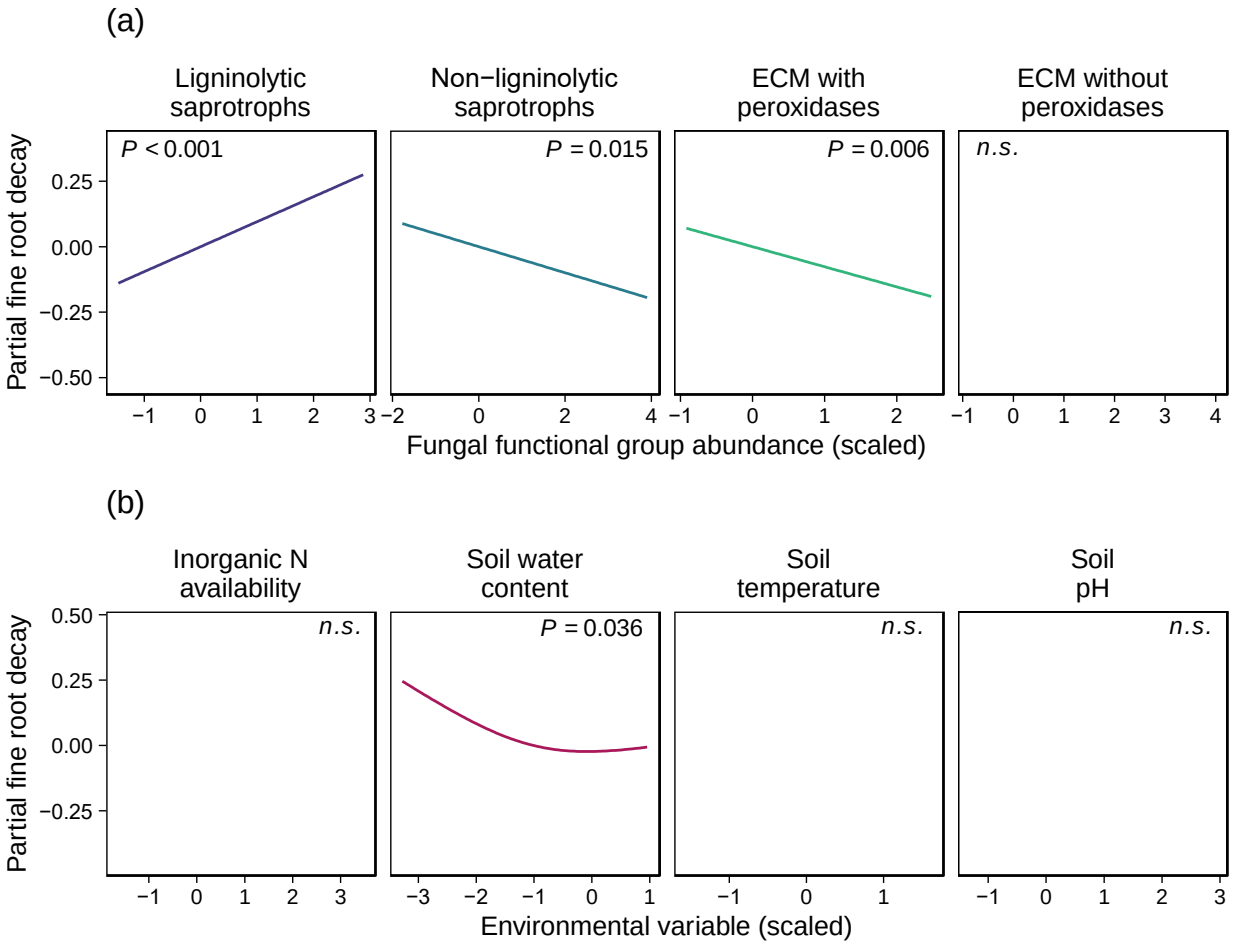

Figure 4.3: Partial regressions showing the relationships between fine root decay and the abundance of fungal functional groups (a) and environmental variables (b). These relationships were evaluated using a single multiple GAMM with four functional groups and four environmental variables as predictors. This model explained 37% of the variance in fine root decay ($R^2_{adj.}$ = 0.365). The abundance of each functional group was scaled to a mean of 0 and SD of 1 to accurately estimate effect sizes. We accounted for potential spatial autocorrelation using a spatial correlation structure in GAMM models that incorporates the geographic coordinates of each plot (n = 70). *n.s.*, not significant.

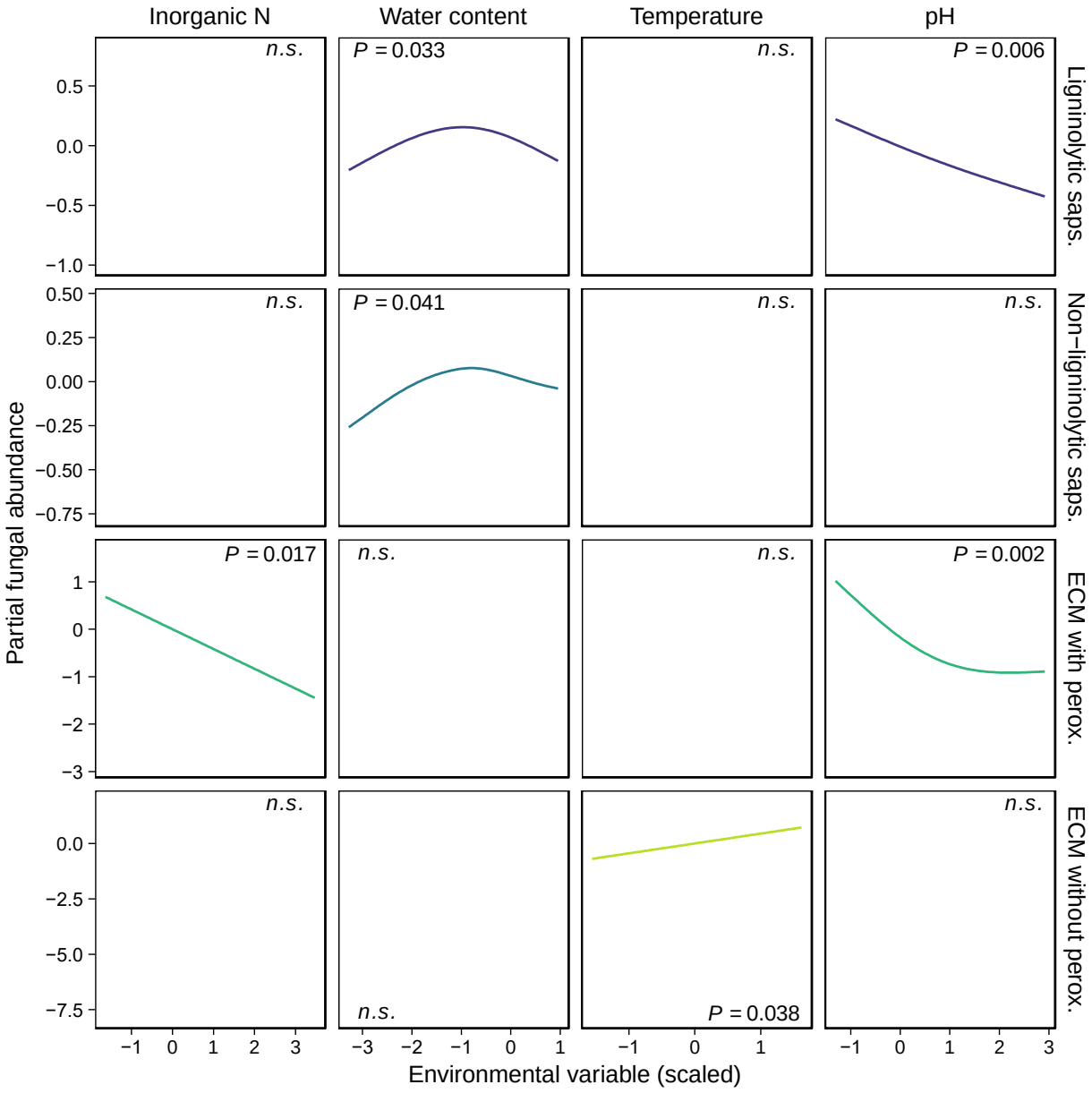

Figure 4.4: Partial regressions showing the relationships between the abundance of fungal functional groups and environmental variables. Each row represents a separate multiple GAMM with a functional group as the response variable and the four environmental variables (columns) as predictors. The statistical significance of these relationships was evaluated using a separate multiple GAMM for each functional group with inorganic N availability and volumetric water content as the predictor variables. The variance explained by the environment in each model is as

follows: ligninolytic saprotrophs, 26% ($R^2_{adj.}$ = 0.260); non-ligninolytic saprotrophs, 13% ($R^2_{adj.}$ = 0.130); ECM with peroxidases, 59% ($R^2_{adj.}$ = 0.585; ECM without peroxidases, 11% ($R^2_{adj.}$ = 0.107). Each environmental variable was scaled to a mean of 0 and SD of 1 to accurately estimate effect sizes. We accounted for spatial autocorrelation using a spatial correlation structure that incorporates the location of each plot (n = 70). *n.s.*, not significant.

CHAPTER 5

Conclusions

- Anthropogenic N deposition indirectly slowed fine root decay by reducing the relative abundance of ligninolytic saprotrophic fungi in decaying fine root litter, thereby enhancing the accumulation of lignin-derived SOM and increasing soil carbon storage (Chapter 2). Anthropogenic N deposition is one factor contributing to a large carbon sink in the Northern Hemisphere (Frey *et al.* 2014), which has partially offset the accumulation of CO_2 emissions in the atmosphere (Keenan *et al.* 2016; Walker *et al.* 2021). Thus, fungal community composition regulates a globally important relationship between inorganic N availability and soil carbon storage.
- ECM fungi with peroxidases declined in relative abundance with increasing N availability across a natural gradient of soil inorganic N (Chapter 3). Lignin-derived SOM and soil carbon storage were negatively correlated with the relative abundance of these ECM fungi and positively correlated with inorganic N availability. These relationships are consistent with the idea that decay of SOM by ECM fungi with peroxidases is greater where inorganic N availability is low, and that this activity restricts the accumulation of SOM. ECM fungi are central to our understanding of SOM dynamics (Frey 2019; Zak *et al.* 2019b), and my results highlight an underappreciated role for ECM fungal composition and its functional consequences for regulating soil carbon storage across forest ecosystems.

- The early stages of fine root decay were controlled by the abundance of ligninolytic fungal saprotrophs and ECM fungi with peroxidases and their effects on community-level genetic decay potentials (Chapter 4). The effects of fungal composition on fine root decay overwhelmed the direct effects of the environment, plausibly explaining why environmental variables appear to be weaker controls over fine root decay than over aboveground litter (Beidler & Pritchard 2017; See *et al.* 2019; Wambsganss *et al.* 2021).
- These findings provide important insights into the ecosystem-level consequences of functional differences among ECM fungal taxa. ECM fungi with peroxidases accelerated the decay of lignin-derived SOM (Chapter 3) and slowed the early stages of fine root decay (Chapter 4), but there was no evidence to suggest ECM fungi without peroxidases elicited these responses. These observations support contentions that ECM fungi cannot be treated as a homogenous fungal functional group (Pellitier & Zak 2018; Zak *et al.* 2019b) and extend the consequences of this functional diversity from tree N nutrition (Pellitier *et al.* 2021b, a) to SOM dynamics.
- The results of my research suggest apparent context dependencies in relationships between N availability, decay, and soil carbon (Averill & Waring 2018) arise due to differential effects on fungal functional groups and their unique roles in the decay of fine root litter and SOM. Increased N availability due to anthropogenic N deposition slowed fine root decay and increased soil carbon by reducing the relative abundance of ligninolytic saprotrophic fungi (Chapter 2). In contrast, naturally high inorganic N availability slowed fine root decay by reducing the abundance of ECM fungi with peroxidases, possibly by alleviating competition with free-living saprotrophs (Chapter 4). However, these early stages of root decay did not determine soil carbon storage (Chapter

3). Rather, ECM fungi with peroxidases accelerated the decay of lignin-derived SOM, ultimately reducing soil carbon storage and causing it to increase with increasing inorganic N availability.

Together, the results of this work demonstrate how environmental conditions (soil inorganic N availability) indirectly regulate the decay of fine root litter into SOM by modifying fungal community composition and functioning, thereby addressing a long-standing goal in ecology (Lavorel & Garnier 2002; Fierer 2017). While these fungal mechanisms resulted in direct correlations between the environment and ecosystem functioning in some cases (Chapters 2-3), these relationships were not always strong enough to result in direct correlations (Chapter 4). Thus, representing fine root decay in biogeochemical models will likely require accounting for the abundance of key fungal functional groups, rather than simple mathematical relationships between the environment and functioning. Our findings provide a set of principles that can inform the development of microbial-explicit ecosystem models (*e.g.*, Wieder *et al.* 2018; Sulman *et al.* 2019) that better represent the complete terrestrial carbon cycle by including fine root decay and its fungal controls.

APPENDIX A

Supporting Information for Chapter 2: Anthropogenic N Deposition Alters Soil Organic Matter Biochemistry and Microbial Communities on Decaying Fine Roots

William A. Argiroff, Donald R. Zak, Rima A. Upchurch, Sydney O. Salley, and A. Stuart Grandy

Figure A.1: Locations of the four forest stands in our long-term N deposition experiment in upper and lower Michigan, USA.

Table A.1: Climatic and edaphic characteristics for the four forest stands in our long-term N deposition experiment.

Characteristic	Site A	Site B	Site C	Site D
Climate[a]				
Mean annual temperature (°C)	4.7	6.0	6.9	7.6
Mean annual precipitation (mm)	873	871	888	812
Ambient N deposition (g N m^{-2} y^{-1})	0.68	0.91	1.17	1.18
Soil (0-10 cm)				
pH (1:1 soil/H_2O)[b]	4.8	5.0	4.5	4.7
C (g kg^{-1}; ambient N)[c]	24.2 (2.8)	37.3 (8.5)	21.3 (1.2)	21.0 (1.4)
C (g kg^{-1}; experimental N)[c]	25.0 (2.6)	74.6 (2.9)	22.0 (2.2)	29.3 (5.4)
N (g kg^{-1}; ambient N)[c]	1.84 (0.36)	2.22 (0.37)	1.72 (0.44)	1.36 (0.01)
N (g kg^{-1}; experimental N)[c]	1.73 (0.16)	4.19 (0.10)	1.72 (0.35)	1.83 (0.18)

[a](Zak *et al.* 2008); [b](Eisenlord & Zak 2010); [c](Pregitzer *et al.* 2008)

Table A.2: Reaction conditions and thermocycler profiles for fungal and bacterial PCR. Values are volumes in 20 μL. Total reaction volume was 25 μL.

Condition	Fungi (28S)	Bacteria (16S)
Reaction		
HF 10X buffer	2.5	2.5
LROR (20 μM)	0.5	-
LR3 (20 μM)	0.5	-
27f (20 μM)	-	0.5
519r (20 μM)	-	0.5
dNTPs (2 mM each)	2.5	2.5
BSA (20 mg mL^{-1})	0.5	0.5
Template DNA	2	2
Molecular-grade H_2O	16.5	16.5
Thermocycler		
Initial denaturation	5 min, 95 °C	5 min, 94 °C
Number of cycles	25	20
Denaturation	30 s, 95 °C	30 s, 94 °C
Annealing	60 s, 54 °C	60 s, 55 °C
Extension	75 s, 72 °C	90 s, 72 °C
Final extension	10 min, 72 °C	10 min, 72 °C

Table A.3: Barcode sequences affixed to forward and reverse primers for sample multiplexing. Barcode sequences were obtained from Pacific Biosciences for use with circular consensus sequencing.

Barcode	Forward	Reverse
Fungi (28S; LROR/LR3)		
B0	gcgctctgtgtgcagc	agagtactacatatga
B2	tatctatcgtatacgc	atgtatctcgactgca
B7	ctgctagagtctacag	cgagctatctcatact
B9	tcatgcacgtctcgct	cagcgactgtgatact
B10	agagcatctctgtact	tgtcgcatcatatgat
B16	cgacgtatctgacagt	cgcgtgcagagtgtca
B19	catacgctgtgtagca	ctactgtctcgcactg
B20	cactgatcgatatgca	gtacactagtgcacat
B26	tcgtagagctcgagac	tcactgctgagagtag
Bacteria (16S; 27f/519r)		
B2	tatctatcgtatacgc	atgtatctcgactgca
B3	atcacactgcatctga	gactcgacgcagagtc
B4	acgtacgctcgtcata	cgatgacgtcgctgta
B6	agagacacgatactca	gctgtatcgcagagac
B7	ctgctagagtctacag	cgagctatctcatact
B10	agagcatctctgtact	tgtcgcatcatatgat
B11	cgcatcgactacgcta	gctgtgatctacgtct
B12	cgtagcgtgctatcac	tgagtagcatgacacg
B13	atgctgatgactgcga	gacatgcagtctcaca

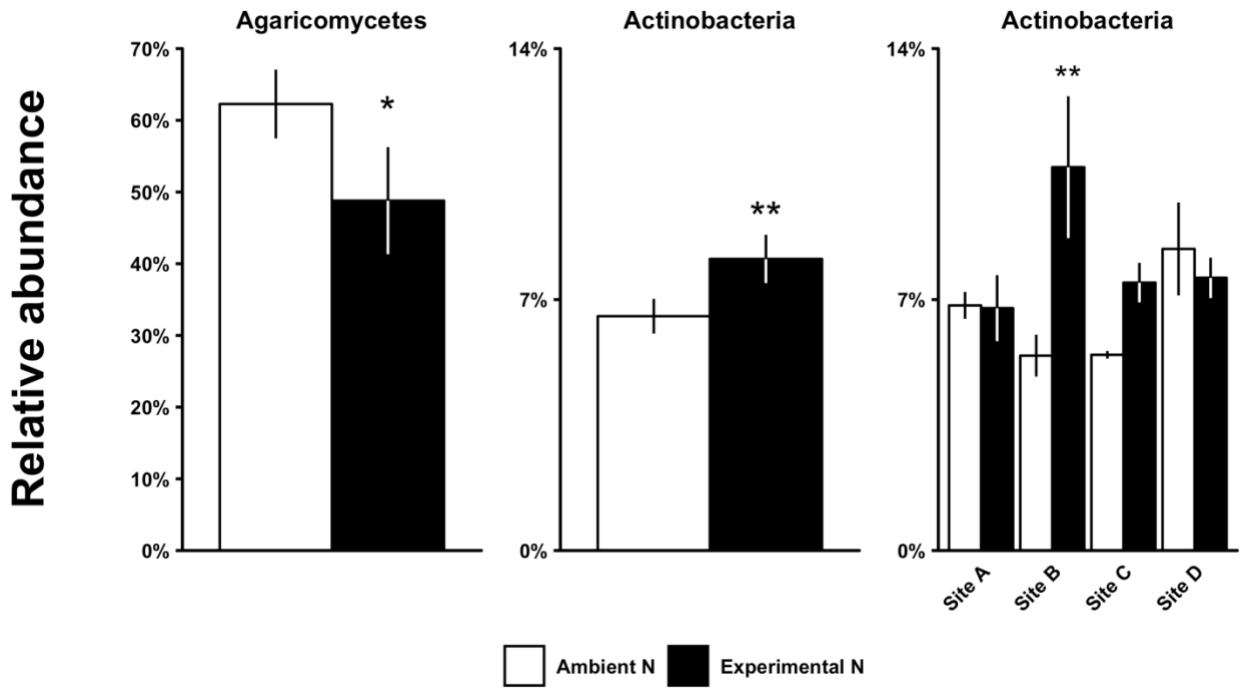

Figure A.2: Relative abundance of Agaricomycetes and Actinobacteria under ambient and experimental N deposition on fine root litter decaying in the field. Bars represent mean relative abundances and error bars are one standard error (n = 12 by treatment, and n = 3 for site by treatment). * $P < 0.1$, ** $P < 0.05$, for effect of experimental N deposition by two-way ANOVA and protected Fisher's LSD test.

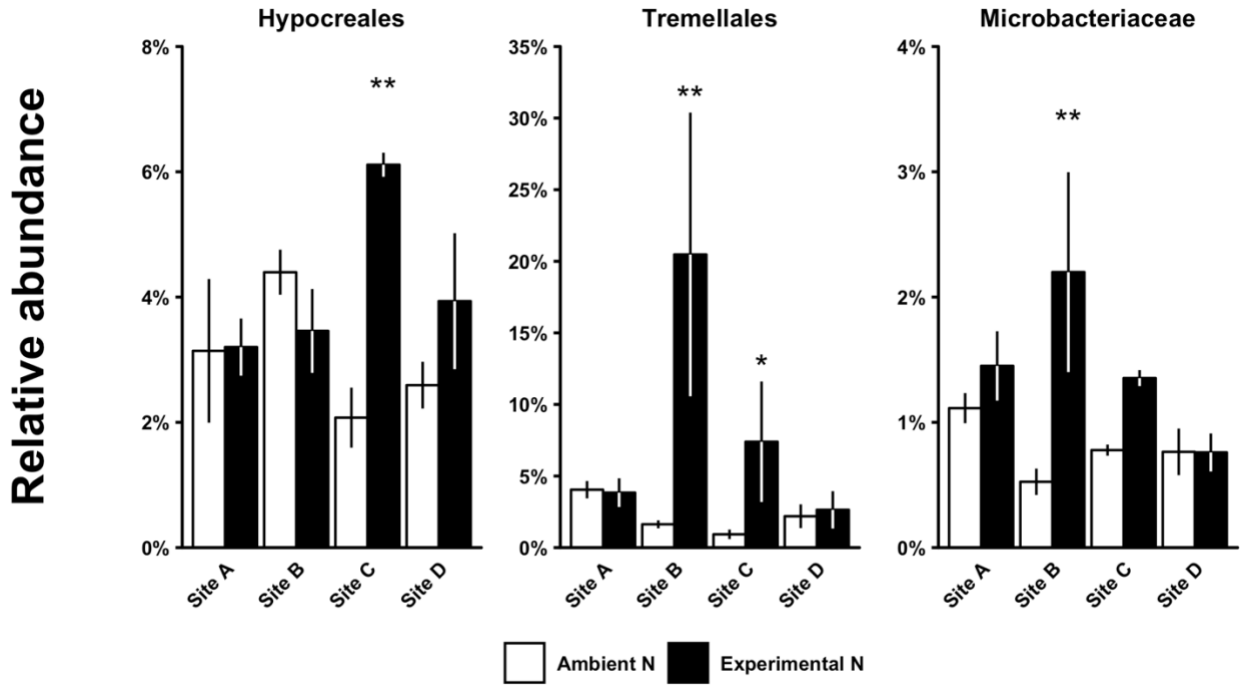

Figure A.3: Responses of relative abundances of select fungal orders and bacterial families to experimental N deposition at each of the four sites in our long-term N deposition experiment. * $P < 0.1$, ** $P < 0.05$, for effect of experimental N deposition by protected Fisher's LSD test.

APPENDIX B

Supporting Information for Chapter 3: Decay by Ectomycorrhizal Fungi Couples Soil Organic Matter to Nitrogen Availability

William A. Argiroff, Donald R. Zak, Peter T. Pellitier, Rima A. Upchurch, and Julia P. Belke

Supporting Methods B.1

Soil organic matter biochemistry

We characterized SOM biochemistry using pyrolysis gas chromatography-mass spectrometry (py-GC/MS). Ground soils were pyrolyzed at 600 °C in quartz tubes for 20 s using a DS pyroprobe 5150 pyrolyzer, and analyzed using a Thermotrace GC Ultra gas chromatograph (Thermo Fisher Scientific) and ITQ 900 mass spectrometer (Thermo Fisher Scientific). AMDIS software and a previously compiled compound library were used to assign spectrometry peaks to compounds, and the relative abundance for each compound was determined by dividing its peak area by the largest peak present in the sample. We summed individual compounds by the classes from which they originated to determine the relative abundances of aromatics, lignin (hereafter "lignin-derived SOM"), lipids, N-bearing, phenols, polysaccharides, proteins, and unknown.

DNA extraction

We extracted DNA from three 0.05 g subsamples of decaying fine roots per plot using the DNeasy Plant Mini Kit (Qiagen) following a modified manufacturer's protocol. We performed physical lysis with four 2.38 mm stainless steel beads at 2,000 rpm for 60 s using the PowerLyzer 24 Bench Top Bead-Based Homogenizer (MoBio Laboratories). Debris was pelleted by centrifugation at 16,000 g for 5 minutes. We isolated DNA from four 0.25 g subsamples of soil per plot using the PowerLyzer PowerSoil DNA Isolation Kit, with bead beating at 2,500 rpm for 45 s. All DNA was purified using the DNeassy PowerClean CleanUp kit, and we verified the quality of extracted and purified DNA with a NanoDrop 8000 Spectrophotometer (Thermo Scientific) and gel electrophoresis.

Full primer sequences

The forward primer consisted of the forward Illumina sequencing adapter (i5), an 8-bp Illumina index, a 10-bp pad sequence, a 2-bp linker sequence, and the base ITS4-Fun primer (5'-AGCCTCCGCTTATTGATATGCTTAART-3'). Similarly, the reverse primer consisted of the reverse Illumina sequencing adapter (i7), an 8-bp Illumina index, a 10-bp pad sequence, a 2-bp linker sequence, and the base 5.8S-Fun primer (5'-AACTTTYRRCAAYGGATCWCT-3'). The sequences for each primer are listed below:

Primer ID	Primer sequence (5'-3')
Forward	
SA501	AATGATACGGCGACCACCGAGATCTACACATCGTACGTATGGTAATTAAAGCCTCCGCTTATTGATATGCTTAART
SA502	AATGATACGGCGACCACCGAGATCTACACACTATCTGTATGGTAATTAAAGCCTCCGCTTATTGATATGCTTAART
SA503	AATGATACGGCGACCACCGAGATCTACACTAGCGAGTTATGGTAATTAAAGCCTCCGCTTATTGATATGCTTAART
SA504	AATGATACGGCGACCACCGAGATCTACACCTGCGTGTTATGGTAATTAAAGCCTCCGCTTATTGATATGCTTAART
SA505	AATGATACGGCGACCACCGAGATCTACACTCATCGAGTATGGTAATTAAAGCCTCCGCTTATTGATATGCTTAART
SA508	AATGATACGGCGACCACCGAGATCTACACGACACCGTTATGGTAATTAAAGCCTCCGCTTATTGATATGCTTAART
SB501	AATGATACGGCGACCACCGAGATCTACACCTACTATATATGGTAATTAAAGCCTCCGCTTATTGATATGCTTAART
SB502	AATGATACGGCGACCACCGAGATCTACACCGTTACTATATGGTAATTAAAGCCTCCGCTTATTGATATGCTTAART
SB503	AATGATACGGCGACCACCGAGATCTACACAGAGTCACTATGGTAATTAAAGCCTCCGCTTATTGATATGCTTAART
SB504	AATGATACGGCGACCACCGAGATCTACACTACGAGACTATGGTAATTAAAGCCTCCGCTTATTGATATGCTTAART
Reverse	
SA701	CAAGCAGAAGACGGCATACGAGATAACTCTCGAGTCAGTCAGGGAACTTTYRRCAAYGGATCWCT
SA702	CAAGCAGAAGACGGCATACGAGATACTATGTCAGTCAGTCAGGGAACTTTYRRCAAYGGATCWCT
SA703	CAAGCAGAAGACGGCATACGAGATAGTAGCGTAGTCAGTCAGGGAACTTTYRRCAAYGGATCWCT

SA704	CAAGCAGAAGACGGCATACGAGATCAGTGAGTAGTCAGTCAGGGAACTTTYRRCAAYGGATCWCT
SA705	CAAGCAGAAGACGGCATACGAGATCGCACTCAAGTCAGTCAGGGAACTTTYRRCAAYGGATCWCT
SA706	CAAGCAGAAGACGGCATACGAGATCTACGCAGAGTCAGTCAGGGAACTTTYRRCAAYGGATCWCT
SA708	CAAGCAGAAGACGGCATACGAGATGTCGCTCGAGTCAGTCAGGGAACTTTYRRCAAYGGATCWCT
SA709	CAAGCAGAAGACGGCATACGAGATGTCGTAGTAGTCAGTCAGGGAACTTTYRRCAAYGGATCWCT
SB702	CAAGCAGAAGACGGCATACGAGATATACTTCGAGTCAGTCAGGGAACTTTYRRCAAYGGATCWCT
SB703	CAAGCAGAAGACGGCATACGAGATAGCTGCTAAGTCAGTCAGGGAACTTTYRRCAAYGGATCWCT

PCR protocols

We used PCR to amplify the ITS2 region from soil samples in 25 µl reactions using the Phusion High Fidelity DNA Polymerase (New England BioLabs, Ipswich, MA, USA). Each reaction contained 5 µl of 5X Phusion buffer, 0.5 µl dNTPs (20 mM each dNTP), 0.5 µl bovine serum albumin (20 mg · ml^{-1}; New England BioLabs), 0.9375 µl each indexed ITS4-Fun and 5.8S-Fun primer (10 µM initial concentration), 0.25 µl Phusion DNA polymerase (2U · $µl^{-1}$), 2 µl purified DNA template, and 14.875 µl molecular-grade water. Thermocycling conditions consisted of a 3 minute initial denaturation step at 95 °C, followed by 30 cycles of 30 s at 95 °C, 45 s at 57 °C, and 90 s at 72 °C. A final extension step was performed at 72 °C for 10 minutes.

For decaying fine root samples, each 25 µl PCR contained 5 µl of 5X Phusion buffer, 0.25 µl dNTPs (20 mM each dNTP), 0.9375 µl of each indexed ITS4-Fun and 5.8S-Fun (10 µM initial concentration), 0.25 µl Phusion DNA polymerase (2U · $µl^{-1}$), 2 µl purified template DNA, and 14.875 µl molecular-grade water. Thermocycling conditions consisted of a Thermocycling conditions consisted of a 3 minute initial denaturation step at 95 °C, followed by 28 cycles of 30

s at 95 °C, 45 s at 57 °C, and 90 s at 72 °C. A final extension step was performed at 72 °C for 10 minutes.

We performed all reactions for each sample in triplicate. Each primer combination for each substrate (*i.e.*, soil or decaying fine root litter) included a negative control (2 µl molecular-grade water instead of template DNA) and a positive control reaction (2 µl template DNA extracted from an *Agaricus bisporus* sporocarp). Reactions were carried out in a Mastercycler ProS thermocycler (Eppendorf), and the quality of all reactions was verified using gel electrophoresis as described above. Minor differences in PCR protocols between soil and decaying fine root samples ensured that samples from each habitat were amplified to a similar extent, as determined by gel electrophoresis.

Amplicon sequencing

The soil PCR library (n = 72 samples) was normalized and purified using a SequalPrep Normalization Plate Kit (ThermoFisher, Waltham, MA, USA) and AMPure XP for PCR Purification (Beckman Coulter Life Sciences, Brea, CA, USA). The library was sequenced on a MiSeq 2x250 bp run using v2 Nano chemistry (Illumina, San Diego, CA, USA) to ensure sequencing would be successful, and then sequenced on a full MiSeq 2x250 bp run using v2 chemistry. Reads from the full and Nano runs were combined during downstream analyses. The decaying fine roots PCR library (n = 72 samples) was normalized and purified as above, and sequenced on a separate full MiSeq 2x250 bp run using v2 chemistry. Library normalization, purification, and sequencing was performed by the UMICH Microbiome Core at the University of Michigan Medical School.

Figure B.1: Locations of 12 study sites in northern Lower Michigan, USA.

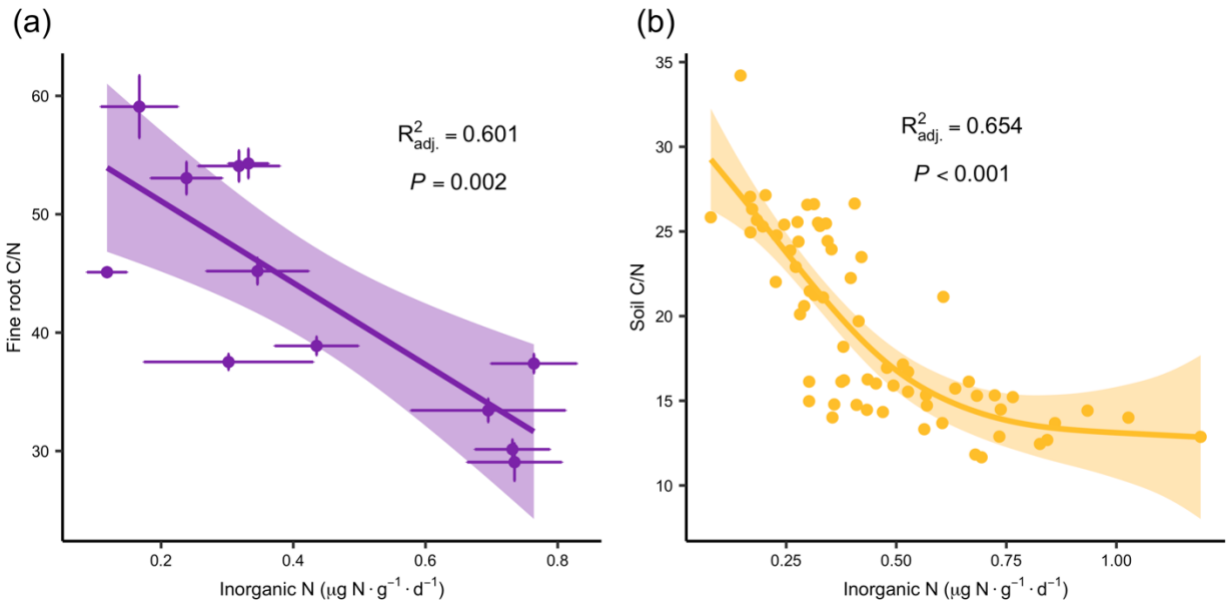

Figure B.2: Relationships between soil inorganic N availability and fine root litter C/N (a) and soil C/N (b). Trend lines, confidence intervals, R^2, and *P*-values were determined using simple linear regression (n = 12) for fine root litter and generalized additive modeling (GAM) for soil C/N (n = 68). We used stand means for fine root C/N because fine root litter was composited by stand (error bars are ± one standard error, n = 3 subsamples); inorganic N availability was determined for the soils from which fine roots were obtained at each tree (n = 5) in May, 2018. Simple GAM without spatial autocorrelation structure was used for soil C/N because our interest was in covariation between inorganic N availability and soil C/N rather than causal inference.

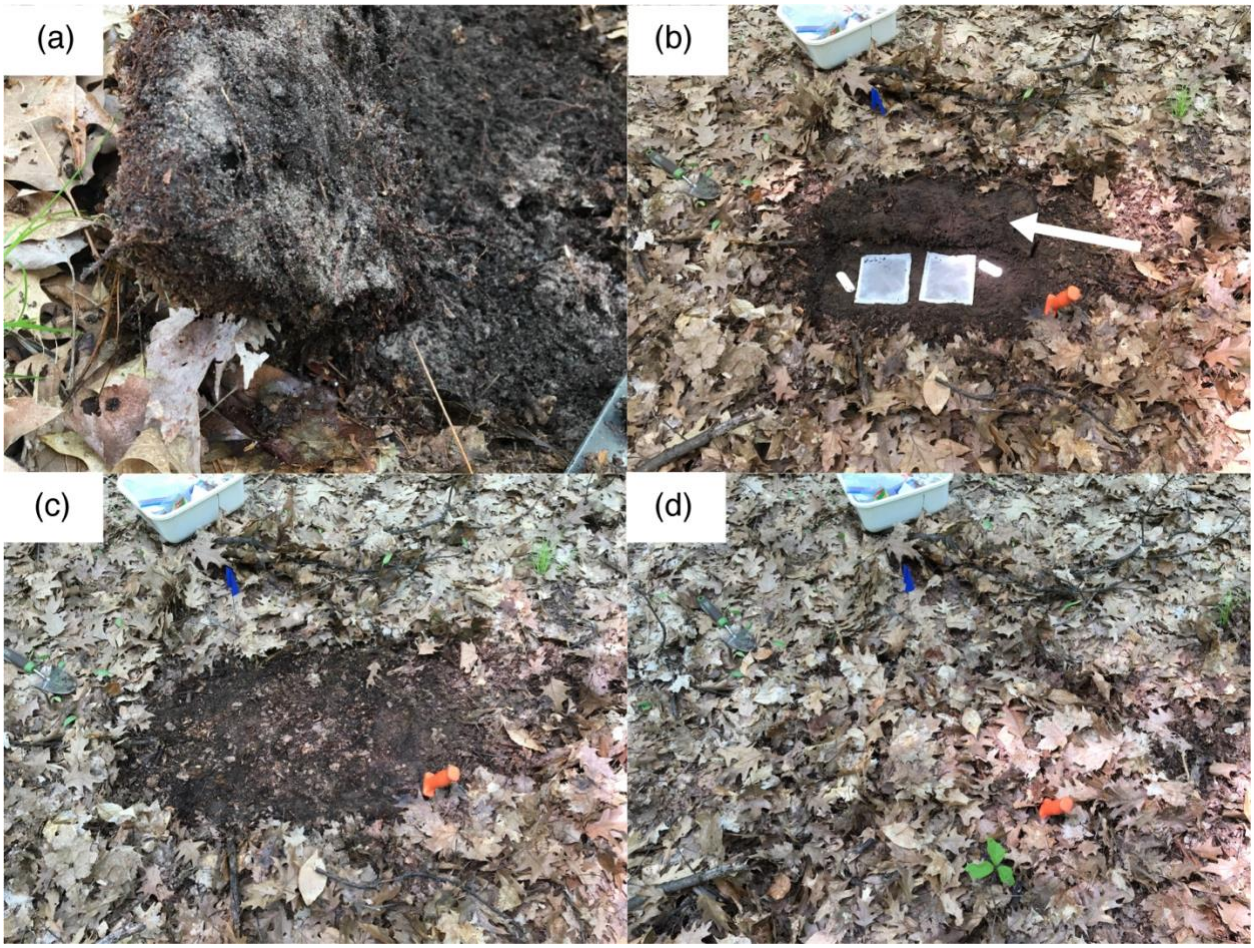

Figure B.3: We placed fine root litter bags at the interface of the Oe and A horizons, which is interpenetrated by a dense mat of fine roots. Mat of fine roots shown peeled away (a) and highlighted by white arrow (b). We replaced the root mat and Oe horizon (c), as well as the Oi horizon (d), over the litter bags. The orange soil knife marks the same location in panels b-d.

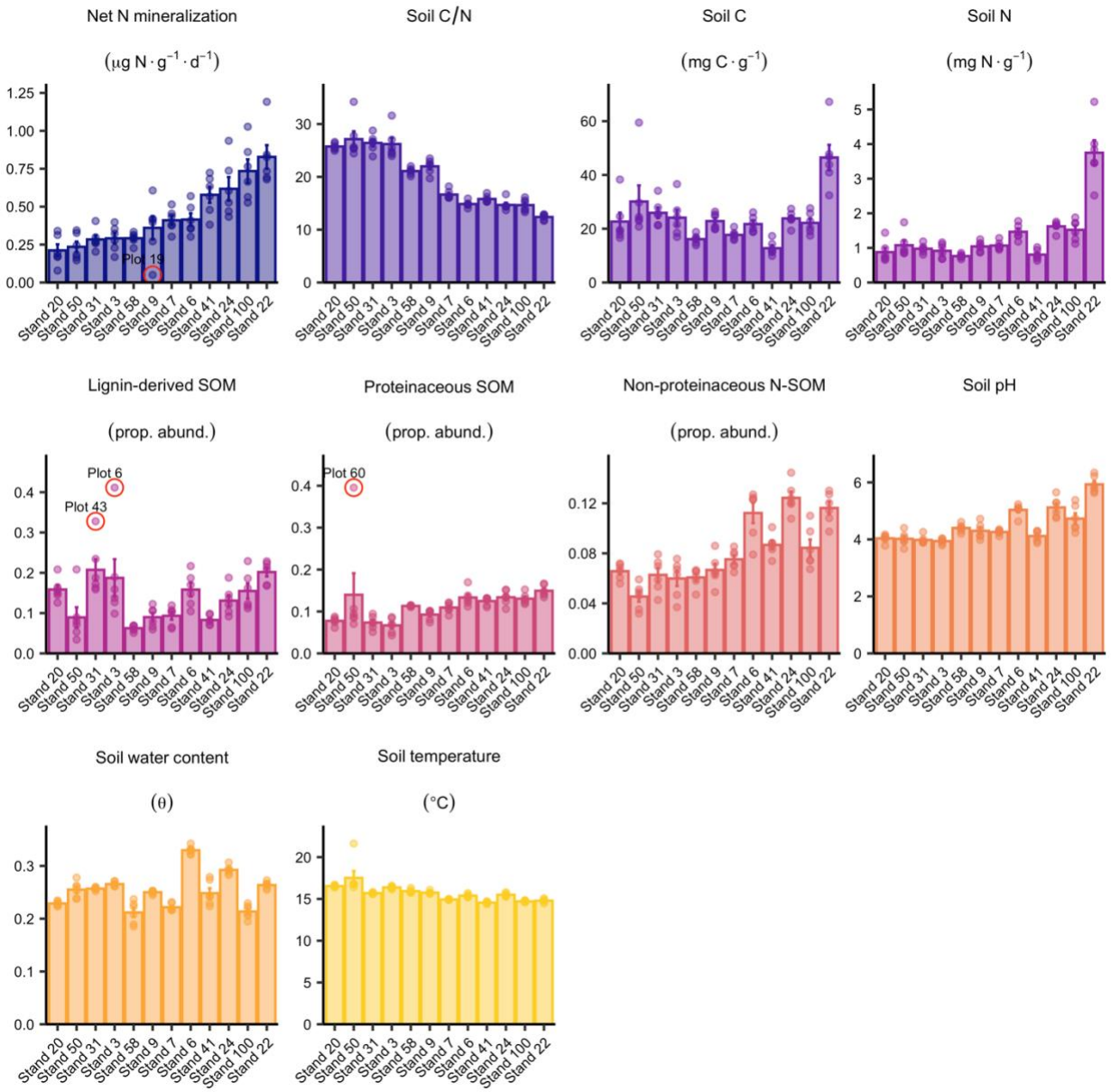

Figure B.4: Environmental data and SOM biochemistry showing stand mean (bars), standard error (error bars), and individual plots (points). Outlier plots that were removed from all analyses are circled in red. We removed Plot 19 because the net N mineralization assay failed, leading to a value near 0 μg · N · g^{-1} · d^{-1} that was far outside the range of values from the stand. Plots 6 and 43 were removed because they contained relative abundances lignin-derived SOM that were >0.3. These values are reflective of fresh fine root litter, suggesting these samples were

contaminated with fresh litter that would bias our analyses. Finally, we removed Plot 60 because it contained a relative abundance of proteinaceous SOM that was far greater than any other plot (~0.4 vs. 0.05-0.15). We do not have an explanation for this result, but its extreme value suggests sampling or analytical error that could bias our analyses.

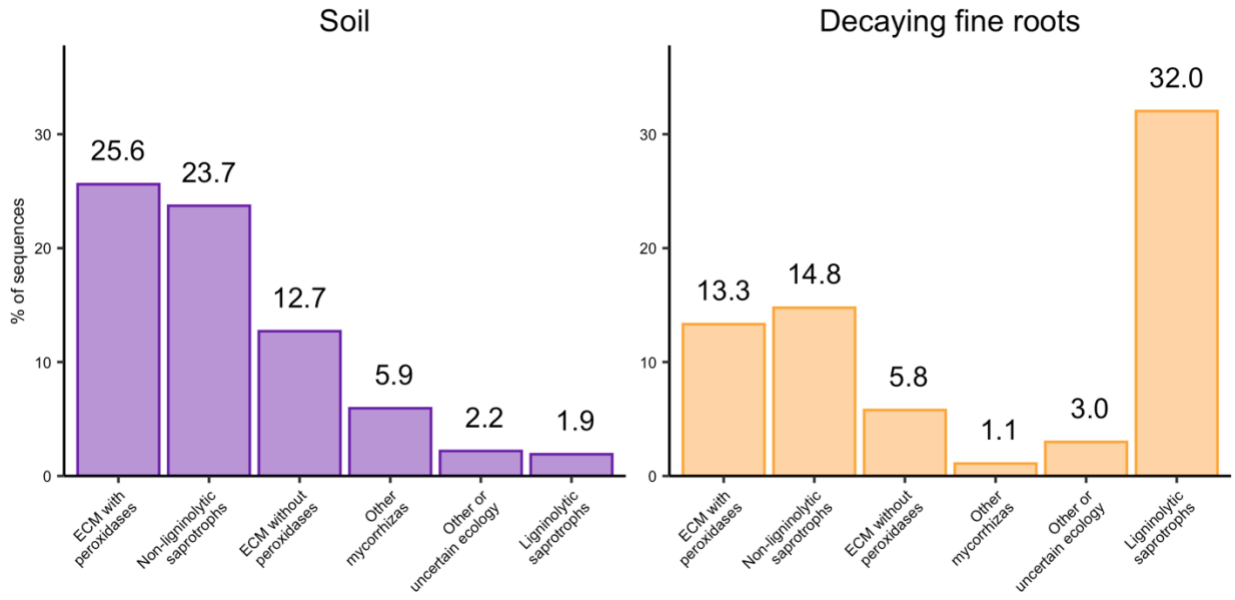

Figure B.5: Percentage of fungal sequences belonging to each fungal functional group in soil and decaying fine root litter. Labels above bars refer to exact percentages. Percentages do not sum to 100% because functional group assignments were only assigned to sequences that were classified at the genus level and belonged to genera that were present in ≥5 plots and accounted for ≥0.1% of sequences (calculated by habitat).

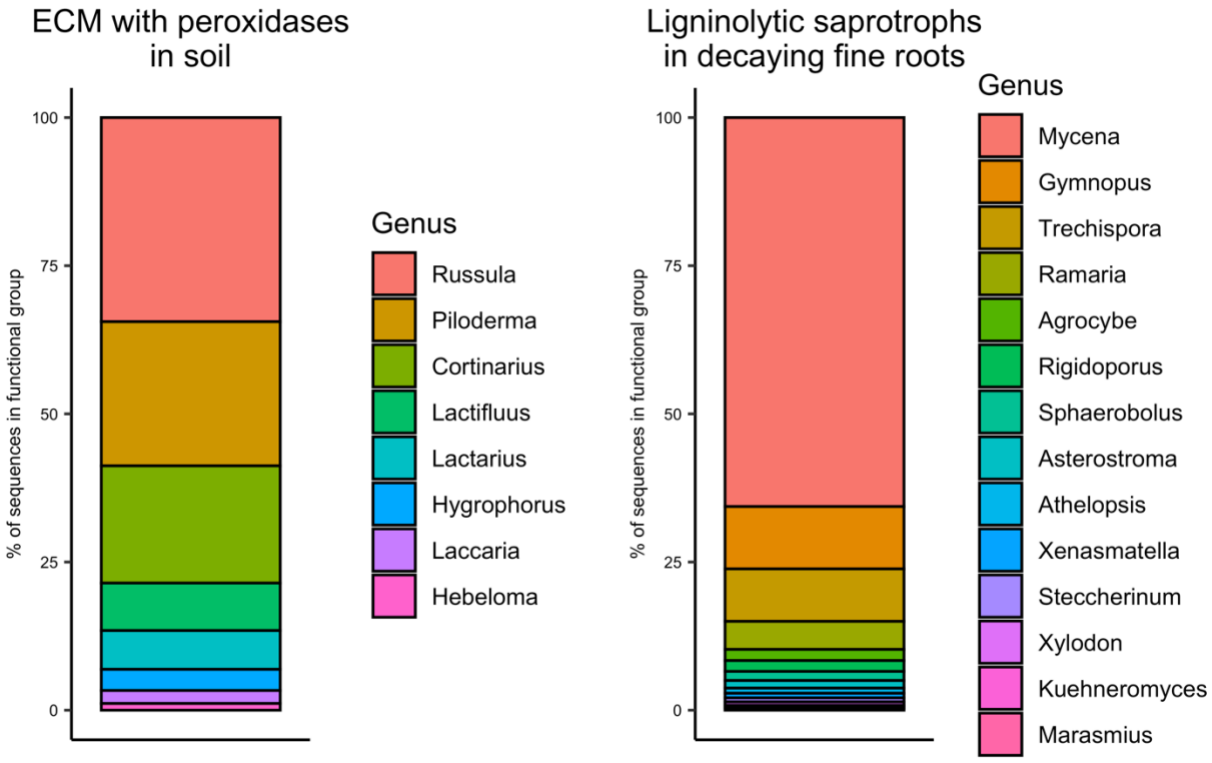

Figure B.6: Percentage of ECM with peroxidases in soil and ligninolytic fungi in decay fine roots belonging to specific genera.

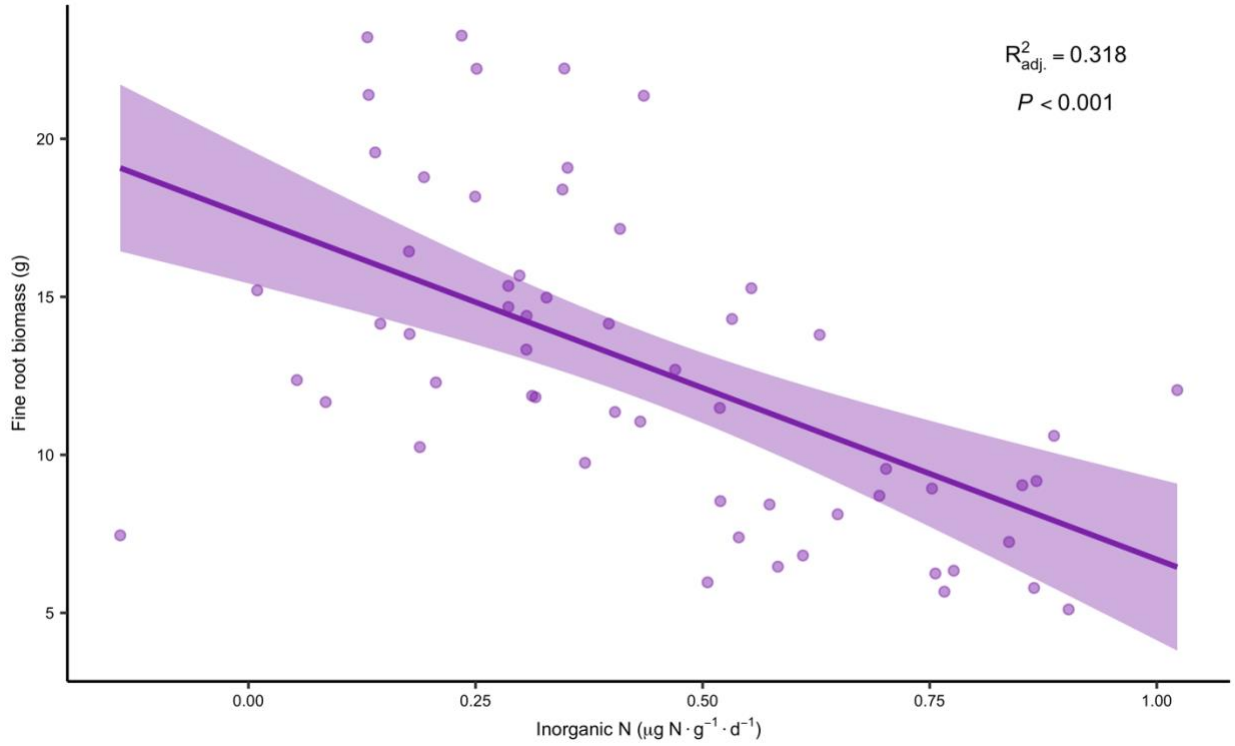

Figure B.7: Fine root biomass (dry mass of roots ≤0.5 mm diameter collected at each *Q. rubra* tree in May 2018) was negatively correlated with soil inorganic N availability at the respective trees (n = 59). This relationship was tested using linear regression.

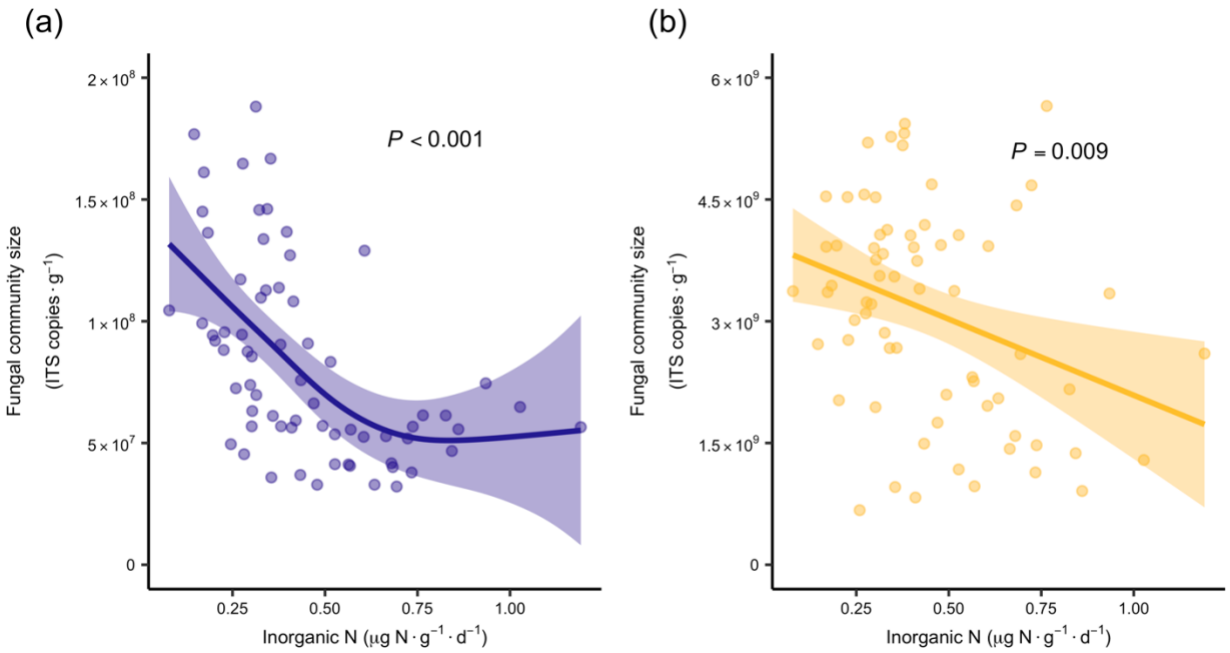

Figure B.8: Absolute abundance of fungi across the inorganic N availability gradient in soil (a) and decaying fine root litter (b) determined as fungal ITS gene copies per g of dry soil or per g ash-free dry roots using qPCR. The significance of these relationships between fungal community size and inorganic N availability were assessed using GAMM (n = 68).

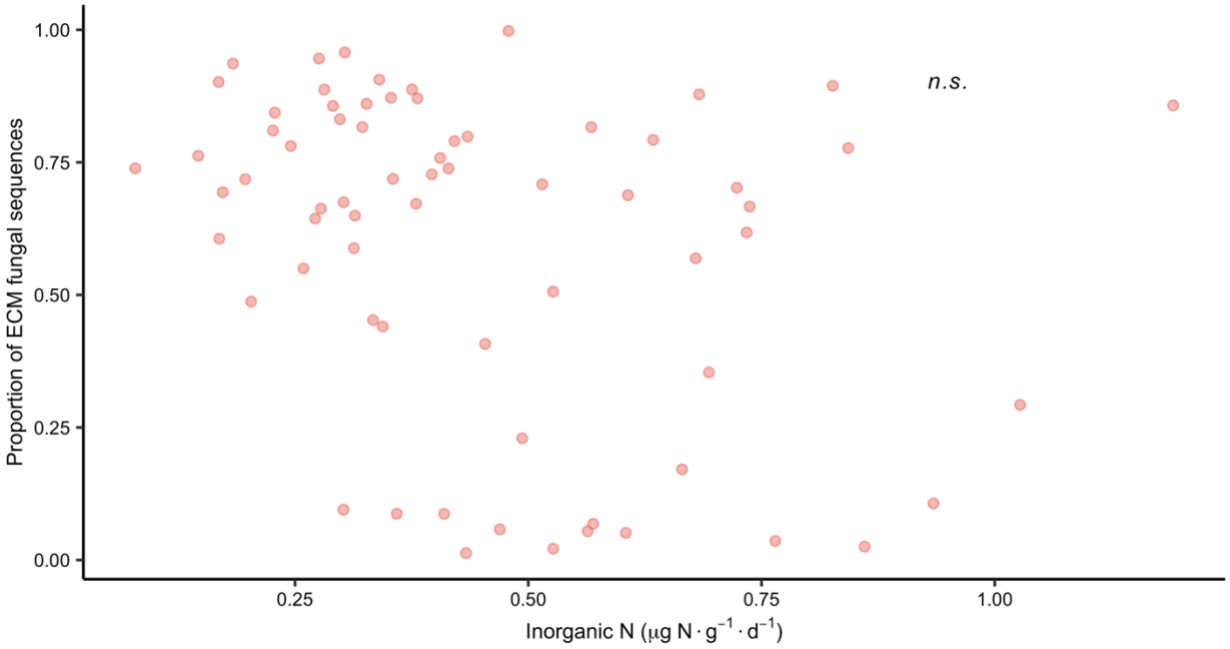

Figure B.9: Proportion of ECM sequences belonging to taxa with peroxidases across the soil inorganic N availability gradient.

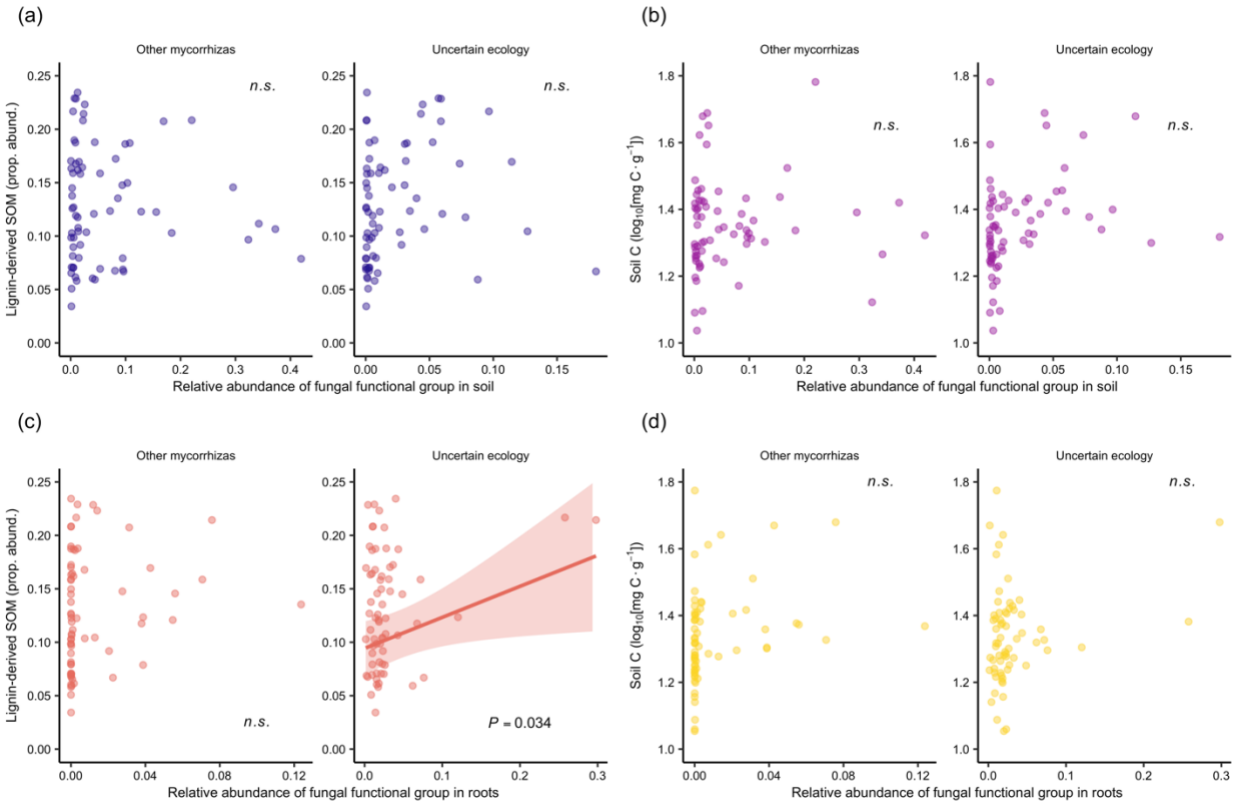

Figure B.10: Partial plots from multiple GAMM showing relationship between lignin-derived SOM and fungal functional groups in soil (a), soil C and fungal functional groups in soil (b), lignin-derived SOM and fungal functional groups in decaying fine roots (c), and soil C and fungal functional groups in soil (d). Each lettered panel represents a separate multiple GAMM with all functional groups as predictor variables (only other mycorrhizas and fungi with other or uncertain ecology are shown here), from which *P*-values and $R^2_{adj.}$ were calculated. We explicitly accounted for spatial autocorrelation in GAMM models with a spatial correlation structure based on the geographic coordinates of each plot (n = 68). Trend lines and confidence intervals are for visualization purposes only.

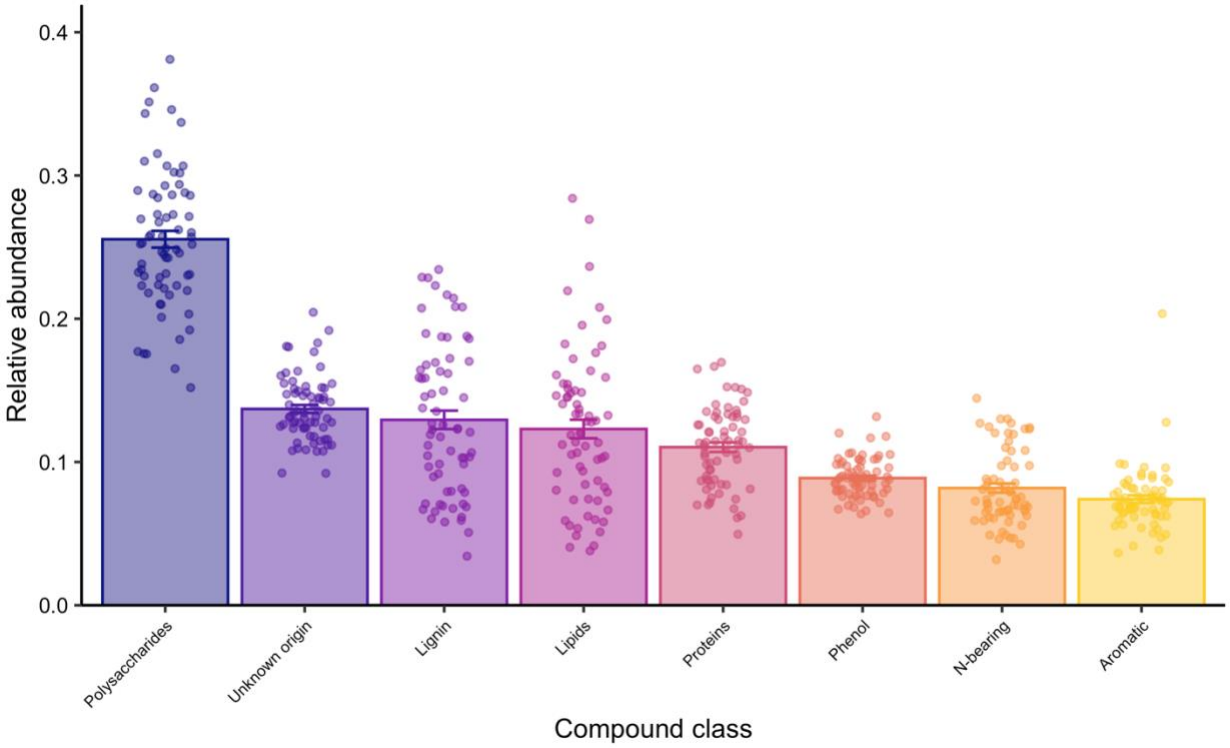

Figure B.11: Relative abundance of compound classes in SOM. Bars are mean values (n = 68), bars are standard error, and points are plot level values.

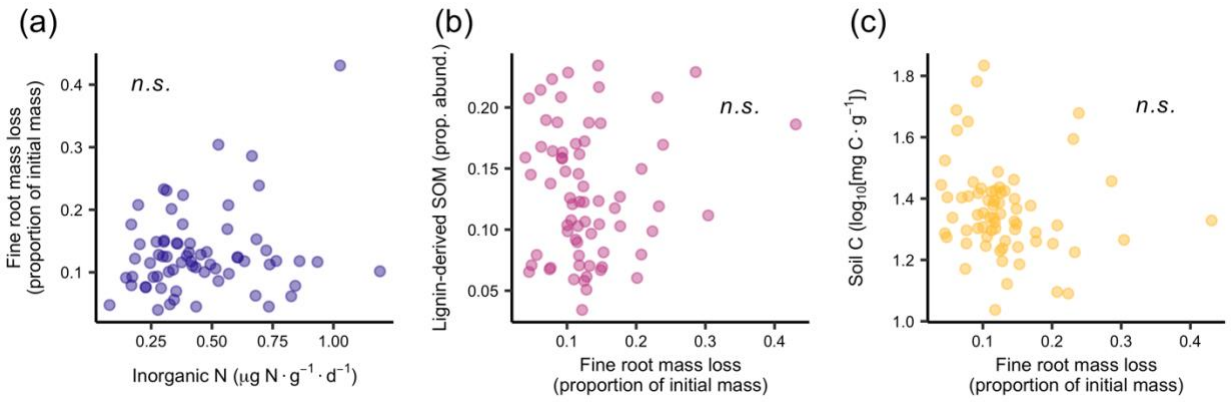

Figure B.12: Fine root mass loss over the 13-month field incubation was not correlated with soil inorganic N availability (a). Lignin-derived SOM (b) and overall soil C storage (c) were not correlated with fine root mass loss. The significance of these relationships was assessed using GAMM (n = 68).

Table B.1: Genera detected in either soil or fine root litter (≥5 plots and ≥0.1% of sequences), manually classified by functional group from the literature or FUNGuild database. Phyla are bolded. Functional groups are as follows: "ECM-P", ECM fungi with peroxidases; ECM-NP, ECM fungi without peroxidases; OM, other mycorrhizas; S-L, ligninolytic saprotrophs; S-NL, non-ligninolytic saprotrophs; O, other or uncertain ecology. References corresponding to numbers are listed below the table. *Lack of peroxidases inferred based on phylogenetic placement of genus outside Auriculariales and residual Agaricomycetes (Floudas *et al.* 2012; Nagy *et al.* 2016). All ECM genera with peroxidases from the literature except *Gautieria* were detected in our data set.

Class	Genus	Functional Group	Refs.
Ascomycota			
Dothideomycetes	*Cenococcum*	ECM-NP	(*1–4*)*
Eurotiomycetes	*Cladophialophora*	S-NL	(*1*, *2*, *5*)*
Eurotiomycetes	*Elaphomyces*	ECM-NP	(*1*, *2*, *5*)*
Eurotiomycetes	*Exophiala*	S-NL	(*1*, *2*, *5*)*
Eurotiomycetes	*Penicillium*	S-NL	(*1*, *2*, *5*)*
Geoglossomycetes	*Geoglossum*	S-NL	(*1*, *2*, *5*)*
Geoglossomycetes	*Glutinoglossum*	S-NL	(*1*, *2*, *5*)*
Geoglossomycetes	*Trichoglossum*	S-NL	(*1*, *2*, *5*)*
Leotiomycetes	*Hyaloscypha*	S-NL	(*1*, *2*, *5*)
Leotiomycetes	*Leohumicola*	S-NL	(*1*, *2*, *5*)*
Leotiomycetes	*Leptodontidium*	O	(*5*)*
Leotiomycetes	*Oidiodendron*	OM	(*1*, *2*, *5*, *6*)*
Leotiomycetes	*Phialocephala*	O	(*5*)*
Leotiomycetes	*Pseudogymnoascus*	O	(*5*)*
Pezizomycetes	*Genea*	ECM-NP	(*1*, *2*, *5*)*
Pezizomycetes	*Humaria*	ECM-NP	(*1*, *2*, *5*)*
Pezizomycetes	*Pachyphlodes*	O	(*5*)*
Pezizomycetes	*Pachyphloeus*	ECM-NP	(*1*, *2*, *5*)*
Pezizomycetes	*Peziza*	O	(*1*, *2*, *5*)*
Pezizomycetes	*Scabropezia*	ECM-NP	(*1*, *2*, *5*)*
Sordariomycetes	*Apodus*	S-NL	(*1*, *2*, *5*)*
Sordariomycetes	*Cephalotheca*	S-NL	(*1*, *2*, *5*)*
Sordariomycetes	*Chloridium*	O	(*1*, *2*, *5*)*
Sordariomycetes	*Humicola*	S-NL	(*1*, *2*, *5*)*
Sordariomycetes	*Ilyonectria*	O	(*1*, *2*, *5*)*
Sordariomycetes	*Metarhizium*	O	(*1*, *2*, *5*)*

Table B.1, continued.

Class	Genus	Functional Group	Refs.
Sordariomycetes	*Trichoderma*	S-NL	(*1, 2, 5*)*
Basidiomycota			
Agaricomycetes	*Agrocybe*	S-L	(*7*)
Agaricomycetes	*Amanita*	ECM-NL	(*4*)
Agaricomycetes	*Armillaria*	S-L	(*5*)
Agaricomycetes	*Asterostroma*	S-L	(*5*)
Agaricomycetes	*Athelia*	O	(*5*)
Agaricomycetes	*Athelopsis*	S-L	(*5*)
Agaricomycetes	*Botryobasidium*	S-NL	(*1, 5*)
Agaricomycetes	*Byssocorticium*	ECM-NL	(*5*)
Agaricomycetes	*Clavaria*	S-NL	(*5*)
Agaricomycetes	*Clavulinopsis*	S-NL	(*5*)
Agaricomycetes	*Clitopilus*	S-NL	(*5*)
Agaricomycetes	*Conocybe*	S-NL	(*5*)
Agaricomycetes	*Cortinarius*	ECM-P	(*4, 8*)
Agaricomycetes	*Craterellus*	ECM-NL	(*1*)
Agaricomycetes	*Cuphophyllus*	S-NL	(*5*)
Agaricomycetes	*Entoloma*	S-NL	(*5, 9*)
Agaricomycetes	*Flagelloscypha*	S-NL	(*5*)
Agaricomycetes	*Gliophorus*	OM	(*5*)
Agaricomycetes	*Gymnopus*	S-L	(*9*)
Agaricomycetes	*Hebeloma*	ECM-P	(*4*)
Agaricomycetes	*Hortiboletus*	ECM-NP	(*1–3*)
Agaricomycetes	*Humidicutis*	OM	(*5*)
Agaricomycetes	*Hydnum*	ECM-NP	(*4*)
Agaricomycetes	*Hygrocybe*	OM	(*5, 9, 10*)
Agaricomycetes	*Hygrophorus*	ECM-P	(*5, 8*)
Agaricomycetes	*Hymenogaster*	ECM-NP	(*5*)
Agaricomycetes	*Inocybe*	ECM-NP	(*5*)
Agaricomycetes	*Kuehneromyces*	S-L	(*5*)
Agaricomycetes	*Laccaria*	ECM-P	(*3, 4*)
Agaricomycetes	*Lactarius*	ECM-P	(*4, 8*)
Agaricomycetes	*Lactifluus*	ECM-P	(*11*)
Agaricomycetes	*Marasmius*	S-L	(*9*)
Agaricomycetes	*Membranomyces*	ECM-NP	(*5*)
Agaricomycetes	*Mycena*	S-L	(*9*)
Agaricomycetes	*Mycenella*	O	(*5*)
Agaricomycetes	*Piloderma*	ECM-P	(*3*)
Agaricomycetes	*Porotheleum*	O	(*5*)
Agaricomycetes	*Protoglossum*	ECM-NL	(*5*)
Agaricomycetes	*Pseudoomphalina*	S-NL	(*5*)
Agaricomycetes	*Pseudotricholoma*	O	(*5*)
Agaricomycetes	*Ramaria*	S-L	(*9*)

Table B.1, continued.

Class	Genus	Functional Group	Refs.
Agaricomycetes	*Rectipilus*	S-NL	(*5*)
Agaricomycetes	*Rhodocollybia*	S-NL	(*5*)
Agaricomycetes	*Rigidoporus*	S-L	(*5*)
Agaricomycetes	*Russula*	ECM-P	(*4*, *8*)
Agaricomycetes	*Scleroderma*	ECM-NP	(*1*, *4*)
Agaricomycetes	*Sebacina*	OM	(*1*, *3*, *4*)
Agaricomycetes	*Sphaerobolus*	S-L	(*5*)
Agaricomycetes	*Steccherinum*	S-L	(*5*)
Agaricomycetes	*Tomentella*	ECM-NP	(*5*)
Agaricomycetes	*Trechispora*	S-L	(*9*)
Agaricomycetes	*Tricholoma*	ECM-NP	(*4*)
Agaricomycetes	*Xenasmatella*	S-L	(*5*)
Agaricomycetes	*Xylodon*	S-L	(*5*)
Geminibasidiomycetes	*Geminibasidium*	S-NL	(*1*, *2*, *5*)*
Tremellomycetes	*Apiotrichum*	S-NL	(*1*, *2*, *5*)*
Tremellomycetes	*Saitozyma*	S-NL	(*1*, *2*, *12*)*
Tremellomycetes	*Solicoccozyma*	S-NL	(*1*, *2*, *12*)*
Calcarisporiellomycota			
Calcarisporiellomycetes	Calcarisporiella	S-NL	(*1*, *2*, *5*)*
Chytridiomycota			
Rhizophydiomycetes	Rhizophydium	O	(*1*, *2*, *5*)*
Glomeromycota			
Glomeromycetes	Glomus	OM	(*13*)
Glomeromycetes	Rhizophagus	OM	(*13*)
Mortierellomycota			
Mortierellomycetes	Mortierella	S-NL	(*1*, *2*, *5*, *14*)*
Mucoromycota			
Mucoromycetes	Absidia	S-NL	(*1*, *2*, *5*)*
Umbelopsidomycetes	Umbelopsis	S-NL	(*1*, *2*, *5*)*

[1](Nagy *et al.* 2016); [2](Floudas *et al.* 2012); [3](Kohler *et al.* 2015); [4](Miyauchi *et al.* 2020); [5](Nguyen *et al.* 2016); [6](Martino *et al.* 2018); [7](Ruiz-Dueñas *et al.* 2021); [8](Bödeker *et al.* 2009); [9](Entwistle *et al.* 2018b); [10](Seitzman *et al.* 2011); [11](De Crop *et al.* 2017); [12](Mašínová *et al.* 2017); [13](Smith & Read 2010); [14](Sterkenburg *et al.* 2018)

Table B.2: GAMM results for relationships between the relative abundance of fungal functional groups and soil inorganic N availability (n = 68). Each row represents an independent GAMM with the relative abundance of a functional group in a habitat (either soil or decaying fine root litter) as the dependent variable and soil inorganic N availability as the independent variable. We explicitly accounted for spatial autocorrelation in GAMM models with a spatial correlation structure using the geographic coordinates of each plot. *P*-values were adjusted for false discovery rate using the Benjamini-Hochberg procedure. Statistically significant relationships are bolded.

Functional group	$R^2_{adj.}$	F	$P_{adj.}$
Soil			
ECM with peroxidases	**0.455**	**9.87**	**<0.001**
ECM without peroxidases	**0.079**	**6.92**	**0.025**
Other mycorrhizas	0.006	1.39	0.323
Ligninolytic saprotrophs	**0.064**	**5.70**	**0.034**
Non-ligninolytic saprotrophs	**0.284**	**28.08**	**<0.001**
Other or uncertain ecology	0	0.01	0.912
Decaying fine roots			
ECM with peroxidases	**0.516**	**11.98**	**<0.001**
ECM without peroxidases	0.061	3.22	0.116
Other mycorrhizas	**0.072**	**6.04**	**0.033**
Ligninolytic saprotrophs	0.002	1.17	0.337
Non-ligninolytic saprotrophs	**0.189**	**16.82**	**<0.001**
Other or uncertain ecology	-0.013	1.05	0.337

Table B.3: GAMM results for relationships between the relative abundance of fungal functional groups or SOM and soil inorganic N availability (n = 68). Each GAMM contained three additional independent variables (soil pH, volumetric water content, and temperature). We explicitly accounted for spatial autocorrelation in GAMM models with a spatial correlation structure using the geographic coordinates of each plot. Significant relationships between fungal functional groups (Table B.2) or SOM (Table B.9) and inorganic N availability were not affected by the inclusion of these additional environmental variables. Statistically significant relationships are bolded.

Dependent variable	Independent variable	$R^2_{adj.}$	F	*P*-value
Decaying fine root litter				
Ligninolytic saprotrophs	Inorg. N availability	0.067	0.03	0.866
	Soil pH		0.42	0.522
	Soil water content		0.65	0.422
	Soil temperature		6.19	0.016
ECM with peroxidases	Inorg. N availability	0.676	**8.086**	**<0.001**
	Soil pH		4.864	0.031272
	Soil water content		3.327	0.052124
	Soil temperature		8.825	0.002929
Soil				
Ligninolytic saprotrophs	Inorg. N availability	0.029	3.79	0.056
	Soil pH		0.39	0.537
	Soil water content		0.49	0.486
	Soil temperature		0.02	0.879
ECM with peroxidases	Inorg. N availability	0.625	**10.42**	**<0.001**
	Soil pH		**4.33**	**0.042**
	Soil water content		**5.29**	**0.008**
	Soil temperature		0.00	0.971
SOM				
Lignin-derived SOM	Inorg. N availability	0.624	**7.98**	**0.001**
	Soil pH		**6.12**	**<0.001**
	Soil water content		1.86	0.178
	Soil temperature		2.55	0.116
Soil C	Inorg. N availability	0.597	**9.46**	**0.003**
	Soil pH		**11.18**	**<0.001**
	Soil water content		0.39	0.536
	Soil temperature		2.20	0.102

Table B.4: Summary of sequencing yield pre- and post-quality filtering. These values do not include the four outlier plots removed from our analyses as described in Figure B.4.

Habitat	Raw reads	High-quality reads	% retained
Decaying fine roots	13,783,181	10,123,975	73.5%
Soil	12,263,093	9,677,542	78.9%
Total	26,046,274	19,801,517	76.0%

Table B.5: Summary of ASVs. These values do not include the four outlier plots removed from our analyses as described in Figure B.4.

Habitat	ASVs
Decaying fine roots	9,388
Soil	18,702
Total	22,911

Table B.6: Percentage of fungal reads classified by phylum for soil and decaying fine root litter. Percentages are based on the total number of reads with the four outlier plots removed (see Figure B.4).

Decaying fine root litter		Soil	
Phylum	% of reads	Phylum	% of reads
Basidiomycota	66.2	Basidiomycota	57.8
Ascomycota	24.4	Ascomycota	17.8
Mortierellomycota	5.9	Mortierellomycota	9.8
unclassified Fungi	1.3	Mucoromycota	7.0
Glomeromycota	1.2	unclassified Fungi	4.9
Mucoromycota	0.8	Chytridiomycota	1.0
Chytridiomycota	0.1	Rozellomycota	0.7
Olpidiomycota	0.1	Glomeromycota	0.6
Rozellomycota	0.1	Calcarisporiellomycota	0.3
Zoopagomycota	<0.1	Kickxellomycota	0.1
Kickxellomycota	<0.1	Olpidiomycota	<0.1
Entomophthoromycota	<0.1	Zoopagomycota	<0.1
Basidiobolomycota	<0.1	Monoblepharomycota	<0.1
Calcarisporiellomycota	<0.1	Blastocladiomycota	<0.1
Blastocladiomycota	<0.1	Basidiobolomycota	<0.1
Monoblepharomycota	<0.1	Aphelidiomycota	<0.1
Aphelidiomycota	0	Entomophthoromycota	<0.1
Entorrhizomycota	0	Entorrhizomycota	<0.1

Table B.7: Abundant genera in decaying fine root litter and soil. We defined abundant as occurring in ≥5 plots in a habitat (soil or decaying fine root litter) and accounting for ≥0.1% of sequences in a habitat.

Soil		Decaying fine roots	
Genus	% of sequences	Genus	% of sequences
Mortierella	9.60	Mycena	21.03
Russula	8.82	Mortierella	5.79
Umbelopsis	6.84	Piloderma	4.60
Piloderma	6.23	Russula	3.94
Cortinarius	5.07	Gymnopus	3.37
Hygrocybe	3.51	Trechispora	2.84
Inocybe	2.42	Tomentella	2.70
Solicoccozyma	2.11	Humicola	2.42
Lactifluus	2.05	Lactarius	2.37
Lactarius	1.68	Trichoderma	1.73
Tricholoma	1.58	Ramaria	1.51
Tomentella	1.46	Laccaria	1.16
Cenococcum	1.29	Cenococcum	1.13
Craterellus	1.26	Sebacina	0.81
Amanita	1.25	Hebeloma	0.69
Gliophorus	1.10	Umbelopsis	0.65
Hygrophorus	0.91	Apodus	0.64
Metarhizium	0.78	Agrocybe	0.60
Mycena	0.77	Ilyonectria	0.60
Scabropezia	0.77	Peziza	0.60
Sebacina	0.74	Rigidoporus	0.58
Clavulinopsis	0.69	Cortinarius	0.56
Rhizophydium	0.57	Hyaloscypha	0.54
Laccaria	0.56	Sphaerobolus	0.49
Ramaria	0.52	Byssocorticium	0.45
Entoloma	0.52	Phialocephala	0.44
Clavaria	0.49	Amanita	0.43
Geoglossum	0.48	Conocybe	0.42
Hydnum	0.45	Asterostroma	0.41
Membranomyces	0.45	Flagelloscypha	0.35
Penicillium	0.41	Pseudoomphalina	0.34
Byssocorticium	0.37	Clavulinopsis	0.34
Protoglossum	0.35	Porotheleum	0.34
Pseudotricholoma	0.34	Scleroderma	0.32
Pachyphloeus	0.31	Humaria	0.29
Hebeloma	0.29	Athelopsis	0.28

Table B.7, continued.

Soil		Decaying fine root litter	
Genus	% of sequences	Genus	% of sequences
Humidicutis	0.29	Geoglossum	0.26
Cuphophyllus	0.27	Leptodontidium	0.26
Trichoglossum	0.27	Xenasmatella	0.25
Calcarisporiella	0.26	Cladophialophora	0.24
Saitozyma	0.25	Membranomyces	0.24
Elaphomyces	0.25	Clitopilus	0.22
Glutinoglossum	0.25	Steccherinum	0.22
Cladophialophora	0.24	Cephalotheca	0.21
Rhodocollybia	0.23	Pseudogymnoascus	0.21
Peziza	0.23	Mycenella	0.20
Genea	0.22	Rectipilus	0.20
Trichoderma	0.21	Athelia	0.19
Agrocybe	0.19	Entoloma	0.19
Geminibasidium	0.19	Xylodon	0.19
Apiotrichum	0.19	Rhizophagus	0.16
Oidiodendron	0.18	Chloridium	0.16
Trechispora	0.18	Kuehneromyces	0.15
Scleroderma	0.17	Hygrocybe	0.12
Pachyphlodes	0.15	Inocybe	0.12
Leohumicola	0.14	Marasmius	0.11
Armillaria	0.13	Hortiboletus	0.11
Exophiala	0.13	Botryobasidium	0.11
Glomus	0.13	Glutinoglossum	0.11
Hymenogaster	0.11		
Absidia	0.10		
Gymnopus	0.10		

Table B.8: GAMM results for lignin-derived SOM or soil C as a function of fungal functional groups in soil or decaying fine root litter (n = 68), which were run as four separate models. We explicitly accounted for spatial autocorrelation in GAMM models with a spatial correlation structure using the geographic coordinates of each plot. Statistically significant relationships are bolded.

Dependent variable	Independent variable	$R^2_{adj.}$	F	*P*-value
Fungal functional groups in soil				
Lignin-derived SOM	ECM with peroxidases	0.056	**4.43**	**0.039**
	ECM without peroxidases		1.81	0.166
	Other mycorrhizas		1.20	0.277
	Ligninolytic saprotrophs		3.16	0.081
	Non-ligninolytic saprotrophs		2.16	0.147
	Other or uncertain		1.09	0.384
Soil C	ECM with peroxidases	0.046	**5.85**	**0.019**
	ECM without peroxidases		1.48	0.228
	Other mycorrhizas		1.12	0.294
	Ligninolytic saprotrophs		1.34	0.252
	Non-ligninolytic saprotrophs		3.63	0.062
	Other or uncertain		0.42	0.522
Fungal functional groups in decaying fine root litter				
Lignin-derived SOM	ECM with peroxidases	0.192	1.99	0.164
	ECM without peroxidases		1.86	0.178
	Other mycorrhizas		0.04	0.833
	Ligninolytic saprotrophs		2.72	0.061
	Non-ligninolytic saprotrophs		**6.56**	**0.013**
	Other or uncertain		**4.73**	**0.034**
Soil C	ECM with peroxidases	0	0.24	0.627
	ECM without peroxidases		1.38	0.244
	Other mycorrhizas		0.02	0.894
	Ligninolytic saprotrophs		0.49	0.488
	Non-ligninolytic saprotrophs		0.68	0.411
	Other or uncertain		1.00	0.321

Table B.9: GAMM results for relationships between lignin-derived SOM and inorganic N availability, soil C and lignin-derived SOM, as well as soil C and inorganic N availability (*n* = 68). Each row represents an independent GAMM. We explicitly accounted for spatial autocorrelation in GAMM models with a spatial correlation structure using the geographic coordinates of each plot. Statistically significant relationships are bolded.

Independent variable	Dependent variable	$R^2_{adj.}$	F	*P*-value
Lignin-derived SOM	Inorganic N availability	**0.085**	**5.39**	**0.045**
Soil C	Lignin-derived SOM	**0.407**	**38.14**	**<0.001**
Soil C	Inorganic N availability	**0.069**	**6.14**	**0.016**

APPENDIX C

Supporting Information for Chapter 4: Fungal Community Composition and Genetic Potential Regulate Fine Root Decay in Northern Temperate Forests

William A. Argiroff, Donald R. Zak, Rima A. Upchurch, Peter T. Pellitier, and Julia P. Belke

Supporting Methods C.1

DNA Isolation

We isolated DNA from 0.15 g (three 0.05 g subsamples) of decaying fine roots from each plot (*n* = 72) using the DNeasy Plant Mini Kit (Qiagen) following a modified manufacturer's protocol. The primary modifications included a physical lysis step with four 2.38 mm stainless steel beads at 2,000 rpm for 60 s using the PowerLyzer 24 Bench Top Bead-Based Homogenizer (MoBio Laboratories). Additionally, we pelleted debris from physical and chemical lysis by centrifugation at 16,000 × *g* for 5 minutes. The extracted DNA was purified using the DNeasy PowerClean CleanUp kit following the manufacturer's protocol. We verified the quality of extracted and purified DNA with a NanoDrop 8000 Spectrophotometer (Thermo Scientific) and gel electrophoresis.

PCR and amplicon sequencing

We amplified the ITS2 region of the universal fungal DNA barcode (*i.e.*, the ribosomal internal transcribed spacer using PCR with ITS4-Fun/5.8S-Fun primers (Table C.1). We performed PCR in 25 µL reactions using Phusion High Fidelity DNA Polymerase (New England BioLabs). Each 25 µL PCR consisted of 5 µL of 5X Phusion buffer, 0.25 µL dNTPs (20 mM each dNTP), 0.9375 µL of each indexed ITS4-Fun and 5.8S-Fun (10 µM initial concentration), 0.25 µL Phusion DNA polymerase ($2U \cdot \mu L^{-1}$), 2 µL purified template DNA, and 14.875 µL molecular-grade water. We performed reactions in triplicate in a Mastercycler ProS thermocycler (Eppendorf). We included a negative control (2 µL molecular-grade water instead of template DNA) and a positive control reaction (2 µL template DNA extracted from an *Agaricus bisporus* sporocarp) for each primer combination, and the quality of all reactions was verified using gel

electrophoresis. PCR libraries were normalized and purified using a SequalPrep Normalization Plate Kit (ThermoFisher) and AMPure XP for PCR Purification (Beckman Coulter Life Sciences), and sequenced using MiSeq 2 × 250 bp with v2 chemistry (Illumina) by the University of Michigan Microbiome Core.

Root biochemistry

We characterized the biochemistry of un-decayed fine root litter using pyrolysis gas chromatography-mass spectrometry (py-GC/MS). Ground fine roots were pyrolyzed at 600 °C in quartz tubes for 20 s with a DS pyroprobe 5150 pyrolyzer, and analyzed using a Thermotrace GC Ultra gas chromatograph (Thermo Fisher Scientific) and ITQ 900 mass spectrometer (Thermo Fisher Scientific). AMDIS software and a previously compiled compound library were used to assign spectrometry peaks to compounds, and the relative abundance for each compound was determined by dividing its peak area by the largest peak present in the sample. We summed compounds by the classes from which they originated to determine the relative abundances of aromatics, lignin, lipids, N-bearing, phenols, polysaccharides, proteins, and unknown origin.

Figure C.1: Locations of 12 study sites in northern Lower Michigan, USA.

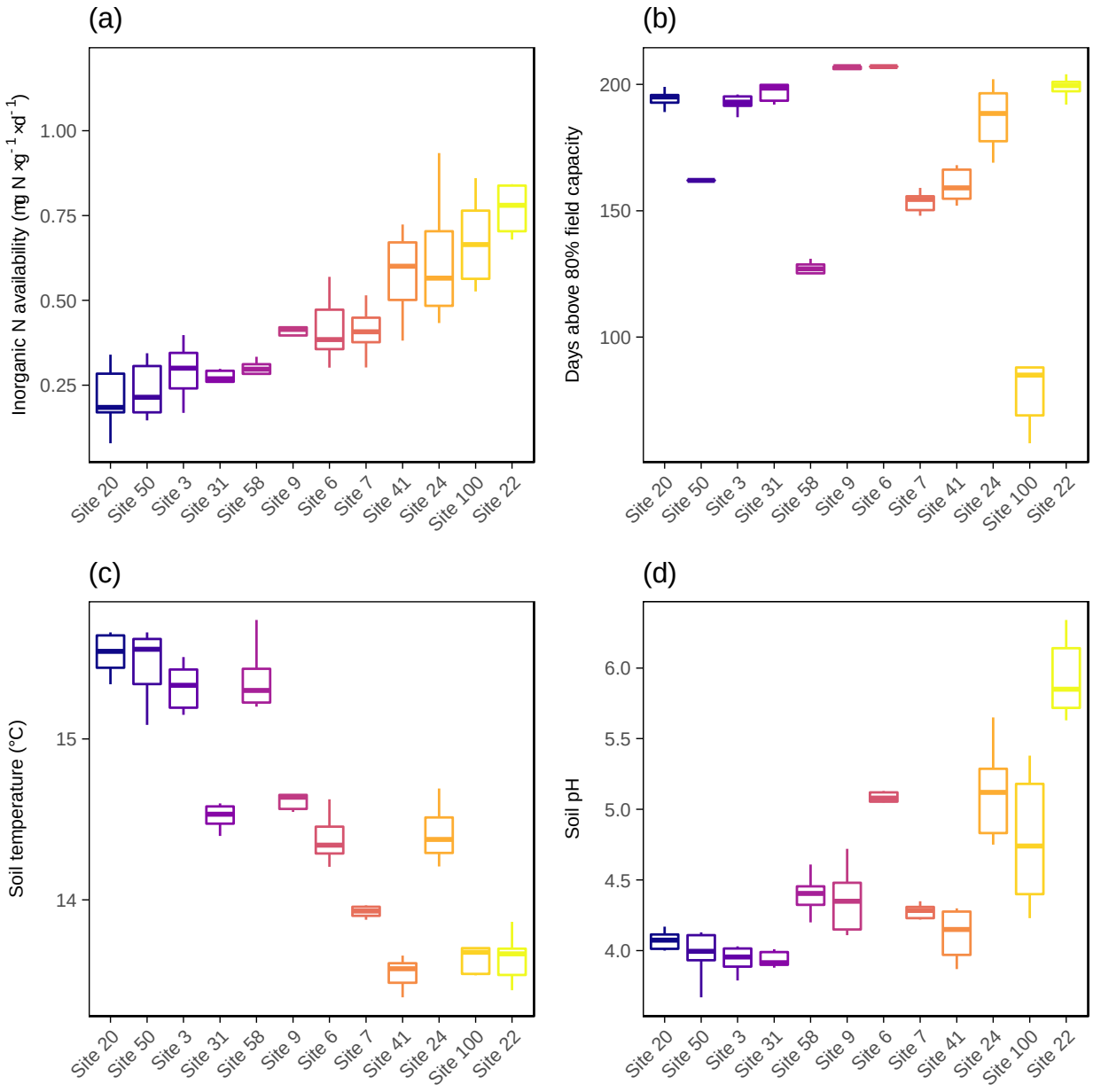

Figure C.2: Inter- and intra-site variation in soil inorganic N availability (a), soil water content (b), soil temperature (c), and soil pH (d) at 70 plots across 12 sites.

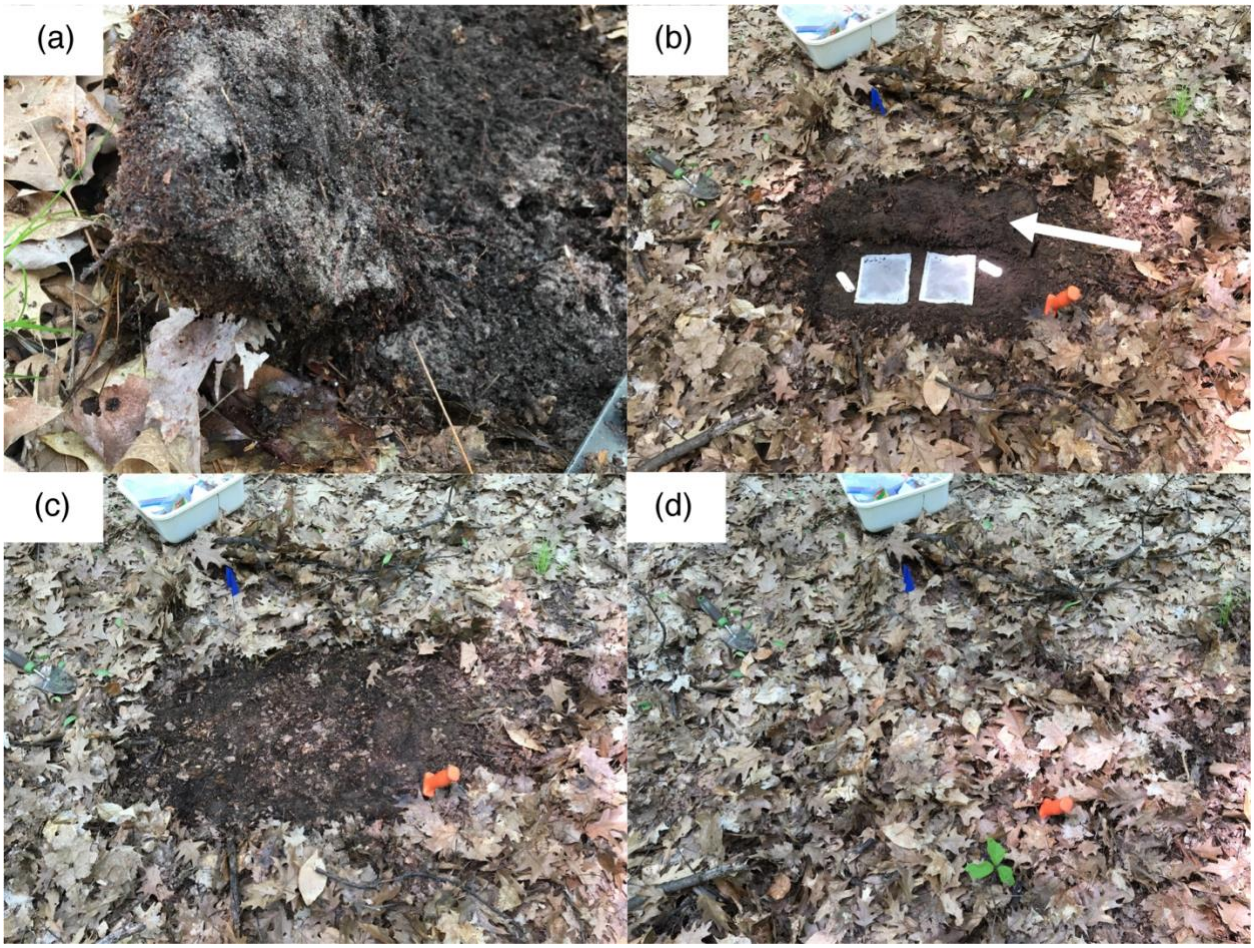

Figure C.3: We placed fine root litter bags at the interface of the Oe and A horizons, which is interpenetrated by a dense mat of fine roots. Mat of fine roots shown peeled away (a) and highlighted by white arrow (b). We replaced the root mat and Oe horizon (c), as well as the Oi horizon (d), over the litter bags. The orange soil knife marks the same location in panels b-d.

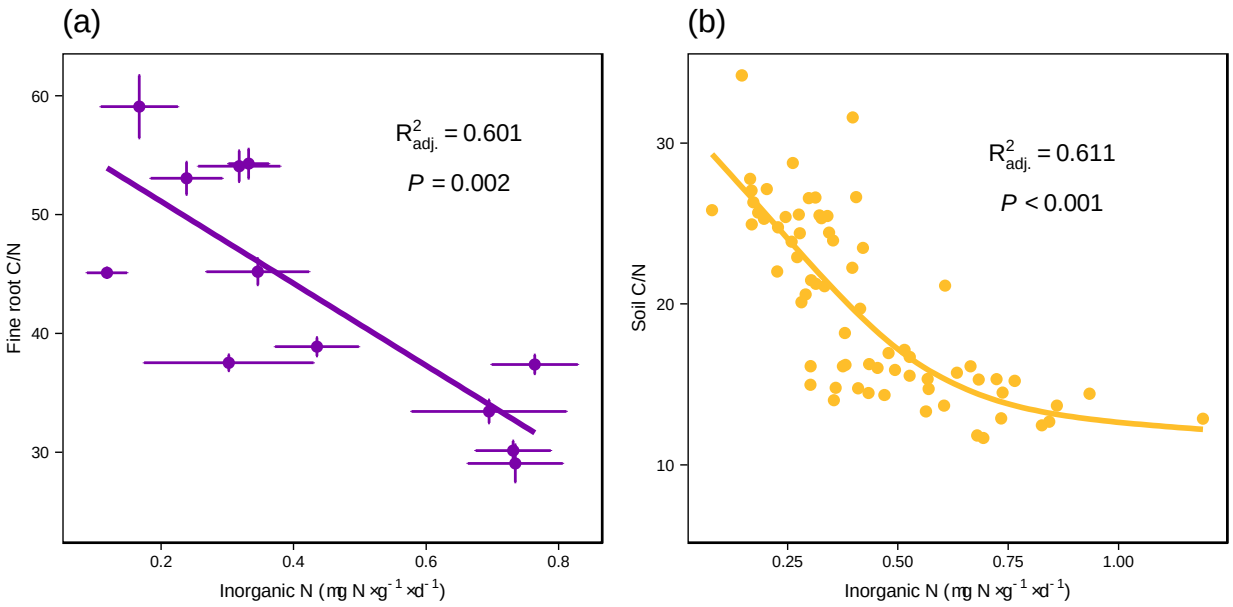

Figure C.4: Relationships between soil inorganic N availability and fine root litter C/N (**a**) and soil C/N (**b**). Trend lines, confidence intervals, R^2, and P-values were determined using simple linear regression (n = 12) for fine root litter and generalized additive modeling (GAM) for soil C/N (n = 70). We used stand means for fine root C/N because fine root litter was composited by stand (error bars are ± one standard error, n = 3 subsamples); inorganic N availability was determined for the soils from which fine roots were obtained at each tree (n = 5) in May, 2018. Simple GAM without spatial autocorrelation structure was used for soil C/N because our interest was in covariation between inorganic N availability and soil C/N rather than causal inference.

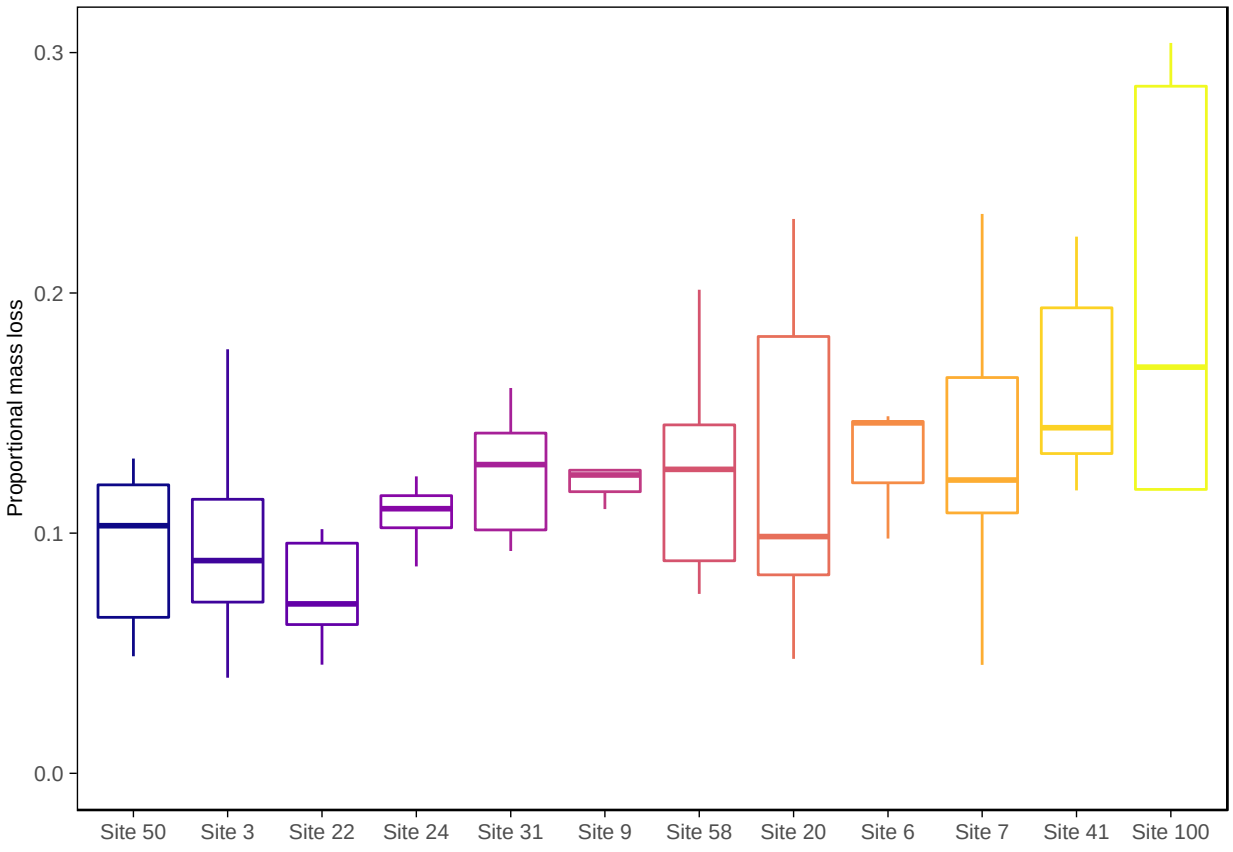

Figure C.5: Fine root decay rates by site.

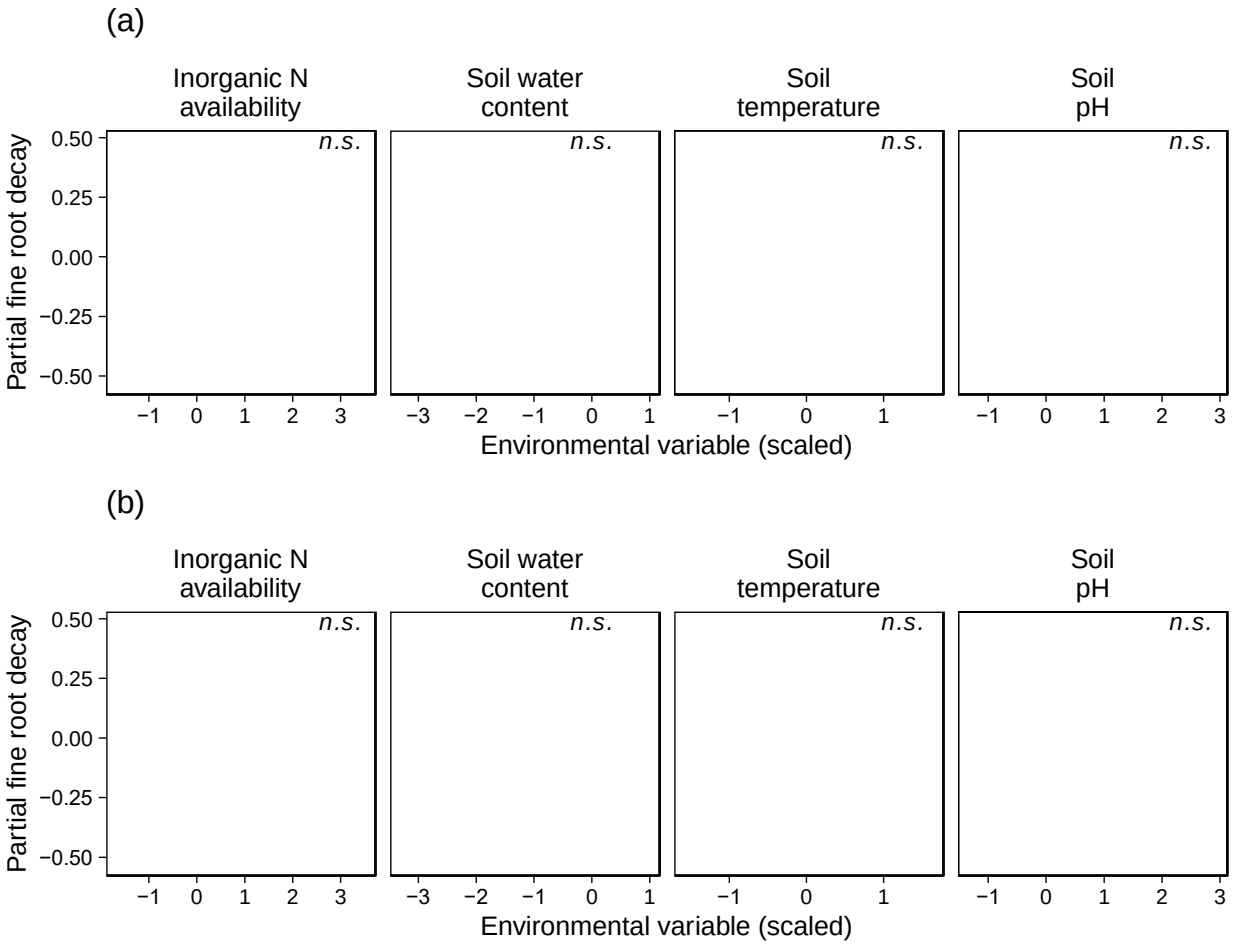

Figure C.6: Partial regression plots showing the relationships between fine root decay and environmental variables included in the GAMMs with the summed abundance of all 58 PCWDEs (a) and rapid decay associated PCWDEs (b) as the additional predictor variable (Figure 4.1b-c and Table C.5). Each predictor was scaled to a mean of 0 and SD of 1 to accurately estimate effect sizes. We accounted for potential spatial autocorrelation using a spatial correlation structure in GAMM models that incorporates the geographic coordinates of each plot (n = 70).

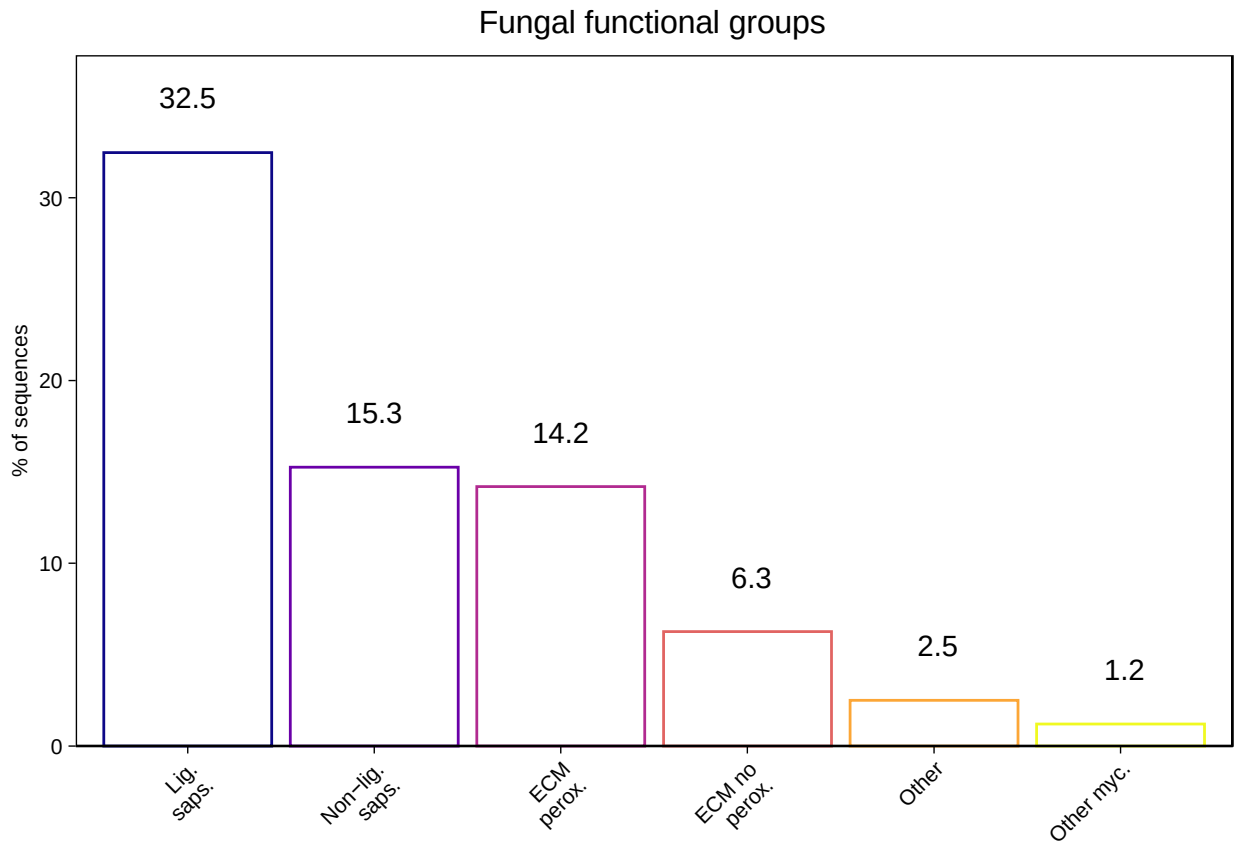

Figure C.7: Percentage of fungal sequences belonging to each fungal functional group in decaying fine root litter. Labels above bars refer to exact percentages. Percentages do not sum to 100% because functional group assignments were only assigned to sequences that were classified at the genus level and belonged to genera that were present in ≥5 plots and accounted for ≥0.1% of sequences. Fungi classified as “other” and “other mycorrhizas” were not included in the analyses because they were a negligible component of the community relative to the four primary groups.

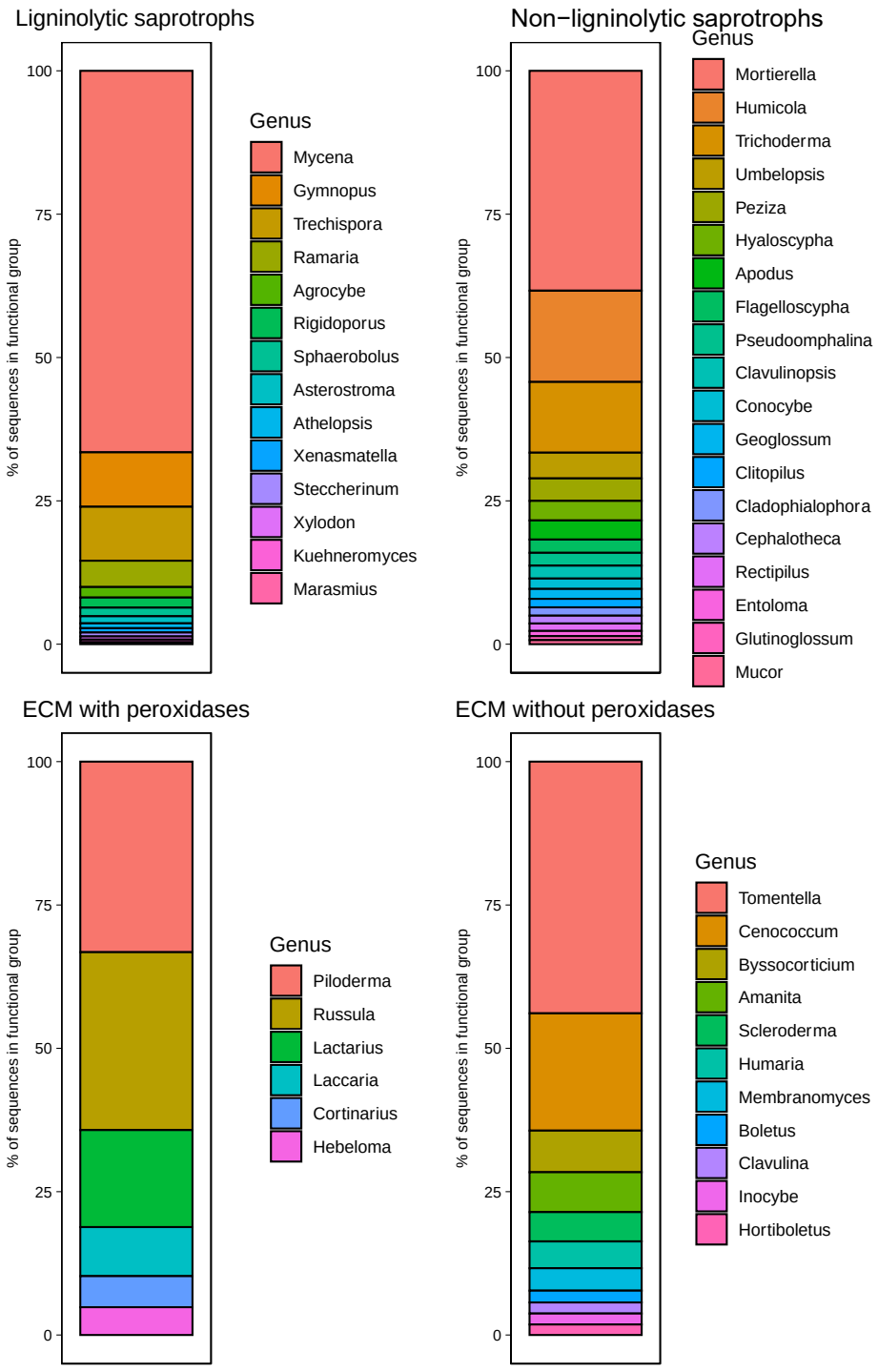

Figure C.8: Percentage of fungal functional groups in decaying roots belonging to specific genera.

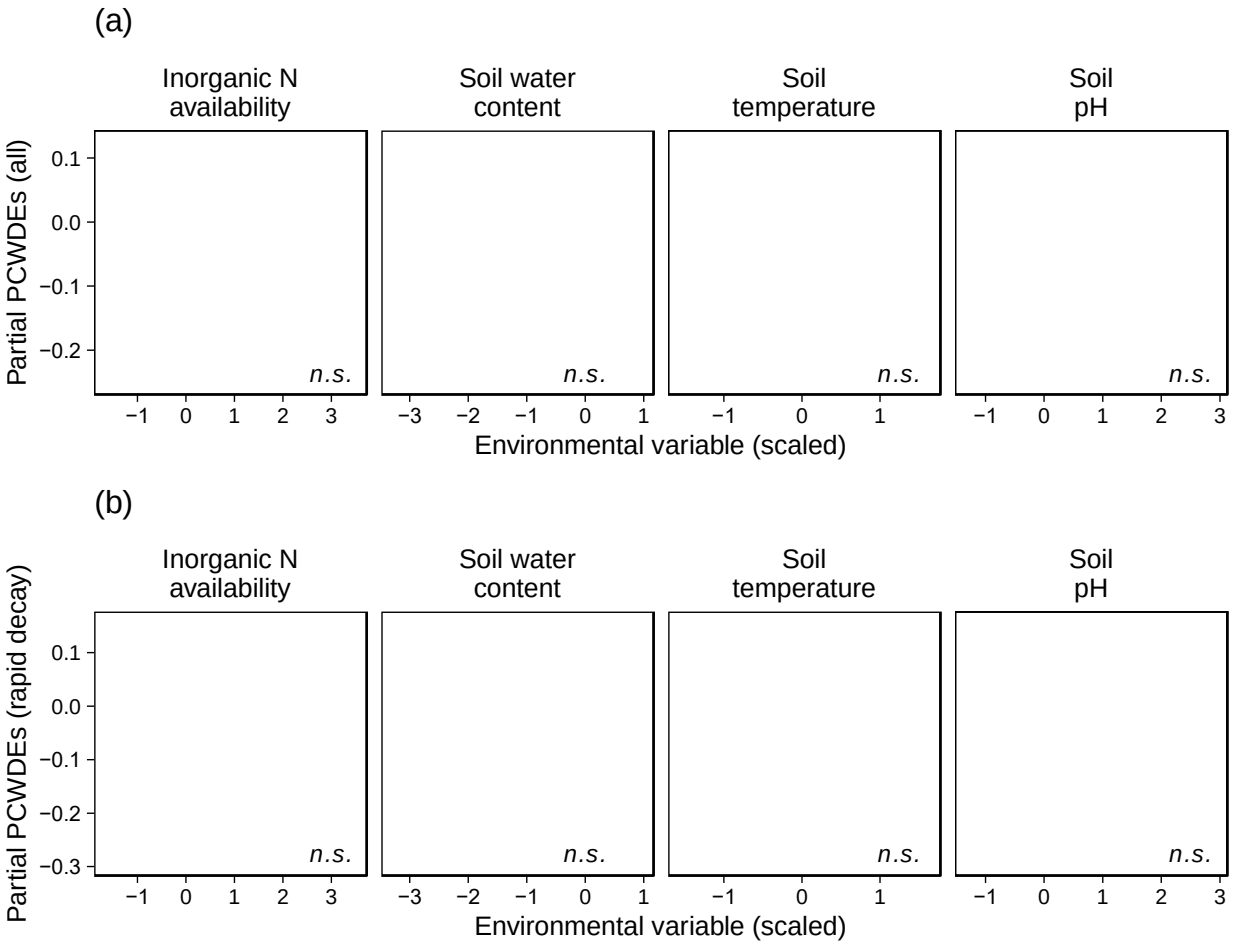

Figure C.9: Partial regression plots showing the relationships between the summed abundance of all 58 PCWDEs (a) and rapid decay associated PCWDEs (b) and environmental variables included in the GAMMs described in Figure 4.2b-c and Table C.9. Each predictor was scaled to a mean of 0 and SD of 1 to accurately estimate effect sizes. We accounted for potential spatial autocorrelation using a spatial correlation structure in GAMM models that incorporates the geographic coordinates of each plot (n = 70).

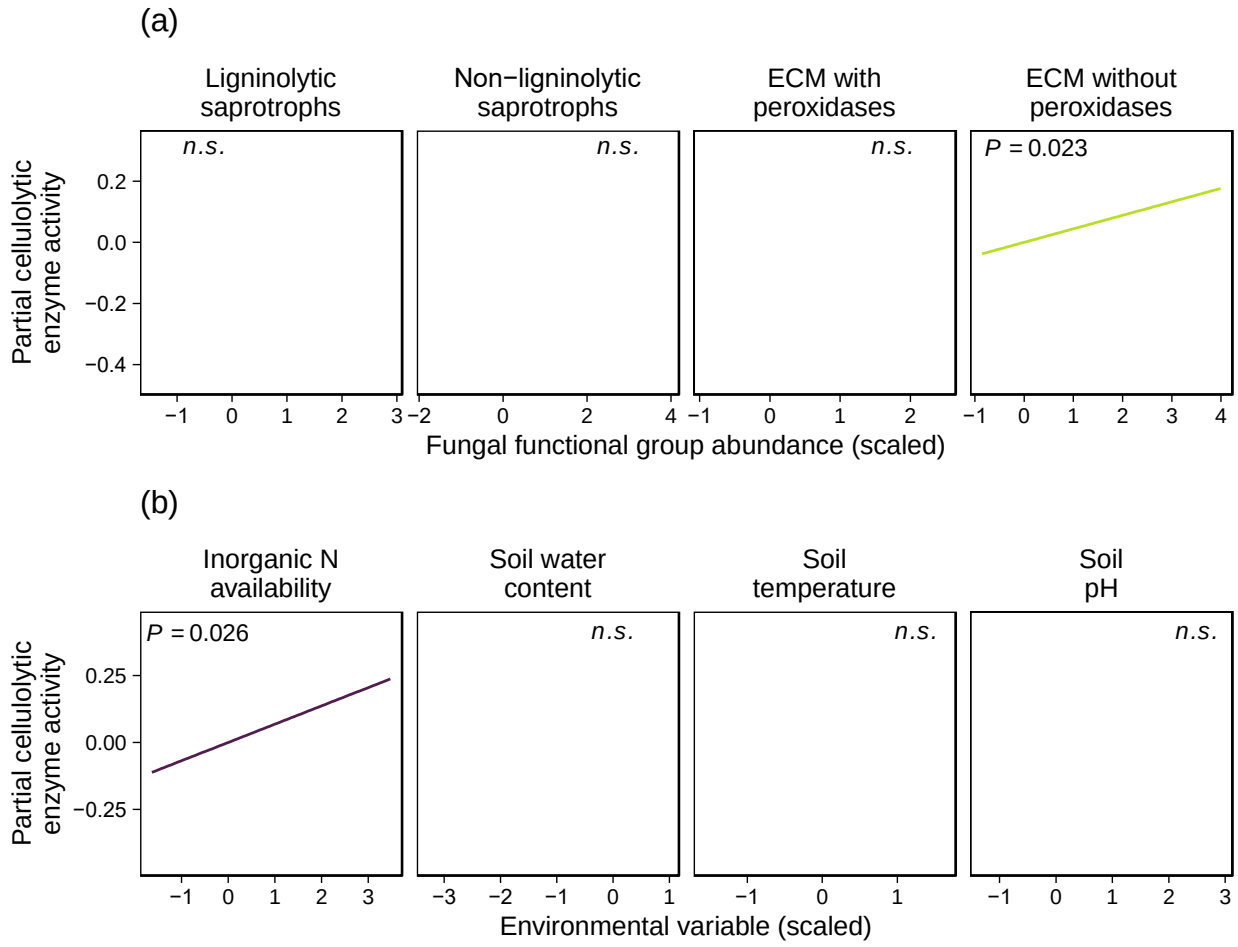

Figure C.10: Partial regressions showing the relationships between cellulolytic enzyme activity and the abundance of fungal functional groups (a) and environmental variables (b). These relationships were evaluated using a single multiple GAMM with four functional groups and four environmental variables as predictors. This model explained 23% of the variance in enzyme activity ($R^2_{adj.}$ = 0.227; Table C.10). The abundance of each functional group was scaled to a mean of 0 and SD of 1 to accurately estimate effect sizes. We accounted for potential spatial autocorrelation using a spatial correlation structure in GAMM models that incorporates the geographic coordinates of each plot (n = 70). *n.s.*, not significant.

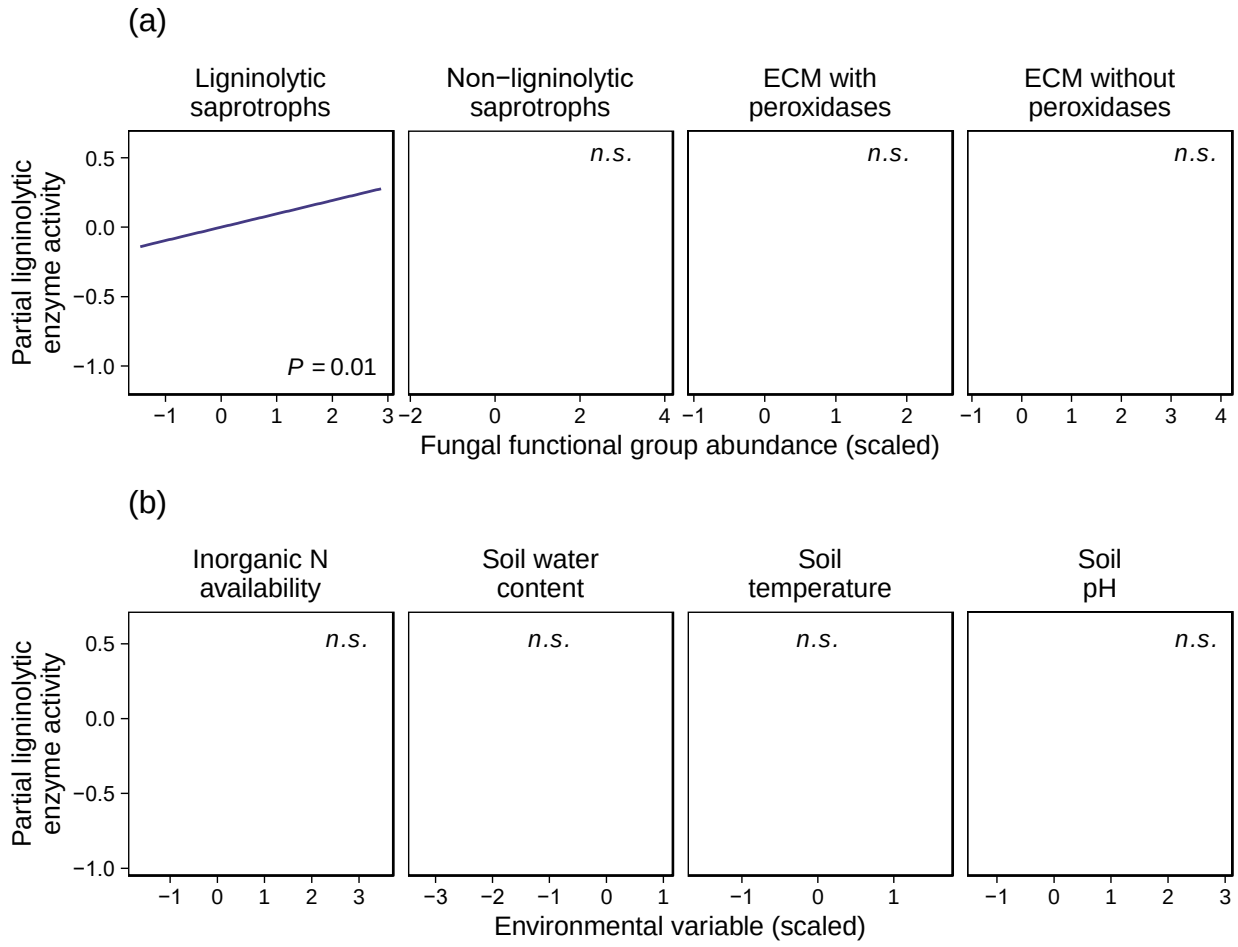

Figure C.11: Partial regressions showing the relationships between ligninolytic enzyme activity and the abundance of fungal functional groups (a) and environmental variables (b). These relationships were evaluated using a single multiple GAMM with four functional groups and four environmental variables as predictors. This model explained 5% of the variance in enzyme activity ($R^2_{adj.}$ = 0.051; Table C.10). The abundance of each functional group was scaled to a mean of 0 and SD of 1 to accurately estimate effect sizes. We accounted for potential spatial autocorrelation using a spatial correlation structure in GAMM models that incorporates the geographic coordinates of each plot (n = 70). *n.s.*, not significant.

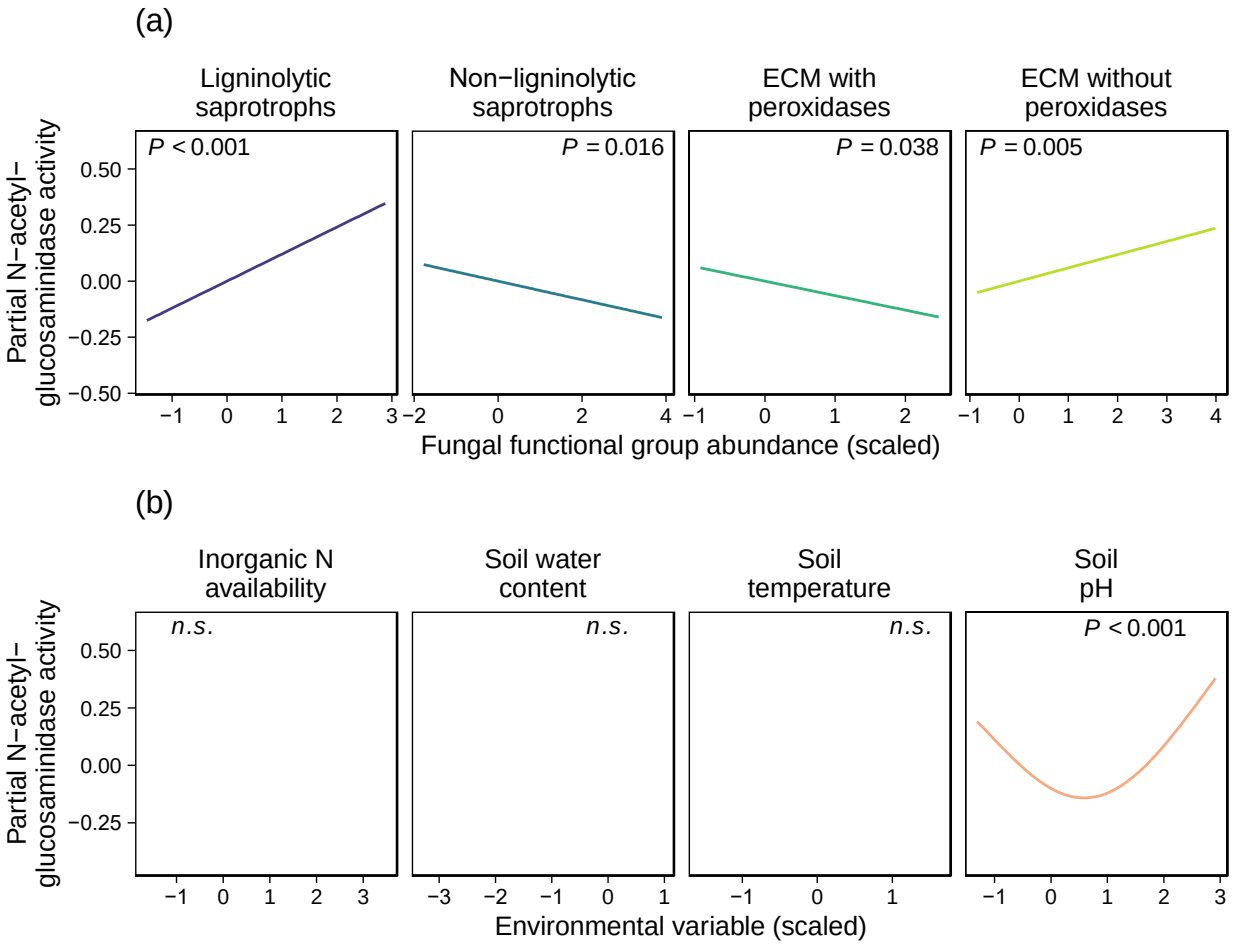

Figure C.12: Partial regressions showing the relationships between N-acetylglucosaminidase activity and the abundance of fungal functional groups (a) and environmental variables (b). These relationships were evaluated using a single multiple GAMM with four functional groups and four environmental variables as predictors. This model explained 38% of the variance in enzyme activity ($R^2_{adj.}$ = 0.379; Table C.10). The abundance of each functional group was scaled to a mean of 0 and SD of 1 to accurately estimate effect sizes. We accounted for potential spatial autocorrelation using a spatial correlation structure in GAMM models that incorporates the geographic coordinates of each plot (n = 70). *n.s.*, not significant.

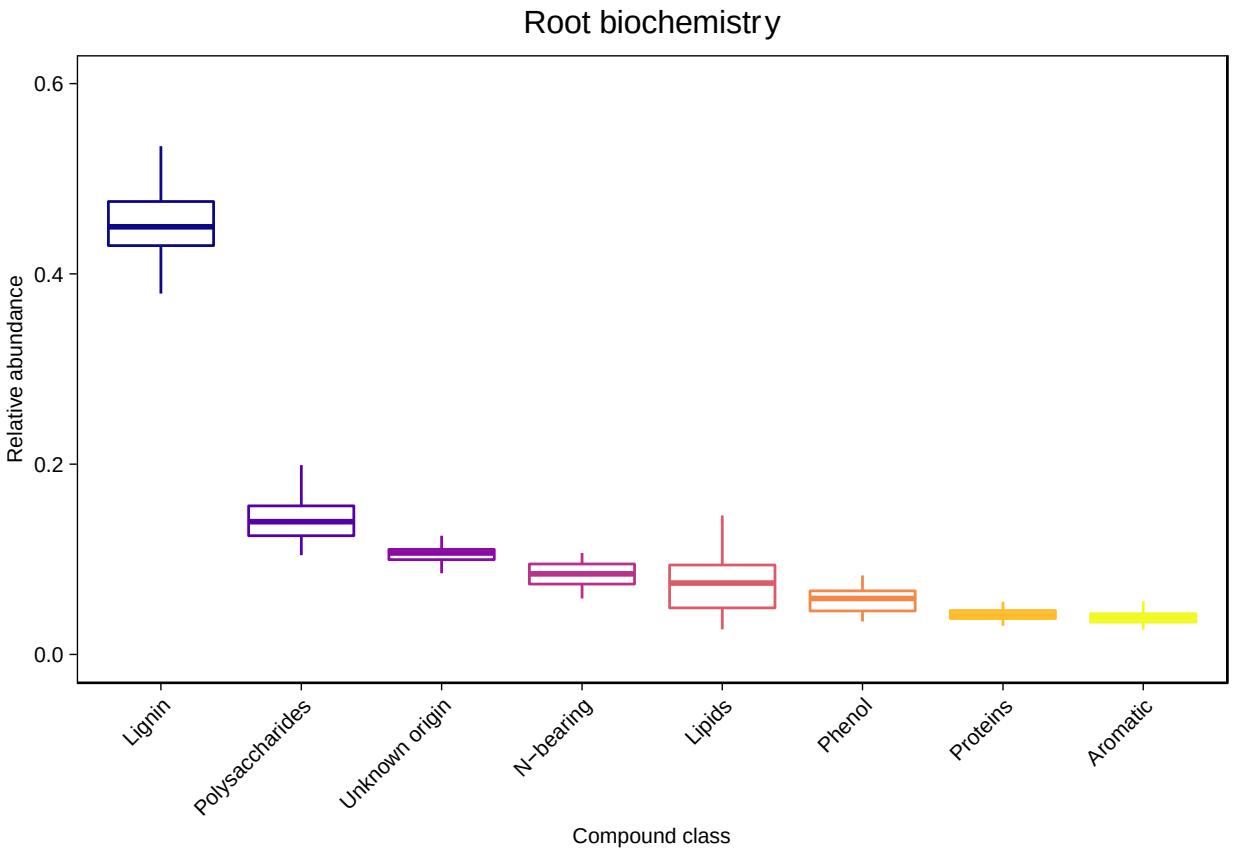

Figure C.13: Fine root biochemistry, represented as the relative abundance of 8 compound classes (n = 36).

Table C.1: Illumina sequencing adapter (i5 or i7), 8-bp Illumina index, 10-bp pad sequence, 2-bp linker sequence, and the base ITS4-Fun or 5.8S-Fun primer.

Primer ID	Primer sequence (5'-3')
Forward	
SA501	AATGATACGGCGACCACCGAGATCTACACATCGTACGTATGGTAATTAAAGCCTCC GCTTATTGATATGCTTAART
SA502	AATGATACGGCGACCACCGAGATCTACACACTATCTGTATGGTAATTAAAGCCTCC GCTTATTGATATGCTTAART
SA503	AATGATACGGCGACCACCGAGATCTACACTAGCGAGTTATGGTAATTAAAGCCTCC GCTTATTGATATGCTTAART
SA504	AATGATACGGCGACCACCGAGATCTACACCTGCGTGTTATGGTAATTAAAGCCTCC GCTTATTGATATGCTTAART
SA505	AATGATACGGCGACCACCGAGATCTACACTCATCGAGTATGGTAATTAAAGCCTCC GCTTATTGATATGCTTAART
SA508	AATGATACGGCGACCACCGAGATCTACACGACACCGTTATGGTAATTAAAGCCTCC GCTTATTGATATGCTTAART
SB501	AATGATACGGCGACCACCGAGATCTACACCTACTATATATGGTAATTAAAGCCTCC GCTTATTGATATGCTTAART
SB502	AATGATACGGCGACCACCGAGATCTACACCGTTACTATATGGTAATTAAAGCCTCC GCTTATTGATATGCTTAART
SB503	AATGATACGGCGACCACCGAGATCTACACAGAGTCACTATGGTAATTAAAGCCTCC GCTTATTGATATGCTTAART
SB504	AATGATACGGCGACCACCGAGATCTACACTACGAGACTATGGTAATTAAAGCCTCC GCTTATTGATATGCTTAART
Reverse	
SA701	CAAGCAGAAGACGGCATACGAGATAACTCTCGAGTCAGTCAGGGAACTTTYRRCA AYGGATCWCT
SA702	CAAGCAGAAGACGGCATACGAGATACTATGTCAGTCAGTCAGGGAACTTTYRRCAA YGGATCWCT
SA703	CAAGCAGAAGACGGCATACGAGATAGTAGCGTAGTCAGTCAGGGAACTTTYRRCA AYGGATCWCT
SA704	CAAGCAGAAGACGGCATACGAGATCAGTGAGTAGTCAGTCAGGGAACTTTYRRCA AYGGATCWCT
SA705	CAAGCAGAAGACGGCATACGAGATCGCACTCAAGTCAGTCAGGGAACTTTYRRCA AYGGATCWCT
SA706	CAAGCAGAAGACGGCATACGAGATCTACGCAGAGTCAGTCAGGGAACTTTYRRCA AYGGATCWCT
SA708	CAAGCAGAAGACGGCATACGAGATGTCGCTCGAGTCAGTCAGGGAACTTTYRRCA AYGGATCWCT
SA709	CAAGCAGAAGACGGCATACGAGATGTCGTAGTAGTCAGTCAGGGAACTTTYRRCA AYGGATCWCT
SB702	CAAGCAGAAGACGGCATACGAGATATACTTCGAGTCAGTCAGGGAACTTTYRRCAA YGGATCWCT
SB703	CAAGCAGAAGACGGCATACGAGATAGCTGCTAAGTCAGTCAGGGAACTTTYRRCA AYGGATCWCT

Table C.2: PCWDE CAZyme families obtained from Ruiz-Dueñas *et al.* (2021).

CAZyme	Enzyme Type	Substrate
GH1	GH	Cellulose and hemicellulose
GH2	GH	Cellulose and hemicellulose
GH3	GH	Cellulose and hemicellulose
GH5_5	GH	Cellulose
GH5_7	GH	Hemicellulose
GH5_22	GH	Hemicellulose
GH6	GH	Cellulose
GH7	GH	Cellulose and hemicellulose
GH9	GH	Cellulose and hemicellulose
GH10	GH	Hemicellulose
GH11	GH	Hemicellulose
GH12	GH	Hemicellulose
GH26	GH	Hemicellulose
GH27	GH	Chitin
GH28	GH	Hemicellulose
GH29	GH	Glycoproteins
GH30_7	GH	Hemicellulose
GH35	GH	Hemicellulose
GH39	GH	Hemicellulose
GH43	GH	Hemicellulose
GH44	GH	Hemicellulose
GH45	GH	Hemicellulose
GH51	GH	Cellulose and hemicellulose
GH53	GH	Hemicellulose
GH54	GH	Hemicellulose
GH62	GH	Hemicellulose
GH67	GH	Hemicellulose
GH74	GH	Cellulose and hemicellulose
GH78	GH	Hemicellulose
GH88	GH	Starch
GH93	GH	Hemicellulose
GH95	GH	Hemicellulose
GH105	GH	Pectin
GH115	GH	Hemicellulose
GH127	GH	Hemicellulose
GH131	GH	Cellulose
GH134	GH	Hemicellulose
PL1	PL	Pectin
PL3	PL	Pectin
PL4	PL	Pectin
PL9	PL	Pectin
PL26	PL	Pectin
CE1	CE	Hemicellulose
CE3	CE	Hemicellulose
CE5	CE	Hemicellulose and cutin
CE8	CE	Pectin
CE12	CE	Hemicellulose and pectin
CE15	CE	Cellulose and hemicellulose
CE16	CE	Hemicellulose
AA1	OX_RE	Lignin
AA2	OX_RE	Lignin

Table C.2, continued.

CAZyme	Enzyme Type	Substrate
AA3	OX_RE	Cellulose and hemicellulose
AA5	OX_RE	Cellulose
AA6	OX_RE	Aromatic compounds
AA9	OX_RE	Cellulose
AA14	OX_RE	Hemicellulose
AA16	OX_RE	Cellulose
CBM1	CBM	Cellulose

Table C.3: Genomes matching genera in decaying root litter, which were used to estimate community-weighted mean decay potentials for fungal communities. NA: genome not available.

Genus	Species	MycoCosm species name	MycoCosm species code
Mycena	albidolilacea	Mycena albidolilacea CBHHK002 v1.0	Mycalb1
Mycena	alexandri	Mycena alexandri CBHHK200 v1.0	Mycale1
Mycena	amicta	Mycena amicta BAPX v1.0	Mycami1
Mycena	belliae	Mycena belliae CBHHK173m v1.0	Mycbel1
Mycena	capillaripes	Mycena capillaripes Frankland 9286 v1.0	Mycrub1
Mycena	crocata	Mycena crocata CBHHK184 v1.0	Myccro1
Mycena	epipterygia	Mycena epipterygia CBHHK145m v1.0	Mycepi1
Mycena	filopes	Mycena filopes CBHHK001 v1.0	Mycfil1
Mycena	floridula	Mycena floridula CBHHK072 v1.0	Mycflo1
Mycena	galericulata	Mycena galericulata CBHHK162m v1.0	Mycgale1
Mycena	galopus	Mycena galopus ATCC-62051 v1.0	Mycgal1
Mycena	haematopus	Mycena haematopus CBHHK189 v1.0	Mychae1
Mycena	latifolia	Mycena latifolia 10383 v1.0	Myclat1
Mycena	leptocephala	Mycena leptocephala CBHHK5/15 v1.0	Myclep1
Mycena	maculata	Mycena maculata CBHHK188m v1.0	Mycmac1
Mycena	metata	Mycena metata CBHHK182m v1.0	Mycmet1
Mycena	olivaceomarginata	Mycena olivaceomarginata CBHHK47/15 v1.0	Mycoli1
Mycena	polygramma	Mycena polygramma CBHHK137 v1.0	Mycpol1
Mycena	pura	Mycena pura 9144 v1.0	Mycpur1
Mycena	rebaudengoi	Mycena rebaudengoi CBHHK068 v1.0	Mycreb1
Mycena	rosella	Mycena rosella CBHHK067 v1.0	Mycros1
Mycena	sanguinolenta	Mycena sanguinolenta CBHHK176m v1.0	Mycsan1
Mycena	sp.	Mycena sp. CBHHK59/15 v1.0	Myc59_1
Mycena	vitilis	Mycena vitilis CBHHK169m v1.0	Mycvit1
Mycena	vulgaris	Mycena vulgaris CBHHK164 v1.0	Mycvul1

Table C.3, continued.

Genus	Species	MycoCosm species name	MycoCosm species code
Umbelopsis	angularis	Umbelopsis angularis P8C34 v1.0	Umban1
Umbelopsis	isabellina	Umbelopsis isabellina AD026 v1.0	Umbisa1
Umbelopsis	ramanniana	Umbelopsis ramanniana AG v1.0	Umbra1
Umbelopsis	sp. nov.	Umbelopsis sp. nov. AD052 v1.0	Umbsp_AD052_1
Umbelopsis	sp_PMI	Umbelopsis sp. PMI123 v1.0	Umbelo1
Piloderma	byssinum	Piloderma byssinum 4S31 v1.0	Pilbys1
Piloderma	olivaceum	Piloderma olivaceum F 1598 v1.0	Pilcr1
Piloderma	sphaerosporum	Piloderma sphaerosporum 354 v1.0	Pilsph1
Russula	brevipes	Russula brevipes BPL707 v1.0	Rusbre1
Russula	compacta	Russula compacta BPL669 v1.0	Ruscom1
Russula	dissimulans	Russula dissimulans BPL704 v1.0	Rusdis1
Russula	earlei	Russula earlei BPL698 v1.0	Rusear1
Russula	emetica	Russula emetica P_ilba v1.0	Ruseme1
Russula	ochroleuca	Russula ochroleuca P_ilba v1.0	Rusoch1
Russula	rugulosa	Russula rugulosa BPL654 v1.0	Rusrug1
Russula	seminuda	Russula seminuda PSC4341-TAS1 v1.0	Russem1
Russula	vinacea	Russula vinacea BPL710 v1.0	Rusvin1
Solicoccozyma	NA	NA	NA
Trechispora	NA	NA	NA
Gymnopus	androsaceus	Gymnopus androsaceus JB14 v1.0	Gyman1
Gymnopus	earleae	Gymnopus earleae GB-263.02 v1.0	Gymear1
Gymnopus	luxurians	Gymnopus luxurians v1.0	Gymlu1
Mortierella	alpina AD266	Mortierella alpina AD266 v1.0	Moralp1_1
Mortierella	alpina KOD1005	Mortierella alpina KOD1005 v1.0	Moramoe1
Mortierella	ambigua	Mortierella ambigua NRRL 28271 v1.0	Moramb1
Mortierella	capitata	Mortierella capitata AV005 v1.0	Morcap1
Mortierella	elongata AG-77	Mortierella elongata AG-77 v2.0	Morel2

Table C.3, continued.

Genus	Species	MycoCosm species name	MycoCosm species code
Mortierella	elongata MPI	Mortierella elongata MPI-CAGE-AA-0104 v1.0	Morel_U14_1
Mortierella	elongata NVP64	Mortierella elongata NVP64 v1.0	MoeNVP64_1
Mortierella	gamsii	Mortierella gamsii AM1032 v1.0	Morgam1
Mortierella	humilis	Mortierella humilis PMI_1414 v1.0	Morhum1
Mortierella	minutissima AD051	Mortierella minutissima AD051 v1.0	Mormin1_1
Mortierella	multidivaricata	Mortierella multidivaricata RSA 2152 T v1.0	Mormul1
Mortierella	sp. AD185	Mortierella sp. AD185 v1.0	MorAD185_1_1
Mortierella	sp. GBAus27b	Mortierella sp. GBAus27b v1.0	MorGBAus27b_1
Mortierella	verticillata	Mortierella verticillata NRRL 6337	Morve1
Mortierella	wolfii	Mortierella wolfii NRRL 6351 v1.0	Morwol1
Lactarius	akahatsu	Lactarius akahatsu QP v1.0	Lacaka1
Lactarius	deliciosus	Lactarius deliciosus 48 v1.0	Lacdel1
Lactarius	hatsudake	Lactarius hatsudake 109 v1.0	Lachat1
Lactarius	hengduanensis	Lactarius hengduanensis 84 v1.0	Lachen1
Lactarius	indigo	Lactarius indigo 2018DUKE089 v1.0	Lacind1
Lactarius	psammicola	Lactarius psammicola BPL869 v1.0	Lacpsa1
Lactarius	pseudohatsudake	Lactarius pseudohatsudake 88 v1.0	Lacpse1
Lactarius	quietus	Lactarius quietus S23C v1.0	Lacqui1
Lactarius	sanguifluus	Lactarius sanguifluus B21 v1.0	Lacsan1
Lactarius	subdulcis	Lactarius subdulcis FM v1.0	Lactsubd1
Lactarius	vividus	Lactarius vividus 141 v1.0	Lacviv1
Laccaria	amethystina	Laccaria amethystina LaAM-08-1 v2.0	Lacam2
Laccaria	bicolor 81306	Laccaria bicolor 81306 v1.0	Lacbi81306_1
Laccaria	bicolor CBS 559.96	Laccaria bicolor CBS 559.96 v1.0	Lacbi55996_1
Laccaria	bicolor CBS 594.89	Laccaria bicolor CBS 594.89 v1.0	Lacbi59489_1

Table C.3, continued.

Genus	Species	MycoCosm species name	MycoCosm species code
Laccaria	bicolor Cham3	Laccaria bicolor Cham3 v1.0	LacbiCham3_1
Laccaria	bicolor D101	Laccaria bicolor D101 v1.0	LacbiD101_1
Laccaria	bicolor DR170	Laccaria bicolor DR170 v1.0	LacbiDR170_1
Laccaria	bicolor N203	Laccaria bicolor N203 v1.0	LacbiN203_1
Laccaria	bicolor S238N 93.12	Laccaria bicolor S238N 93.12 v1.1	Lacbi9312_2
Laccaria	bicolor S238N	Laccaria bicolor S238N v1.0	LacbiS238N_1
Laccaria	bicolor S238N-H53	Laccaria bicolor S238N-H53 v1.0	LacbiH53_1
Laccaria	bicolor S238N-H70	Laccaria bicolor S238N-H70 v1.0	LacbiH70_1
Laccaria	bicolor S238N-H82	Laccaria bicolor S238N-H82 v1.0	LacbiH82_1
Laccaria	bicolor S238N-H82xH70	Laccaria bicolor S238N-H82xH70 v1.0	LacbiH82xH70_1
Laccaria	bicolor S238O	Laccaria bicolor S238O v1.0	LacbiS238O_1
Amanita	muscaria Koide	Amanita muscaria Koide v1.0	Amamu1
Amanita	muscaria var. formosa	Amanita muscaria var. formosa 2016PMI152 v1.0	Amaapr1
Amanita	rubescens	Amanita rubescens P_ilba v1.0	Amarub1
Amanita	thiersii	Amanita thiersii Skay4041 v1.0	Amath1
Trichoderma	arundinaceum IBT 40837	Trichoderma arundinaceum IBT 40837	Triaru1
Trichoderma	asperelloides	Trichoderma asperelloides TR356 v1.0	Triasp1
Trichoderma	asperellum	Trichoderma asperellum CBS 433.97 v1.0	Trias1
Trichoderma	atrobrunneum	Trichoderma atrobrunneum ITEM 908	Triatrob1
Trichoderma	atroviride B10	Trichoderma atroviride B10 v1.0	Triatr1
Trichoderma	atroviride F7	Trichoderma atroviride F7 v1.0	Triatro1
Trichoderma	atroviride P1	Trichoderma atroviride P1 v1.0	Triatrov1
Trichoderma	atroviride	Trichoderma atroviride v2.0	Triat2
Trichoderma	brevicompactum IBT40841	Trichoderma brevicompactum IBT40841	Tribre1
Trichoderma	citrinoviride	Trichoderma citrinoviride TUCIM 6016 v4.0	Trici4

Table C.3, continued.

Genus	Species	MycoCosm species name	MycoCosm species code
Trichoderma	gamsii	Trichoderma gamsii T6085	Trigam1
Trichoderma	guizhouense	Trichoderma guizhouense NJAU 4742	Trigui1
Trichoderma	harzianum CBS	Trichoderma harzianum CBS 226.95 v1.0	Triha1
Trichoderma	harzianum M10	Trichoderma harzianum M10 v1.0	TriharM10_1
Trichoderma	harzianum T22	Trichoderma harzianum T22 v1.0	TriharT22_1
Trichoderma	harzianum TR274	Trichoderma harzianum TR274 v1.0	Trihar1
Trichoderma	longibrachiatum	Trichoderma longibrachiatum ATCC 18648 v3.0	Trilo3
Trichoderma	longibrachiatum	Trichoderma longibrachiatum MK1 v1.0	Trilon1
Trichoderma	parareesei	Trichoderma parareesei CBS 125925	Tripar1
Trichoderma	pleuroti TPhu1	Trichoderma pleuroti TPhu1	Triple1
Trichoderma	reesei QM6a	Trichoderma reesei QM6a	Trire_Chr
Trichoderma	reesei RUT C-30	Trichoderma reesei RUT C-30 v1.0	TrireRUTC30_1
Trichoderma	reesei v2.0	Trichoderma reesei v2.0	Trire2
Trichoderma	virens	Trichoderma virens Gv29-8 v2.0	TriviGv29_8_2
Trichoderma	hamatum	Trichoderma hamatum GD12	Triham1
Cenococcum	geophilum	Cenococcum geophilum 1.58 v2.0	Cenge3
Inocybe	NA	NA	NA
Hebeloma	brunneifolium	Hebeloma brunneifolium PMI1Jessy v2.0	Hebvel2
Hebeloma	cylindrosporum	Hebeloma cylindrosporum h7 v2.0	Hebcy2
Lactifluus	subvellereus	Lactifluus cf. subvellereus BPL653 v1.0	Lacsub1
Lactifluus	volemus	Lactifluus cf. volemus BPL652 v1.0	Lacvol1
Ramaria	rubella	Ramaria rubella (R. acris) UT-36052-T v1.0	Ramac1
Craterellus	NA	NA	NA
Tomentella	NA	NA	NA
Membranomyces	NA	NA	NA
Scabropezia	NA	NA	NA
Metarhizium	acridum	Metarhizium acridum CQMa 102	Metac1
Metarhizium	anisopliae	Metarhizium anisopliae ARSEF 549	Metani1

Table C.3, continued.

Genus	Species	MycoCosm species name	MycoCosm species code
Metarhizium	brunneum	Metarhizium brunneum ARSEF3297	Metbr1
Metarhizium	robertsii	Metarhizium robertsii ARSEF 23	Metro1
Cortinarius	aff. campbellae	Cortinarius aff. campbellae TAS5-PSC4363 v1.0	Corcam1
Cortinarius	austrovenetus	Cortinarius austrovenetus TL2843-KIS7R v1.0	Coraus1
Cortinarius	glaucopus	Cortinarius glaucopus AT 2004 276 v2.0	Corgl3
Cortinarius	sp.	Cortinarius sp. KIS3-TL2766 v1.0	CorKIS3_1
Peziza	echinospora	Peziza echinospora CBS 144458 v1.0	Pezech1
Hygrocybe	NA	NA	NA
Gliophorus	NA	NA	NA
Clavaria	NA	NA	NA
Hydnum	rufescens	Hydnum rufescens UP504 v2.0	Hydru2
Conocybe	apala	Conocybe apala SZMC-NL-8967 v1.0	Conapa1
Sebacina	vermifera	Sebacina vermifera MAFF 305830 v1.0	Sebve1
Porotheleum	NA	NA	NA
Pseudoomphalina	NA	NA	NA
Tricholoma	populinum	Tricholoma populinum 2016PMI031 v1.0	Tripop1
Tricholoma	matsutake	Tricholoma matsutake 945 v3.0	Trima3
Rigidoporus	microporus	Rigidoporus microporus ED310 v1.0	Rigmic1
Humaria	NA	NA	NA
Geoglossum	NA	NA	NA
Phialocephala	scopiformis	Phialocephala scopiformis 5WS22E1 v1.0	Phisc1
Leptodontidium	sp.	Leptodontidium sp. MPI-SDFR-AT-0119 v2.0	Lepor2
Leptodontidium	sp.	Leptodontium sp. PMI_412 v1.0	Leptod1
Hyaloscypha	finlandica	Hyaloscypha finlandica PMI_746 v1.0	Hyafin1
Scleroderma	citrinum	Scleroderma citrinum hr. v1.0	Sclcihr1
Scleroderma	citrinum	Scleroderma citrinum Foug A v1.0	Sclci1
Hygrophorus	NA	NA	NA
Rhizophydium	NA	NA	NA
Humidicutis	NA	NA	NA
Clavulinopsis	NA	NA	NA
Pseudogymnoascus	destructans	Pseudogymnoascus destructans 20631-21	Pseudest1

Table C.3, continued.

Genus	Species	MycoCosm species name	MycoCosm species code
Byssocorticium	NA	NA	NA
Apiotrichum	NA	NA	NA
Saitozyma	NA	NA	NA
Humicola	NA	NA	NA
Pachyphloeus	NA	NA	NA
Rhodocollybia	butyracea	Rhodocollybia butyracea CCBAS 279 v1.0	Rhobu1
Rhodocollybia	butyracea	Rhodocollybia butyracea AH 40177 v1.0	Rhobut1_1
Cuphophyllus	NA	NA	NA
Pseudotricholoma	NA	NA	NA
Athelopsis	NA	NA	NA
Apodus	NA	NA	NA
Flagelloscypha	sp.	Flagelloscypha sp. PMI_526 v1.0	FlaPMI526_1
Clitopilus	NA	NA	NA
Protoglossum	NA	NA	NA
Xylodon	NA	NA	NA
Xenasmatella	tulasnelloidea	Xenasmatella tulasnelloidea OMC1662 v1.0	Xentul1
Xenasmatella	vaga	Xenasmatella vaga CBS212.54 v1.0	Xenvag1
Sphaerobolus	stellatus	Sphaerobolus stellatus v1.0	Sphst1
Genea	NA	NA	NA
Penicillium	sp.	Penicillium sp. DTU1 v1.0	Aspcris1
Penicillium	antarcticum	Penicillium antarcticum DTO 356-E5 v1.0	Penanta1
Penicillium	atramentosum	Penicillium atramentosum RS17 v1.0	Penatra1
Penicillium	bilaiae	Penicillium bilaiae ATCC 20851 v1.0	Penbi1
Penicillium	brevicompactum	Penicillium brevicompactum 1011305 v2.0	Penbr2
Penicillium	brevicompactum	Penicillium brevicompactum AgRF18 v1.0	PenbrAgRF18_1
Penicillium	canescens	Penicillium canescens ATCC 10419 v1.0	Penca1
Penicillium	chrysogenum	Penicillium chrysogenum v1.0	Pench1
Penicillium	chrysogenum	Penicillium chrysogenum Wisconsin 54-1255	PenchWisc1_1
Penicillium	citreonigrum	Penicillium citreonigrum cont 1189274 v1.0	Pencit1
Penicillium	digitatum	Penicillium digitatum PHI26	Pendi1
Penicillium	expansum	Penicillium expansum ATCC 24692 v1.0	Penex1

Table C.3, continued.

Genus	Species	MycoCosm species name	MycoCosm species code
Penicillium	fellutanum	Penicillium fellutanum ATCC 48694 v1.0	Penfe1
Penicillium	glabrum	Penicillium glabrum DAOM 239074 v1.0	Pengl1
Penicillium	janthinellum	Penicillium janthinellum ATCC 10455 v1.0	Penja1
Penicillium	lanosocoeruleum	Penicillium lanosocoeruleum ATCC 48919 v1.0	Penla1
Penicillium	malodoratum	Penicillium malodoratum CBS 490.65 v1.0	Penmal1
Penicillium	oxalicum	Penicillium oxalicum 114-2	Penox1
Penicillium	raistrickii	Penicillium raistrickii ATCC 10490 v1.0	Penra1
Penicillium	solitum	Penicillium solitum IBT 30036 v1.0	Pensoli1
Penicillium	subrubescens	Penicillium subrubescens FBCC1632 / CBS132785	Pensub1
Penicillium	swiecickii	Penicillium swiecickii 182 6C1 v1.0	Penswi1
Penicillium	thymicola	Penicillium thymicola DAOMC 180753 v1.0	Penth1
Penicillium	vulpinum	Penicillium vulpinum IBT 29486	Penvul1
Penicillium	sp.	Penicillium sp. NC0857 v1.0	ThyNC0857_1
Glutinoglossum	NA	NA	NA
Agrocybe	praecox	Agrocybe praecox OKM6292 v1.0	Agrpra2
Agrocybe	pediades	Agrocybe pediades AH 40210 v1.0	Agrped1
Boletus	coccyginus	Boletus coccyginus 2016PMI039 v1.0	Bolcoc1
Boletus	edulis	Boletus edulis BED1 v4.0	Boled5
Boletus	edulis	Boletus edulis P_ilba v1.0	Boledp1
Exophiala	alcalophila	Exophiala alcalophila ATCC 48519 v1.0	Exoalc1
Exophiala	alcalophila	Exophiala alcalophila J33 v1.0	Exoalc1_J33
Exophiala	aquamarina	Exophiala aquamarina CBS 119918	Exoaq1
Exophiala	limosus	Exophiala limosus JF 03-4F Slimy v1.0	EurotioJF034F_1
Exophiala	mesophila	Exophiala mesophila CBS40295	Exome1
Exophiala	oligosperma	Exophiala oligosperma CBS72588	Exool1
Exophiala	sideris	Exophiala sideris CBS121828	Exosi1
Exophiala	sp.	Exophiala sp. JF 06-1F Fuzzy v1.0	ExoJF061F_1

Table C.3, continued.

Genus	Species	MycoCosm species name	MycoCosm species code
Exophiala	spinifera	Exophiala spinifera CBS89968	Exosp1
Exophiala	viscosium	Exophiala viscosium JF 03-3F Goopy v1.0	EurotioJF033F_1
Exophiala	xenobiotica	Exophiala xenobiotica CBS118157	Exoxe1
Mycenella	NA	NA	NA
Clavulina	NA	NA	NA
Chloridium	NA	NA	NA
Steccherinum	NA	NA	NA
Calcarisporiella	NA	NA	NA
Asterostroma	NA	NA	NA
Cladophialophora	bantiana	Cladophialophora bantiana CBS 173.52	Claba1
Cladophialophora	carrionii	Cladophialophora carrionii CBS 160.54	Claca1
Cladophialophora	immunda	Cladophialophora immunda CBS83496	Claim1
Cladophialophora	yegresii	Cladophialophora yegresii CBS 114405	Claye1
Elaphomyces	NA	NA	NA
Trichoglossum	NA	NA	NA
Hortiboletus	NA	NA	NA
Kuehneromyces	NA	NA	NA
Ilyonectria	europaea	Ilyonectria europaea PMI82 v1.0	Ilysp1
Ilyonectria	robusta	Ilyonectria robusta PMI_751 v1.0	Ilyrob1
Ilyonectria	sp.	Ilyonectria sp. MPI-CAGE-AT-0026 v1.0	Ilyeu1
Ilyonectria	sp.	Ilyonectria sp. MPI-CAGE-AT-0134 v1.0	Neora1
Entoloma	NA	NA	NA
Rectipilus	NA	NA	NA
Marasmius	fiardii	Marasmius fiardii PR-910 v1.0	Marfi1
Mucor	lusitanicus	Mucor lusitanicus (circinelloides) MU402 v1.0	Muccir1_3
Mucor	lusitanicus	Mucor lusitanicus CBS277.49 v2.0	Mucci2
Mucor	mucedo	Mucor mucedo NRRL 3635 v1.0	Mucmuc1
Mucor	cordense	Mucor cordense RSA 1222 v1.0	Kircor1
Mucor	heterogamus	Mucor heterogamus NRRL 1489 v1.0	Zyghet1
Hymenogaster	NA	NA	NA
Geminibasidium	NA	NA	NA
Pachyphlodes	NA	NA	NA
Botryobasidium	botryosum	Botryobasidium botryosum v1.0	Botbo1

Table C.3, continued.

Genus	Species	MycoCosm species name	MycoCosm species code
Athelia	NA	NA	NA
Cephalotheca	NA	NA	NA
Armillaria	borealis	Armillaria borealis FPL87.14 v1.0	Armbor1
Armillaria	cepistipes	Armillaria cepistipes B5	Armcep1
Armillaria	ectypa	Armillaria ectypa FPL83.16 v1.0	Armect1
Armillaria	fumosa	Armillaria fumosa CBS 122221 v1.0	Armfum1
Armillaria	gallica	Armillaria gallica 21-2 v1.0	Armga1
Armillaria	luteobubalina	Armillaria luteobubalina HWK02 v1.0	Armlut1
Armillaria	mellea	Armillaria mellea DSM 3731	Armme1_1
Armillaria	nabsnona	Armillaria nabsnona CMW6904 v1.0	Armnab1
Armillaria	novae-zelandiae	Armillaria novae-zelandiae 2840 v1.0	Armnov1
Armillaria	ostoyae	Armillaria ostoyae C18/9	Armosto1
Armillaria	solidipes	Armillaria solidipes 28-4 v1.0	Armost1
Armillaria	tabescens	Armillaria tabescens CCBAS 213 v1.0	Armtab1
Oidiodendron	maius	Oidiodendron maius Zn v1.0	Oidma1
Leohumicola	NA	NA	NA
Rhizophagus	cerebriforme	Rhizophagus cerebriforme DAOM 227022 v1.0	Rhice1_1
Rhizophagus	diaphanus	Rhizophagus diaphanus v1.0	Rhidi1
Rhizophagus	irregularis	Rhizophagus irregularis A1 v1.0	RhiirA1_1
Rhizophagus	irregularis	Rhizophagus irregularis A4 v1.0	RhiirA4
Rhizophagus	irregularis	Rhizophagus irregularis A5 v1.0	RhiirA5
Rhizophagus	irregularis	Rhizophagus irregularis B3 v1.0	RhiirB3
Rhizophagus	irregularis	Rhizophagus irregularis C2 v1.0	RhiirC2
Rhizophagus	irregularis	Rhizophagus irregularis DAOM 181602 v1.0	Gloin1
Rhizophagus	irregularis	Rhizophagus irregularis DAOM 197198 v2.0	Rhiir2_1
Glomus	NA	NA	NA

Table C.4: Genera detected in decomposing fine root litter (≥5 plots and ≥0.1% of sequences), manually classified by functional group from the literature or FUNGuild database. Phyla are bolded. Functional groups are as follows: "ECM-P", ECM fungi with peroxidases; ECM-NP, ECM fungi without peroxidases; OM, other mycorrhizas; S-L, ligninolytic saprotrophs; S-NL, non-ligninolytic saprotrophs; O, other or uncertain ecology. References corresponding to numbers are listed below the table. *Lack of peroxidases inferred based on phylogenetic placement of genus outside Auriculariales and residual Agaricomycetes (1, 2).

Class	Genus	Functional Group	Refs.
Ascomycota			
Dothideomycetes	*Cenococcum*	ECM-NP	(1-4)*
Eurotiomycetes	*Cladophialophora*	S-NL	(1, 2, 5)*
Geoglossomycetes	*Geoglossum*	S-NL	(1, 2, 5)*
Geoglossomycetes	*Glutinoglossum*	S-NL	(1, 2, 5)*
Leotiomycetes	*Hyaloscypha*	S-NL	(1, 2, 5)
Leotiomycetes	*Leptodontidium*	O	(5)*
Leotiomycetes	*Phialocephala*	O	(5)*
Leotiomycetes	*Pseudogymnoascus*	O	(5)*
Pezizomycetes	*Humaria*	ECM-NP	(1, 2, 5)*
Pezizomycetes	*Peziza*	O	(1, 2, 5)*
Sordariomycetes	*Apodus*	S-NL	(1, 2, 5)*
Sordariomycetes	*Cephalotheca*	S-NL	(1, 2, 5)*
Sordariomycetes	*Chloridium*	O	(1, 2, 5)*
Sordariomycetes	*Humicola*	S-NL	(1, 2, 5)*
Sordariomycetes	*Ilyonectria*	O	(1, 2, 5)*
Sordariomycetes	*Trichoderma*	S-NL	(1, 2, 5)*
Basidiomycota			
Agaricomycetes	*Agrocybe*	S-L	(6)
Agaricomycetes	*Amanita*	ECM-NL	(4)
Agaricomycetes	*Asterostroma*	S-L	(5)
Agaricomycetes	*Athelia*	O	(5)
Agaricomycetes	*Athelopsis*	S-L	(5)
Agaricomycetes	*Boletus*	ECM-NL	(1, 2, 4)
Agaricomycetes	*Byssocorticium*	ECM-NL	(5)
Agaricomycetes	*Clavulina*	ECM-NL	(1, 5)
Agaricomycetes	*Clavulinopsis*	S-NL	(5)
Agaricomycetes	*Clitopilus*	S-NL	(5)
Agaricomycetes	*Conocybe*	S-NL	(5)

Table C.4, continued.

Class	Genus	Functional Group	Refs.
Agaricomycetes	*Cortinarius*	ECM-P	(4, 7)
Agaricomycetes	*Entoloma*	S-NL	(5, 8)
Agaricomycetes	*Flagelloscypha*	S-NL	(5)
Agaricomycetes	*Gymnopus*	S-L	(8)
Agaricomycetes	*Hebeloma*	ECM-P	(4)
Agaricomycetes	*Hortiboletus*	ECM-NP	(1-3)
Agaricomycetes	*Hygrocybe*	OM	(5, 8, 9)
Agaricomycetes	*Inocybe*	ECM-NP	(5)
Agaricomycetes	*Kuehneromyces*	S-L	(5)
Agaricomycetes	*Laccaria*	ECM-P	(3, 4)
Agaricomycetes	*Lactarius*	ECM-P	(4, 7)
Agaricomycetes	*Marasmius*	S-L	(8)
Agaricomycetes	*Membranomyces*	ECM-NP	(5)
Agaricomycetes	*Mycena*	S-L	(8)
Agaricomycetes	*Mycenella*	O	(5)
Agaricomycetes	*Piloderma*	ECM-P	(3)
Agaricomycetes	*Porotheleum*	O	(5)
Agaricomycetes	*Pseudoomphalina*	S-NL	(5)
Agaricomycetes	*Ramaria*	S-L	(8)
Agaricomycetes	*Rectipilus*	S-NL	(5)
Agaricomycetes	*Rigidoporus*	S-L	(5)
Agaricomycetes	*Russula*	ECM-P	(4, 7)
Agaricomycetes	*Scleroderma*	ECM-NP	(1, 4)
Agaricomycetes	*Sebacina*	OM	(1, 3, 4)
Agaricomycetes	*Sphaerobolus*	S-L	(5)
Agaricomycetes	*Steccherinum*	S-L	(5)
Agaricomycetes	*Tomentella*	ECM-NP	(5)
Agaricomycetes	*Trechispora*	S-L	(8)
Agaricomycetes	*Xenasmatella*	S-L	(5)
Agaricomycetes	*Xylodon*	S-L	(5)
Glomeromycota			
Glomeromycetes	*Rhizophagus*	OM	(100
Mortierellomycota			
Mortierellomycetes	*Mortierella*	S-NL	(1, 2, 5, 11)*
Mucoromycota			
Mucoromycetes	*Mucor*	S-NL	(1, 2, 5)*
Umbelopsidomycetes	*Umbelopsis*	S-NL	(Floudas *et al.* 2012; Nagy *et al.* 2016; Nguyen *et al.* 2016)*

[1](Nagy *et al.* 2016); [2](Floudas *et al.* 2012); [3](Kohler *et al.* 2015); [4](Miyauchi *et al.* 2020); [5](Nguyen *et al.* 2016); [6](Ruiz-Dueñas *et al.* 2021); [7](Bödeker *et al.* 2009); [8](Entwistle *et al.* 2018b); [9](Seitzman *et al.* 2011); [10](Smith & Read 2010); [11](Sterkenburg *et al.* 2018)

Table C.5: GAMM results for relationships between fine root decay and the total estimated community-weighted abundance of PCWDE genes (n = 70). Each GAMM contained four additional independent variables (soil inorganic N availability, soil pH, volumetric water content, temperature). We explicitly accounted for spatial autocorrelation in GAMM models with a spatial correlation structure using the geographic coordinates of each plot. Statistically significant relationships are bolded.

Dependent variable	Independent variable	$R^2_{adj.}$	F	*P*-value
	Sum of all PCWDE genes		**4.19**	**0.032**
	Inorg. N availability		1.68	0.199
Fine root decay	Soil water content	0.138	3.82	0.055
	Soil temperature		2.52	0.118
	Soil pH		0.08	0.774
	Sum of rapid-decay PCWDE genes		**8.57**	**0.005**
	Inorg. N availability		1.64	0.205
Fine root decay	Soil water content	0.179	3.94	0.051
	Soil temperature		1.38	0.244
	Soil pH		0.13	0.720

Table C.6: Percentage of fungal reads classified by phylum in decaying fine root litter.

Percentages are based on the total number of reads with the three outlier plots removed.

Phylum	% of sequences
Basidiomycota	66.3
Ascomycota	24.5
Mortierellomycota	5.8
unclassified Fungi	1.2
Glomeromycota	1.1
Mucoromycota	0.8
Chytridiomycota	0.1
Rozellomycota	0.1
Olpidiomycota	0.1
Zoopagomycota	<0.1
Entomophthoromycota	<0.1
Kickxellomycota	<0.1
Basidiobolomycota	<0.1
Calcarisporiellomycota	<0.1
Blastocladiomycota	<0.1
Monoblepharomycota	<0.1

Table C.7: Percentage of fungal reads classified by genus in decaying fine root litter.

Percentages are based on the total number of reads with the three outlier plots removed.

Genus	% of sequences
Mycena	21.6
Mortierella	5.7
Piloderma	4.7
Russula	4.4
Gymnopus	3.1
Trechispora	3.0
Tomentella	2.7
Lactarius	2.4
Humicola	2.4
Trichoderma	1.8
Ramaria	1.5
Cenococcum	1.2
Laccaria	1.2
Sebacina	0.8
Cortinarius	0.8
Hebeloma	0.7
Umbelopsis	0.7
Agrocybe	0.6
Ilyonectria	0.6
Peziza	0.6
Rigidoporus	0.6
Hyaloscypha	0.5
Apodus	0.5
Sphaerobolus	0.5
Phialocephala	0.5
Byssocorticium	0.4
Amanita	0.4
Asterostroma	0.4
Flagelloscypha	0.3
Pseudoomphalina	0.3
Clavulinopsis	0.3
Porotheleum	0.3
Scleroderma	0.3
Humaria	0.3
Athelopsis	0.3
Conocybe	0.3
Leptodontidium	0.3
Geoglossum	0.3
Xenasmatella	0.2
Membranomyces	0.2
Clitopilus	0.2
Cladophialophora	0.2

Table C.7, continued.

Genus	% of sequences
Steccherinum	0.2
Cephalotheca	0.2
Pseudogymnoascus	0.2
Rectipilus	0.2
Mycenella	0.2
Athelia	0.2
Xylodon	0.2
Chloridium	0.2
Rhizophagus	0.2
Kuehneromyces	0.1
Entoloma	0.1
Boletus	0.1
Hygrocybe	0.1
Clavulina	0.1
Inocybe	0.1
Marasmius	0.1
Hortiboletus	0.1
Glutinoglossum	0.1
Mucor	0.1

Table C.8: Summary of sequencing yield pre- and post-quality filtering, and total ASVs. These values do not include the three outlier plots removed from our analyses.

Habitat	Raw reads	High-quality reads	% retained	ASVs
Decaying fine roots	13,860,743	10,305,553	73.4%	9,367

Table C.9: GAMM results for relationships between community-weighted abundance of PCWDEs and the four fungal functional groups (n = 70). Each GAMM contained four additional independent variables (soil inorganic N availability, soil pH, volumetric water content, temperature). We explicitly accounted for spatial autocorrelation in GAMM models with a spatial correlation structure using the geographic coordinates of each plot. Statistically significant relationships are bolded.

Dependent variable	Independent variable	$R^2_{adj.}$	F	*P*-value
All PCWDEs	**Ligninolytic saprotrophs**	0.526	**30.60**	**<0.001**
	Non-ligninolytic saprotrophs		0.03	0.857
	ECM with peroxidases		**22.53**	**<0.001**
	ECM without peroxidases		0.01	0.908
	Inorg. N availability		0.07	0.800
	Soil water content		0.10	0.756
	Soil temperature		0.75	0.391
	Soil pH		0.04	0.850
Rapid decay PCWDEs	**Ligninolytic saprotrophs**	0.601	**33.66**	**<0.001**
	Non-ligninolytic saprotrophs		0.12	0.729
	ECM with peroxidases		**40.20**	**<0.001**
	ECM without peroxidases		0.09	0.770
	Inorg. N availability		0.04	0.839
	Soil water content		0.14	0.707
	Soil temperature		0.46	0.501
	Soil pH		0.17	0.686

Table C.10: GAMM results for relationships between extracellular enzyme activities and the four fungal functional groups and environmental variables as predictors (n = 70). We explicitly accounted for spatial autocorrelation in GAMM models with a spatial correlation structure using the geographic coordinates of each plot. Statistically significant relationships are bolded.

Dependent variable	Independent variable	$R^2_{adj.}$	F	*P*-value
Cellulolytic enzymes	Ligninolytic saprotrophs	0.227	2.95	0.053
	Non-ligninolytic saprotrophs		0.80	0.375
	ECM with peroxidases		2.35	0.130
	ECM without peroxidases		**5.47**	**0.023**
	Inorg. N availability		**5.23**	**0.026**
	Soil water content		0.66	0.419
	Soil temperature		1.26	0.212
	Soil pH		0.35	0.556
Ligninolytic enzymes	**Ligninolytic saprotrophs**	0.051	**7.14**	**0.010**
	Non-ligninolytic saprotrophs		1.61	0.209
	ECM with peroxidases		2.71	0.105
	ECM without peroxidases		2.38	0.128
	Inorg. N availability		0.00	0.950
	Soil water content		1.78	0.187
	Soil temperature		1.69	0.199
	Soil pH		0.30	0.587
N-acetylglucosaminidase	**Ligninolytic saprotrophs**	0.379	**38.39**	**<0.001**
	Non-ligninolytic saprotrophs		**6.10**	**0.016**
	ECM with peroxidases		**4.51**	**0.038**
	ECM without peroxidases		**8.71**	**0.005**
	Inorg. N availability		0.55	0.460
	Soil water content		0.48	0.489
	Soil temperature		0.01	0.940
	Soil pH		**12.50**	**<0.001**

Table C.11: GAMM results for relationships between fine root decay and the four fungal functional groups and environmental variables as predictors (n = 70). We explicitly accounted for spatial autocorrelation in GAMM models with a spatial correlation structure using the geographic coordinates of each plot. Statistically significant relationships are bolded.

Dependent variable	Independent variable	$R^2_{adj.}$	F	*P*-value
Fine root decay	**Ligninolytic saprotrophs**	0.365	**19.88**	**<0.001**
	Non-ligninolytic saprotrophs		**6.32**	**0.015**
	ECM with peroxidases		**8.21**	**0.006**
	ECM without peroxidases		1.14	0.290
	Inorg. N availability		2.46	0.122
	Soil water content		**5.10**	**0.036**
	Soil temperature		0.09	0.768
	Soil pH		0.21	0.651

Table C.12: GAMM results for relationships between fungal functional groups and environmental variables (n = 70). We explicitly accounted for spatial autocorrelation in GAMM models with a spatial correlation structure using the geographic coordinates of each plot. Statistically significant relationships are bolded.

Dependent variable	Independent variable	$R^2_{adj.}$	F	*P*-value
Ligninolytic saprotrophs	**Inorg. N availability**	0.260	**0.33**	**0.568**
	Soil water content		5.21	0.033
	Soil temperature		1.58	0.213
	Soil pH		**8.62**	**0.006**
Non-ligninolytic saprotrophs	Inorg. N availability	0.130	0.02	0.887
	Soil water content		**2.81**	**0.041**
	Soil temperature		1.36	0.248
	Soil pH		2.49	0.120
ECM with peroxidases	**Inorg. N availability**	0.585	**5.97**	**0.017**
	Soil water content		0.24	0.623
	Soil temperature		1.90	0.173
	Soil pH		**12.32**	**0.002**
ECM without peroxidases	Inorg. N availability	0.107	0.70	0.406
	Soil water content		1.65	0.204
	Soil temperature		**4.49**	**0.038**
	Soil pH		0.72	0.399

REFERENCES

Ahmad, M., Taylor, C.R., Pink, D., Burton, K., Eastwood, D., Bending, G.D., *et al.* (2010). Development of novel assays for lignin degradation: comparative analysis of bacterial and fungal lignin degraders. *Mol. Biosyst.*, 6, 815–821.

Allison, S.D. (2012). A trait-based approach for modelling microbial litter decomposition. *Ecol. Lett.*, 15, 1058–1070.

Allison, S.D. & Martiny, J.B.H. (2008). Resistance, resilience, and redundancy in microbial communities. *Proc. Natl. Acad. Sci. U. S. A.*, 105 Suppl 1, 11512–11519.

Anderson, M.J. (2001). A new method for non-parametric multivariate analysis of variance. *Austral Ecol.*, 26, 32–46.

Anderson, M.J. (2004). *PERMDISP: a FORTRAN computer program for permutational analysis of multivariate dispersions (for any two-factor ANOVA design) using permutation tests*.

Angst, G., Mueller, K.E., Nierop, K.G.J. & Simpson, M.J. (2021). Plant- or microbial-derived? A review on the molecular composition of stabilized soil organic matter. *Soil Biol. Biochem.*, 156, 108189.

Anthony, M.A., Crowther, T.W., van der Linde, S., Suz, L.M., Bidartondo, M.I., Cox, F., *et al.* (2022). Forest tree growth is linked to mycorrhizal fungal composition and function across Europe. *ISME J.*, 1–10.

Argiroff, W.A., Zak, D.R., Pellitier, P.T., Upchurch, R.A. & Belke, J.P. (2022). Decay by ectomycorrhizal fungi couples soil organic matter to nitrogen availability. *Ecol. Lett.*, 25, 391–404.

Argiroff, W.A., Zak, D.R., Upchurch, R.A., Salley, S.O. & Grandy, A.S. (2019). Anthropogenic N deposition alters soil organic matter biochemistry and microbial communities on decaying fine roots. *Glob. Chang. Biol.*, 25, 4369–4382.

Assavanig, A., Amornikitticharoen, B., Ekpaisal, N., Meevootisom, V. & Flegel, T.W. (1992). Isolation, characterization and function of laccase from Trichoderma. *Appl. Microbiol. Biotechnol.*, 38, 198–202.

Averill, C., Dietze, M.C. & Bhatnagar, J.M. (2018). Continental-scale nitrogen pollution is shifting forest mycorrhizal associations and soil carbon stocks. *Glob. Chang. Biol.*, 24, 4544–4553.

Averill, C. & Hawkes, C.V. (2016). Ectomycorrhizal fungi slow soil carbon cycling. *Ecol. Lett.*, 19, 937–947.

Averill, C. & Waring, B. (2018). Nitrogen limitation of decomposition and decay: How can it occur? *Glob. Chang. Biol.*, 24, 1417–1427.

Baker, M.E. & King, R.S. (2010). A new method for detecting and interpreting biodiversity and ecological community thresholds. *Methods Ecol. Evol.*, 1, 25–37.

Baldrian, P. (2008). Enzymes of saprotrophic basidiomycetes. In: *British Mycological Society Symposia Series* (eds. Boddy, L., Frankland, J.C. & van West, P.). Academic Press, pp. 19–41.

Baldrian, P. (2009). Ectomycorrhizal fungi and their enzymes in soils: is there enough evidence for their role as facultative soil saprotrophs? *Oecologia*.

Barnes, B.V., Barnes, R., Jr, Zak, D.R., Spurr, S.H. & Denton, S.R. (1998). *Forest Ecology*. Wiley.

Baskaran, P., Hyvönen, R., Berglund, S.L., Clemmensen, K.E., Ågren, G.I., Lindahl, B.D., *et al.* (2017). Modelling the influence of ectomycorrhizal decomposition on plant nutrition and soil carbon sequestration in boreal forest ecosystems. *New Phytol.*, 213, 1452–1465.

Batjes, N.H. (1996). Total carbon and nitrogen in the soils of the world. *Eur. J. Soil Sci.*, 47, 151–163.

Beidler, K.V. & Pritchard, S.G. (2017). Maintaining connectivity: understanding the role of root order and mycelial networks in fine root decomposition of woody plants. *Plant Soil*, 420, 19–36.

de Bello, F., Carmona, C.P., Dias, A.T.C., Götzenberger, L., Moretti, M. & Berg, M.P. (2021). *Handbook of Trait-Based Ecology: From Theory to R Tools*. Cambridge University Press.

Benjamini, Y. & Hochberg, Y. (1995). Controlling the false discovery rate: A practical and powerful approach to multiple testing. *J. R. Stat. Soc.*, 57, 289–300.

Berg, B. (2014). Decomposition patterns for foliar litter – A theory for influencing factors. *Soil Biol. Biochem.*, 78, 222–232.

Berg, B., Berg, M.P., Bottner, P., Box, E., Breymeyer, A., de Anta, R.C., *et al.* (1993). Litter mass loss rates in pine forests of Europe and Eastern United States: some relationships with climate and litter quality. *Biogeochemistry*, 20, 127–159.

Berg, B. & McClaugherty, C. (2020). *Plant Litter: Decomposition, Humus Formation, Carbon Sequestration*. Springer, Cham.

Blankinship, J.C., Berhe, A.A., Crow, S.E., Druhan, J.L., Heckman, K.A., Keiluweit, M., *et al.* (2018). Improving understanding of soil organic matter dynamics by triangulating theories, measurements, and models. *Biogeochemistry*, 140, 1–13.

Bödeker, I.T.M., Clemmensen, K.E., de Boer, W., Martin, F., Olson, Å. & Lindahl, B.D. (2014). Ectomycorrhizal Cortinarius species participate in enzymatic oxidation of humus in northern forest ecosystems. *New Phytol.*, 203, 245–256.

Bödeker, I.T.M., Nygren, C.M.R., Taylor, A.F.S., Olson, A. & Lindahl, B.D. (2009). ClassII peroxidase-encoding genes are present in a phylogenetically wide range of ectomycorrhizal fungi. *ISME J.*, 3, 1387–1395.

Bogar, L., Peay, K., Kornfeld, A., Huggins, J., Hortal, S., Anderson, I., *et al.* (2019). Plant-mediated partner discrimination in ectomycorrhizal mutualisms. *Mycorrhiza*, 29, 97–111.

Bradford, M.A., Berg, B., Maynard, D.S., Wieder, W.R. & Wood, S.A. (2016). Understanding the dominant controls on litter decomposition. *J. Ecol.*, 104, 229–238.

Bradford, M.A., Veen, G.F.C., Bonis, A., Bradford, E.M., Classen, A.T., Cornelissen, J.H.C., *et al.* (2017). A test of the hierarchical model of litter decomposition. *Nat Ecol Evol*, 1, 1836–1845.

Bradford, M.A., Wood, S.A., Addicott, E.T., Fenichel, E.P., Fields, N., González-Rivero, J., *et al.* (2021). Quantifying microbial control of soil organic matter dynamics at macrosystem scales. *Biogeochemistry*, 156, 19–40.

Bugg, T.D.H., Ahmad, M., Hardiman, E.M. & Singh, R. (2011). The emerging role for bacteria in lignin degradation and bio-product formation. *Curr. Opin. Biotechnol.*, 22, 394–400.

Burton, A.J., Pregitzer, K.S., Crawford, J.N., Zogg, G.P. & Zak, D.R. (2004). Simulated chronic NO3 − deposition reduces soil respiration in northern hardwood forests. *Glob. Chang. Biol.*, 10, 1080–1091.

Burton, A.J., Ramm, C.W., Pregitzer, K.S. & Reed, D.D. (1991). Use of multivariate methods in forest research site selection. *Can. J. For. Res.*, 21, 1573–1580.

Callahan, B.J., McMurdie, P.J. & Holmes, S.P. (2017). Exact sequence variants should replace operational taxonomic units in marker-gene data analysis. *ISME J.*, 11, 2639–2643.

Callahan, B.J., McMurdie, P.J., Rosen, M.J., Han, A.W., Johnson, A.J.A. & Holmes, S.P. (2016). DADA2: High-resolution sample inference from Illumina amplicon data. *Nat. Methods*, 13, 581–583.

Campbell, J.E., Berry, J.A., Seibt, U., Smith, S.J., Montzka, S.A., Launois, T., *et al.* (2017). Large historical growth in global terrestrial gross primary production. *Nature*, 544, 84–87.

del Cerro, C., Erickson, E., Dong, T., Wong, A.R., Eder, E.K., Purvine, S.O., *et al.* (2021). Intracellular pathways for lignin catabolism in white-rot fungi. *Proc. Natl. Acad. Sci. U. S. A.*, 118, e2017381118.

Chen, J., Luo, Y., van Groenigen, K.J., Hungate, B.A., Cao, J., Zhou, X., *et al.* (2018). A keystone microbial enzyme for nitrogen control of soil carbon storage. *Sci Adv*, 4, eaaq1689.

Clemmensen, K.E., Durling, M.B., Michelsen, A., Hallin, S., Finlay, R.D. & Lindahl, B.D. (2021). A tipping point in carbon storage when forest expands into tundra is related to mycorrhizal recycling of nitrogen. *Ecol. Lett.*, 24, 1193–1204.

Clemmensen, K.E., Finlay, R.D., Dahlberg, A., Stenlid, J., Wardle, D.A. & Lindahl, B.D. (2015). Carbon sequestration is related to mycorrhizal fungal community shifts during long-term succession in boreal forests. *New Phytol.*, 205, 1525–1536.

Cline, L.C., Schilling, J.S., Menke, J., Groenhof, E. & Kennedy, P.G. (2018). Ecological and functional effects of fungal endophytes on wood decomposition. *Funct. Ecol.*, 32, 181–191.

Cline, L.C. & Zak, D.R. (2015). Initial colonization, community assembly and ecosystem function: fungal colonist traits and litter biochemistry mediate decay rate. *Mol. Ecol.*, 24, 5045–5058.

Cole, J.R., Wang, Q., Fish, J.A., Chai, B., McGarrell, D.M., Sun, Y., *et al.* (2014). Ribosomal Database Project: data and tools for high throughput rRNA analysis. *Nucleic Acids Res.*, 42, D633-42.

Cotrufo, M.F., Soong, J.L., Horton, A.J., Campbell, E.E., Haddix, M.L., Wall, D.H., *et al.* (2015). Formation of soil organic matter via biochemical and physical pathways of litter mass loss. *Nat. Geosci.*, 8, 776–779.

De Crop, E., Nuytinck, J., Van de Putte, K., Wisitrassameewong, K., Hackel, J., Stubbe, D., *et al.* (2017). A multi-gene phylogeny of Lactifluus (Basidiomycota, Russulales) translated into a new infrageneric classification of the genus. *Persoonia*, 38, 58–80.

DeForest, J.L., Zak, D.R., Pregitzer, K.S. & Burton, A.J. (2004). Atmospheric nitrate deposition, microbial community composition, and enzyme activity in northern hardwood forests. *Soil Sci. Soc. Am. J.*, 68, 132–138.

Defrenne, C.E., Philpott, T.J., Guichon, S.H.A., Roach, W.J., Pickles, B.J. & Simard, S.W. (2019). Shifts in Ectomycorrhizal Fungal Communities and Exploration Types Relate to the Environment and Fine-Root Traits Across Interior Douglas-Fir Forests of Western Canada. *Front. Plant Sci.*, 10, 643.

Edgar, R.C., Haas, B.J., Clemente, J.C., Quince, C. & Knight, R. (2011). UCHIME improves sensitivity and speed of chimera detection. *Bioinformatics*, 27, 2194–2200.

Eisenlord, S.D., Freedman, Z., Zak, D.R., Xue, K., He, Z. & Zhou, J. (2013). Microbial mechanisms mediating increased soil C storage under elevated atmospheric N deposition. *Appl. Environ. Microbiol.*, 79, 1191–1199.

Eisenlord, S.D. & Zak, D.R. (2010). Simulated atmospheric nitrogen deposition alters actinobacterial community composition in forest soils. *Soil Sci. Soc. Am. J.*, 74, 1157–1166.

Entwistle, E.M., Romanowicz, K.J., Argiroff, W.A., Freedman, Z.B., Morris, J.J. & Zak, D.R. (2018a). Anthropogenic N Deposition Alters the Composition of Expressed Class II Fungal Peroxidases. *Appl. Environ. Microbiol.*, 84.

Entwistle, E.M., Zak, D.R. & Argiroff, W.A. (2018b). Anthropogenic N deposition increases soil C storage by reducing the relative abundance of lignolytic fungi. *Ecol. Monogr.*, 88, 225–244.

Fernandez, C.W. & Kennedy, P.G. (2016). Revisiting the "Gadgil effect": do interguild fungal interactions control carbon cycling in forest soils? *New Phytol.*, 209, 1382–1394.

Fernandez, C.W., See, C.R. & Kennedy, P.G. (2020). Decelerated carbon cycling by ectomycorrhizal fungi is controlled by substrate quality and community composition. *New Phytol.*, 226, 569–582.

Fichot, E.B. & Norman, R.S. (2013). Microbial phylogenetic profiling with the Pacific Biosciences sequencing platform. *Microbiome*, 1, 10.

Fierer, N. (2017). Embracing the unknown: disentangling the complexities of the soil microbiome. *Nat. Rev. Microbiol.*, 15, 579–590.

Floudas, D., Binder, M., Riley, R., Barry, K., Blanchette, R.A., Henrissat, B., *et al.* (2012). The Paleozoic origin of enzymatic lignin decomposition reconstructed from 31 fungal genomes. *Science*, 336, 1715–1719.

Freedman, Z. & Zak, D.R. (2014). Atmospheric N deposition increases bacterial laccase-like multicopper oxidases: implications for organic matter decay. *Appl. Environ. Microbiol.*, 80, 4460–4468.

Freedman, Z.B., Upchurch, R.A., Zak, D.R. & Cline, L.C. (2016). Anthropogenic N Deposition Slows Decay by Favoring Bacterial Metabolism: Insights from Metagenomic Analyses. *Front. Microbiol.*, 7, 259.

Freschet, G.T., Cornwell, W.K., Wardle, D.A., Elumeeva, T.G., Liu, W., Jackson, B.G., *et al.* (2013). Linking litter decomposition of above- and below-ground organs to plant-soil feedbacks worldwide. *J. Ecol.*, 101, 943–952.

Frey, S.D. (2019). Mycorrhizal Fungi as Mediators of Soil Organic Matter Dynamics. *Annu. Rev. Ecol. Evol. Syst.*, 50, 237–259.

Frey, S.D., Ollinger, S., Nadelhoffer, K., Bowden, R., Brzostek, E., Burton, A., *et al.* (2014). Chronic nitrogen additions suppress decomposition and sequester soil carbon in temperate forests. *Biogeochemistry*, 121, 305–316.

Gadgil, R.L. & Gadgil, P.D. (1971). Mycorrhiza and litter decomposition. *Nature*, 233, 133.

Galloway, J.N., Dentener, F.J., Capone, D.G., Boyer, E.W., Howarth, R.W., Seitzinger, S.P., *et al.* (2004). Nitrogen Cycles: Past, Present, and Future. *Biogeochemistry*, 70, 153–226.

Galloway, J.N., Townsend, A.R., Erisman, J.W., Bekunda, M., Cai, Z., Freney, J.R., *et al.* (2008). Transformation of the nitrogen cycle: recent trends, questions, and potential solutions. *Science*, 320, 889–892.

Ghosh, A., Frankland, J.C., Thurston, C.F. & Robinson, C.H. (2003). Enzyme production by Mycena galopus mycelium in artificial media and in Picea sitchensis F1 horizon needle litter. *Mycol. Res.*, 107, 996–1008.

Glassman, S.I., Weihe, C., Li, J., Albright, M.B.N., Looby, C.I., Martiny, A.C., *et al.* (2018). Decomposition responses to climate depend on microbial community composition. *Proc. Natl. Acad. Sci. U. S. A.*, 115, 11994–11999.

Grandy, A.S., Neff, J.C. & Weintraub, M.N. (2007). Carbon structure and enzyme activities in alpine and forest ecosystems. *Soil Biol. Biochem.*, 39, 2701–2711.

Grandy, A.S., Sinsabaugh, R.L., Neff, J.C., Stursova, M. & Zak, D.R. (2008). Nitrogen deposition effects on soil organic matter chemistry are linked to variation in enzymes, ecosystems and size fractions. *Biogeochemistry*, 91, 37–49.

Grandy, A.S., Strickland, M.S., Lauber, C.L., Bradford, M.A. & Fierer, N. (2009). The influence of microbial communities, management, and soil texture on soil organic matter chemistry. *Geoderma*, 150, 278–286.

Grigoriev, I.V., Nikitin, R., Haridas, S., Kuo, A., Ohm, R., Otillar, R., *et al.* (2014). MycoCosm portal: gearing up for 1000 fungal genomes. *Nucleic Acids Res.*, 42, D699-704.

Guo, D., Xia, M., Wei, X., Chang, W., Liu, Y. & Wang, Z. (2008). Anatomical traits associated with absorption and mycorrhizal colonization are linked to root branch order in twenty-three Chinese temperate tree species. *New Phytol.*, 180, 673–683.

Hall, E.K., Bernhardt, E.S., Bier, R.L., Bradford, M.A., Boot, C.M., Cotner, J.B., *et al.* (2018). Understanding how microbiomes influence the systems they inhabit. *Nat Microbiol*, 3, 977–982.

Hassett, J.E., Zak, D.R., Blackwood, C.B. & Pregitzer, K.S. (2009). Are basidiomycete laccase gene abundance and composition related to reduced lignolytic activity under elevated atmospheric NO3(-) deposition in a northern hardwood forest? *Microb. Ecol.*, 57, 728–739.

Hawkes, C.V. & Keitt, T.H. (2015). Resilience vs. historical contingency in microbial responses to environmental change. *Ecol. Lett.*, 18, 612–625.

Hibbett, D.S., Bauer, R., Binder, M., Giachini, A.J., Hosaka, K., Justo, A., *et al.* (2014). Agaricomycetes. In: *Systematics and Evolution: Part A* (eds. McLaughlin, D.J. & Spatafora, J.W.). Springer Berlin Heidelberg, Berlin, Heidelberg, pp. 373–429.

Hobbie, S.E. (2005). Contrasting Effects of Substrate and Fertilizer Nitrogen on the Early Stages of Litter Decomposition. *Ecosystems*, 8, 644–656.

Hobbie, S.E., Oleksyn, J., Eissenstat, D.M. & Reich, P.B. (2010). Fine root decomposition rates do not mirror those of leaf litter among temperate tree species. *Oecologia*, 162, 505–513.

Hofrichter, M. (2002). Review: lignin conversion by manganese peroxidase (MnP). *Enzyme Microb. Technol.*, 30, 454–466.

Hölker, U., Dohse, J. & Höfer, M. (2002). Extracellular laccases in ascomycetes Trichoderma atroviride and Trichoderma harzianum. *Folia Microbiol.* , 47, 423–427.

Hortal, S., Plett, K.L., Plett, J.M., Cresswell, T., Johansen, M., Pendall, E., *et al.* (2017). Role of plant-fungal nutrient trading and host control in determining the competitive success of ectomycorrhizal fungi. *ISME J.*, 11, 2666–2676.

Jackson, R.B., Lajtha, K., Crow, S.E., Hugelius, G., Kramer, M.G. & Piñeiro, G. (2017). The Ecology of Soil Carbon: Pools, Vulnerabilities, and Biotic and Abiotic Controls. *Annu. Rev. Ecol. Evol. Syst.*, 48, 419–445.

Janssens, I.A., Dieleman, W., Luyssaert, S., Subke, J.-A., Reichstein, M., Ceulemans, R., *et al.* (2010). Reduction of forest soil respiration in response to nitrogen deposition. *Nat. Geosci.*, 3, 315–322.

Jansson, J.K. & Hofmockel, K.S. (2018). The soil microbiome-from metagenomics to metaphenomics. *Curr. Opin. Microbiol.*, 43, 162–168.

Janusz, G., Pawlik, A., Sulej, J., Swiderska-Burek, U., Jarosz-Wilkolazka, A. & Paszczynski, A. (2017). Lignin degradation: microorganisms, enzymes involved, genomes analysis and evolution. *FEMS Microbiol. Rev.*, 41, 941–962.

Keenan, T.F., Prentice, I.C., Canadell, J.G., Williams, C.A., Wang, H., Raupach, M., *et al.* (2016). Recent pause in the growth rate of atmospheric CO2 due to enhanced terrestrial carbon uptake. *Nat. Commun.*, 7, 13428.

Kellner, H., Luis, P., Pecyna, M.J., Barbi, F., Kapturska, D., Krüger, D., *et al.* (2014). Widespread occurrence of expressed fungal secretory peroxidases in forest soils. *PLoS One*, 9, e95557.

Kirk, T.K. & Farrell, R.L. (1987). Enzymatic "combustion": the microbial degradation of lignin. *Annu. Rev. Microbiol.*, 41, 465–505.

Kohler, A., Kuo, A., Nagy, L.G., Morin, E., Barry, K.W., Buscot, F., *et al.* (2015). Convergent losses of decay mechanisms and rapid turnover of symbiosis genes in mycorrhizal mutualists. *Nat. Genet.*, 47, 410–415.

Kohout, P., Charvátová, M., Štursová, M., Mašínová, T., Tomšovský, M. & Baldrian, P. (2018). Clearcutting alters decomposition processes and initiates complex restructuring of fungal communities in soil and tree roots. *ISME J.*, 12, 692–703.

Kohout, P., Sudová, R., Brabcová, V., Vosolsobě, S., Baldrian, P. & Albrechtová, J. (2021). Forest Microhabitat Affects Succession of Fungal Communities on Decomposing Fine Tree Roots. *Front. Microbiol.*, 12, 541583.

Koide, R.T., Fernandez, C. & Malcolm, G. (2014). Determining place and process: functional traits of ectomycorrhizal fungi that affect both community structure and ecosystem function. *New Phytol.*, 201, 433–439.

Kõljalg, U., Nilsson, R.H., Abarenkov, K., Tedersoo, L., Taylor, A.F.S., Bahram, M., *et al.* (2013). Towards a unified paradigm for sequence-based identification of fungi. *Mol. Ecol.*, 22, 5271–5277.

Kou, L., Jiang, L., Fu, X., Dai, X., Wang, H. & Li, S. (2018). Nitrogen deposition increases root production and turnover but slows root decomposition in Pinus elliottii plantations. *New Phytol.*, 218, 1450–1461.

Kyaschenko, J., Clemmensen, K.E., Karltun, E. & Lindahl, B.D. (2017). Below-ground organic matter accumulation along a boreal forest fertility gradient relates to guild interaction within fungal communities. *Ecol. Lett.*, 20, 1546–1555.

Lane, D.J. (1991). 16S/23S rRNA sequencing. In: *Nucleic acid techniques in bacterial systematics* (eds. Stackebrandt, E. & Goodfellow, M.). John Wiley & Sons, Inc., West Sussex, UK, pp. 115–175.

Lavorel, S. & Garnier, E. (2002). Predicting changes in community composition and ecosystem functioning from plant traits: revisiting the Holy Grail. *Funct. Ecol.*, 16, 545–556.

Legendre, P. & Legendre, L. (2012). *Numerical Ecology*. Elsevier.

Lehmann, J. & Kleber, M. (2015). The contentious nature of soil organic matter. *Nature*, 528, 60–68.

Levasseur, A., Drula, E., Lombard, V., Coutinho, P.M. & Henrissat, B. (2013). Expansion of the enzymatic repertoire of the CAZy database to integrate auxiliary redox enzymes. *Biotechnol. Biofuels*, 6, 41.

Li, A., Fahey, T.J., Pawlowska, T.E., Fisk, M.C. & Burtis, J. (2015). Fine root decomposition, nutrient mobilization and fungal communities in a pine forest ecosystem. *Soil Biol. Biochem.*, 83, 76–83.

Liang, C., Schimel, J.P. & Jastrow, J.D. (2017). The importance of anabolism in microbial control over soil carbon storage. *Nat Microbiol*, 2, 17105.

Lilleskov, E.A., Fahey, T.J., Horton, T.R. & Lovett, G.M. (2002). Belowground ectomycorrhizal fungal community change over a nitrogen deposition gradient in Alaska. *Ecology*, 83, 104–115.

Lindahl, B.D., Kyaschenko, J., Varenius, K., Clemmensen, K.E., Dahlberg, A., Karltun, E., *et al.* (2021). A group of ectomycorrhizal fungi restricts organic matter accumulation in boreal forest. *Ecol. Lett.*, 24, 1341–1351.

Lindahl, B.D. & Tunlid, A. (2015). Ectomycorrhizal fungi - potential organic matter decomposers, yet not saprotrophs. *New Phytol.*, 205, 1443–1447.

Liu, K.-L., Porras-Alfaro, A., Kuske, C.R., Eichorst, S.A. & Xie, G. (2012). Accurate, rapid taxonomic classification of fungal large-subunit rRNA genes. *Appl. Environ. Microbiol.*, 78, 1523–1533.

Lombard, V., Golaconda Ramulu, H., Drula, E., Coutinho, P.M. & Henrissat, B. (2014). The carbohydrate-active enzymes database (CAZy) in 2013. *Nucleic Acids Res.*, 42, D490-5.

Luo, C., Xie, S., Sun, W., Li, X. & Cupples, A.M. (2009). Identification of a novel toluene-degrading bacterium from the candidate phylum TM7, as determined by DNA stable isotope probing. *Appl. Environ. Microbiol.*, 75, 4644–4647.

Maaroufi, N.I., Nordin, A., Hasselquist, N.J., Bach, L.H., Palmqvist, K. & Gundale, M.J. (2015). Anthropogenic nitrogen deposition enhances carbon sequestration in boreal soils. *Glob. Chang. Biol.*, 21, 3169–3180.

Martin, M. (2011). Cutadapt removes adapter sequences from high-throughput sequencing reads. *EMBnet.journal*, 17, 10–12.

Martinez, D., Berka, R.M., Henrissat, B., Saloheimo, M., Arvas, M., Baker, S.E., *et al.* (2008). Genome sequencing and analysis of the biomass-degrading fungus Trichoderma reesei (syn. Hypocrea jecorina). *Nat. Biotechnol.*, 26, 553–560.

Martino, E., Morin, E., Grelet, G.-A., Kuo, A., Kohler, A., Daghino, S., *et al.* (2018). Comparative genomics and transcriptomics depict ericoid mycorrhizal fungi as versatile saprotrophs and plant mutualists. *New Phytol.*, 217, 1213–1229.

Mašínová, T., Bahnmann, B.D., Větrovský, T., Tomšovský, M., Merunková, K. & Baldrian, P. (2017). Drivers of yeast community composition in the litter and soil of a temperate forest. *FEMS Microbiol. Ecol.*, 93.

Mayer, M., Rewald, B., Matthews, B., Sandén, H., Rosinger, C., Katzensteiner, K., *et al.* (2021). Soil fertility relates to fungal-mediated decomposition and organic matter turnover in a temperate mountain forest. *New Phytol.*, 231, 777–790.

Maynard, D.S., Covey, K.R., Crowther, T.W., Sokol, N.W., Morrison, E.W., Frey, S.D., *et al.* (2018). Species associations overwhelm abiotic conditions to dictate the structure and function of wood-decay fungal communities. *Ecology*, 99, 801–811.

McCormack, M.L., Dickie, I.A., Eissenstat, D.M., Fahey, T.J., Fernandez, C.W., Guo, D., *et al.* (2015). Redefining fine roots improves understanding of below-ground contributions to terrestrial biosphere processes. *New Phytol.*, 207, 505–518.

McMurdie, P.J. & Holmes, S. (2013). phyloseq: an R package for reproducible interactive analysis and graphics of microbiome census data. *PLoS One*, 8, e61217.

McMurdie, P.J. & Holmes, S. (2014). Waste not, want not: why rarefying microbiome data is inadmissible. *PLoS Comput. Biol.*, 10, e1003531.

de Mendiburu, F. (2017). *agricolae: Statistical procedures for agricultural research*.

Miyamoto, T., Igarashi, T. & Takahashi, K. (2000). Lignin-degrading ability of litter-decomposing basidiomycetes from Picea forests of Hokkaido. *Mycoscience*, 41, 105–110.

Miyauchi, S., Kiss, E., Kuo, A., Drula, E., Kohler, A., Sánchez-García, M., *et al.* (2020). Large-scale genome sequencing of mycorrhizal fungi provides insights into the early evolution of symbiotic traits. *Nat. Commun.*, 11, 5125.

Morgan, M., Anders, S., Lawrence, M., Aboyoun, P., Pagès, H. & Gentleman, R. (2009). ShortRead: a bioconductor package for input, quality assessment and exploration of high-throughput sequence data. *Bioinformatics*, 25, 2607–2608.

Morrison, E.W., Frey, S.D., Sadowsky, J.J., van Diepen, L.T.A., Thomas, W.K. & Pringle, A. (2016). Chronic nitrogen additions fundamentally restructure the soil fungal community in a temperate forest. *Fungal Ecol.*, 23, 48–57.

Morrison, E.W., Pringle, A., van Diepen, L.T.A. & Frey, S.D. (2018). Simulated nitrogen deposition favors stress-tolerant fungi with low potential for decomposition. *Soil Biol. Biochem.*, 125, 75–85.

Mueller, R.C., Balasch, M.M. & Kuske, C.R. (2014). Contrasting soil fungal community responses to experimental nitrogen addition using the large subunit rRNA taxonomic marker and cellobiohydrolase I functional marker. *Mol. Ecol.*, 23, 4406–4417.

Nagy, L.G., Riley, R., Tritt, A., Adam, C., Daum, C., Floudas, D., *et al.* (2016). Comparative Genomics of Early-Diverging Mushroom-Forming Fungi Provides Insights into the Origins of Lignocellulose Decay Capabilities. *Mol. Biol. Evol.*, 33, 959–970.

Nguyen, N.H., Song, Z., Bates, S.T., Branco, S., Tedersoo, L., Menke, J., *et al.* (2016). FUNGuild: An open annotation tool for parsing fungal community datasets by ecological guild. *Fungal Ecol.*, 20, 241–248.

Nilsson, R.H., Anslan, S., Bahram, M., Wurzbacher, C., Baldrian, P. & Tedersoo, L. (2019a). Mycobiome diversity: high-throughput sequencing and identification of fungi. *Nat. Rev. Microbiol.*, 17, 95–109.

Nilsson, R.H., Larsson, K.-H., Taylor, A.F.S., Bengtsson-Palme, J., Jeppesen, T.S., Schigel, D., *et al.* (2019b). The UNITE database for molecular identification of fungi: handling dark taxa and parallel taxonomic classifications. *Nucleic Acids Res.*, 47, D259–D264.

Oksanen, J., Blanchet, F.G., Friendly, M., Kindt, R., Legendre, P., McGlinn, D., *et al.* (2018). *vegan: Community ecology package*.

Orwin, K.H., Kirschbaum, M.U.F., St John, M.G. & Dickie, I.A. (2011). Organic nutrient uptake by mycorrhizal fungi enhances ecosystem carbon storage: a model-based assessment. *Ecol. Lett.*, 14, 493–502.

Pagès, H., Aboyoun, P., Gentleman, R. & DebRoy, S. (2020). *Biostrings: Efficient manipulation of biological strings*.

Pan, Y., Birdsey, R.A., Fang, J., Houghton, R., Kauppi, P.E., Kurz, W.A., *et al.* (2011). A large and persistent carbon sink in the world's forests. *Science*, 333, 988–993.

Pauvert, C., Buée, M., Laval, V., Edel-Hermann, V., Fauchery, L., Gautier, A., *et al.* (2019). Bioinformatics matters: The accuracy of plant and soil fungal community data is highly dependent on the metabarcoding pipeline. *Fungal Ecol.*, 41, 23–33.

Pellitier, P.T., Ibáñez, I., Zak, D.R., Argiroff, W.A. & Acharya, K. (2021a). Ectomycorrhizal access to organic nitrogen mediates CO2 fertilization response in a dominant temperate tree. *Nat. Commun.*, 12, 5403.

Pellitier, P.T. & Zak, D.R. (2018). Ectomycorrhizal fungi and the enzymatic liberation of nitrogen from soil organic matter: why evolutionary history matters. *New Phytol.*, 217, 68–73.

Pellitier, P.T. & Zak, D.R. (2021a). Ectomycorrhizal fungal decay traits along a soil nitrogen gradient. *New Phytol.*, 232, 2152–2164.

Pellitier, P.T. & Zak, D.R. (2021b). Ectomycorrhizal root tips harbor distinctive fungal associates along a soil nitrogen gradient. *Fungal Ecol.*, 54, 101111.

Pellitier, P.T., Zak, D.R., Argiroff, W.A. & Upchurch, R.A. (2021b). Coupled Shifts in Ectomycorrhizal Communities and Plant Uptake of Organic Nitrogen Along a Soil Gradient: An Isotopic Perspective. *Ecosystems*, 24, 1976–1990.

Pellitier, P.T., Zak, D.R. & Salley, S.O. (2019). Environmental filtering structures fungal endophyte communities in tree bark. *Mol. Ecol.*, 28, 5188–5198.

Phillips, R.P., Brzostek, E. & Midgley, M.G. (2013). The mycorrhizal-associated nutrient economy: a new framework for predicting carbon-nutrient couplings in temperate forests. *New Phytol.*, 199, 41–51.

Philpott, T.J., Barker, J.S., Prescott, C.E. & Grayston, S.J. (2018). Limited Effects of Variable-Retention Harvesting on Fungal Communities Decomposing Fine Roots in Coastal Temperate Rainforests. *Appl. Environ. Microbiol.*, 84.

Pold, G., Grandy, A.S., Melillo, J.M. & DeAngelis, K.M. (2017). Changes in substrate availability drive carbon cycle response to chronic warming. *Soil Biol. Biochem.*, 110, 68–78.

Porter, T.M. & Golding, G.B. (2012). Factors that affect large subunit ribosomal DNA amplicon sequencing studies of fungal communities: classification method, primer choice, and error. *PLoS One*, 7, e35749.

Pregitzer, K.S., Burton, A.J., Zak, D.R. & Talhelm, A.F. (2008). Simulated chronic nitrogen deposition increases carbon storage in Northern Temperate forests. *Glob. Chang. Biol.*, 14, 142–153.

Pregitzer, K.S., DeForest, J.L., Burton, A.J., Allen, M.F., Ruess, R.W. & Hendrick, R.L. (2002). Fine root architecture of nine north American trees. *Ecol. Monogr.*, 72, 293–309.

Pregitzer, K.S., Zak, D.R., Burton, A.J., Ashby, J.A. & MacDonald, N.W. (2004). Chronic nitrate additions dramatically increase the export of carbon and nitrogen from northern hardwood ecosystems. *Biogeochemistry*, 68, 179–197.

Prosser, J.I. (2020). Putting science back into microbial ecology: a question of approach. *Philos. Trans. R. Soc. Lond. B Biol. Sci.*, 375, 20190240.

Quast, C., Pruesse, E., Yilmaz, P., Gerken, J., Schweer, T., Yarza, P., *et al.* (2013). The SILVA ribosomal RNA gene database project: improved data processing and web-based tools. *Nucleic Acids Res.*, 41, D590-6.

R Core Team. (2018). *R: A language and environment for statistical computing*.

R Core Team. (2020). *R: A language and environment for statistical computing*.

Rasse, D.P., Rumpel, C. & Dignac, M.-F. (2005). Is soil carbon mostly root carbon? Mechanisms for a specific stabilisation. *Plant Soil*, 269, 341–356.

Riley, R., Salamov, A.A., Brown, D.W., Nagy, L.G., Floudas, D., Held, B.W., *et al.* (2014). Extensive sampling of basidiomycete genomes demonstrates inadequacy of the white-rot/brown-rot paradigm for wood decay fungi. *Proc. Natl. Acad. Sci. U. S. A.*, 111, 9923–9928.

Rineau, F., Roth, D., Shah, F., Smits, M., Johansson, T., Canbäck, B., *et al.* (2012). The ectomycorrhizal fungus Paxillus involutus converts organic matter in plant litter using a trimmed brown-rot mechanism involving Fenton chemistry. *Environ. Microbiol.*, 14, 1477–1487.

Romero-Olivares, A.L., Morrison, E.W., Pringle, A. & Frey, S.D. (2021). Linking Genes to Traits in Fungi. *Microb. Ecol.*, 82, 145–155.

Rosen, M.J., Callahan, B.J., Fisher, D.S. & Holmes, S.P. (2012). Denoising PCR-amplified metagenome data. *BMC Bioinformatics*, 13, 283.

RStudio Team. (2018). *RStudio: integrated development for R*.

RStudio Team. (2020). *RStudio: integrated development for R*.

Ruiz-Dueñas, F.J., Barrasa, J.M., Sánchez-García, M., Camarero, S., Miyauchi, S., Serrano, A., *et al.* (2021). Genomic Analysis Enlightens Agaricales Lifestyle Evolution and Increasing Peroxidase Diversity. *Mol. Biol. Evol.*, 38, 1428–1446.

Saiya-Cork, K.R., Sinsabaugh, R.L. & Zak, D.R. (2002). The effects of long term nitrogen deposition on extracellular enzyme activity in an Acer saccharum forest soil. *Soil Biol. Biochem.*, 34, 1309–1315.

Schimel, J.P. & Schaeffer, S.M. (2012). Microbial control over carbon cycling in soil. *Front. Microbiol.*, 3, 348.

Schlesinger, W.H. & Bernhardt, E.S. (2013). *Biogeochemistry: An Analysis of Global Change*. Academic Press.

Schloss, P.D., Westcott, S.L., Ryabin, T., Hall, J.R., Hartmann, M., Hollister, E.B., *et al.* (2009). Introducing mothur: open-source, platform-independent, community-supported software for describing and comparing microbial communities. *Appl. Environ. Microbiol.*, 75, 7537–7541.

Schoch, C.L., Seifert, K.A., Huhndorf, S., Robert, V., Spouge, J.L., Levesque, C.A., *et al.* (2012). Nuclear ribosomal internal transcribed spacer (ITS) region as a universal DNA barcode marker for Fungi. *Proc. Natl. Acad. Sci. U. S. A.*, 109, 6241–6246.

See, C.R., Luke McCormack, M., Hobbie, S.E., Flores-Moreno, H., Silver, W.L. & Kennedy, P.G. (2019). Global patterns in fine root decomposition: climate, chemistry, mycorrhizal association and woodiness. *Ecol. Lett.*, 22, 946–953.

Seitzman, B.H., Ouimette, A., Mixon, R.L., Hobbie, E.A. & Hibbett, D.S. (2011). Conservation of biotrophy in Hygrophoraceae inferred from combined stable isotope and phylogenetic analyses. *Mycologia*, 103, 280–290.

Shah, F., Nicolás, C., Bentzer, J., Ellström, M., Smits, M., Rineau, F., *et al.* (2016). Ectomycorrhizal fungi decompose soil organic matter using oxidative mechanisms adapted from saprotrophic ancestors. *New Phytol.*, 209, 1705–1719.

Silver, W.L. & Miya, R.K. (2001). Global patterns in root decomposition: comparisons of climate and litter quality effects. *Oecologia*, 129, 407–419.

Smith, G.R. & Peay, K.G. (2021). Multiple distinct, scale-dependent links between fungi and decomposition. *Ecol. Lett.*, 24, 1352–1362.

Smith, G.R. & Wan, J. (2019). Resource-ratio theory predicts mycorrhizal control of litter decomposition. *New Phytol.*, 223, 1595–1606.

Smith, S.E. & Read, D.J. (2010). *Mycorrhizal Symbiosis*. Academic Press.

Sorouri, B. & Allison, S.D. (2022). Microbial extracellular enzyme activity with simulated climate change. *Elementa (Wash., DC)*, 10.

Starke, R., Mondéjar, R.L., Human, Zander Rainer, Navrátilová, D., Štursová, M., Větrovský, T., *et al.* (2021). Niche differentiation of bacteria and fungi in carbon and nitrogen cycling of different habitats in a temperate coniferous forest: A metaproteomic approach. *Soil Biol. Biochem.*, 155, 108170.

Steidinger, B.S., Bhatnagar, J.M., Vilgalys, R., Taylor, J.W., Qin, C., Zhu, K., *et al.* (2020). Ectomycorrhizal fungal diversity predicted to substantially decline due to climate changes in North American Pinaceae forests. *J. Biogeogr.*, 47, 772–782.

Sterkenburg, E., Bahr, A., Brandström Durling, M., Clemmensen, K.E. & Lindahl, B.D. (2015). Changes in fungal communities along a boreal forest soil fertility gradient. *New Phytol.*, 207, 1145–1158.

Sterkenburg, E., Clemmensen, K.E., Ekblad, A., Finlay, R.D. & Lindahl, B.D. (2018). Contrasting effects of ectomycorrhizal fungi on early and late stage decomposition in a boreal forest. *ISME J.*, 12, 2187–2197.

Suding, K.N., Lavorel, S., Chapin, F.S., III, Cornelissen, J.H.C., Díaz, S., Garnier, E., *et al.* (2008). Scaling environmental change through the community-level: a trait-based response-and-effect framework for plants. *Glob. Chang. Biol.*, 14, 1125–1140.

Sulman, B.N., Moore, J.A.M., Abramoff, R., Averill, C., Kivlin, S., Georgiou, K., *et al.* (2018). Multiple models and experiments underscore large uncertainty in soil carbon dynamics. *Biogeochemistry*, 141, 109–123.

Sulman, B.N., Shevliakova, E., Brzostek, E.R., Kivlin, S.N., Malyshev, S., Menge, D.N.L., *et al.* (2019). Diverse mycorrhizal associations enhance terrestrial C storage in a global model. *Global Biogeochem. Cycles*, 33, 501–523.

Sun, T., Dong, L., Wang, Z., Lü, X. & Mao, Z. (2016). Effects of long-term nitrogen deposition on fine root decomposition and its extracellular enzyme activities in temperate forests. *Soil Biol. Biochem.*, 93, 50–59.

Sun, T., Hobbie, S.E., Berg, B., Zhang, H., Wang, Q., Wang, Z., *et al.* (2018). Contrasting dynamics and trait controls in first-order root compared with leaf litter decomposition. *Proc. Natl. Acad. Sci. U. S. A.*, 115, 10392–10397.

Talbot, J.M., Martin, F., Kohler, A., Henrissat, B. & Peay, K.G. (2015). Functional guild classification predicts the enzymatic role of fungi in litter and soil biogeochemistry. *Soil Biol. Biochem.*, 88, 441–456.

Talbot, J.M. & Treseder, K.K. (2012). Interactions among lignin, cellulose, and nitrogen drive litter chemistry-decay relationships. *Ecology*, 93, 345–354.

Talbot, J.M., Yelle, D.J., Nowick, J. & Treseder, K.K. (2012). Litter decay rates are determined by lignin chemistry. *Biogeochemistry*, 108, 279–295.

Tanunchai, B., Ji, L., Schroeter, S.A., Wahdan, S.F.M., Hossen, S., Delelegn, Y., *et al.* (2022). FungalTraits vs. FUNGuild: Comparison of ecological functional assignments of leaf- and needle-associated fungi across 12 temperate tree species. *Microb. Ecol.*

Taylor, C.R., Hardiman, E.M., Ahmad, M., Sainsbury, P.D., Norris, P.R. & Bugg, T.D.H. (2012). Isolation of bacterial strains able to metabolize lignin from screening of environmental samples. *J. Appl. Microbiol.*, 113, 521–530.

Taylor, D.L., Hollingsworth, T.N., McFarland, J.W., Lennon, N.J., Nusbaum, C. & Ruess, R.W. (2014). A first comprehensive census of fungi in soil reveals both hyperdiversity and fine-scale niche partitioning. *Ecol. Monogr.*, 84, 3–20.

Taylor, D.L., Walters, W.A., Lennon, N.J., Bochicchio, J., Krohn, A., Caporaso, J.G., *et al.* (2016). Accurate Estimation of Fungal Diversity and Abundance through Improved Lineage-Specific Primers Optimized for Illumina Amplicon Sequencing. *Appl. Environ. Microbiol.*, 82, 7217–7226.

Tedersoo, L., Bahram, M., Põlme, S., Kõljalg, U., Yorou, N.S., Wijesundera, R., *et al.* (2014). Fungal biogeography. Global diversity and geography of soil fungi. *Science*, 346, 1256688.

Teixeira, M.M., Moreno, L.F., Stielow, B.J., Muszewska, A., Hainaut, M., Gonzaga, L., *et al.* (2017). Exploring the genomic diversity of black yeasts and relatives (Chaetothyriales, Ascomycota). *Stud. Mycol.*, 86, 1–28.

Tenney, F.G. & Waksman, S.A. (1929). Composition of natural organic materials and their decomposition in the doil: IV. The nature and rapidity of decomposition of the various organic complexes in different plant materials under aerobic conditions. *Soil Sci.*, 28, 55.

Terrer, C., Phillips, R.P., Hungate, B.A., Rosende, J., Pett-Ridge, J., Craig, M.E., *et al.* (2021). A trade-off between plant and soil carbon storage under elevated CO2. *Nature*, 591, 599–603.

Terrer, C., Vicca, S., Hungate, B.A., Phillips, R.P. & Prentice, I.C. (2016). Mycorrhizal association as a primary control of the CO_2 fertilization effect. *Science*, 353, 72–74.

Thomas, D.C., Zak, D.R. & Filley, T.R. (2012). Chronic N deposition does not apparently alter the biochemical composition of forest floor and soil organic matter. *Soil Biol. Biochem.*, 54, 7–13.

Travers, K.J., Chin, C.-S., Rank, D.R., Eid, J.S. & Turner, S.W. (2010). A flexible and efficient template format for circular consensus sequencing and SNP detection. *Nucleic Acids Res.*, 38, e159.

Treseder, K.K., Alster, C.J., Cat, L.A., Gorris, M.E., Kuhn, A.L., Lovero, K.G., *et al.* (2021). Nutrient and stress tolerance traits linked to fungal responses to global change. *Elementa (Wash., DC)*, 9.

Treseder, K.K., Balser, T.C., Bradford, M.A., Brodie, E.L., Dubinsky, E.A., Eviner, V.T., *et al.* (2012). Integrating microbial ecology into ecosystem models: challenges and priorities. *Biogeochemistry*, 109, 7–18.

Treseder, K.K. & Lennon, J.T. (2015). Fungal Traits That Drive Ecosystem Dynamics on Land. *Microbiol. Mol. Biol. Rev.*, 79, 243–262.

Treseder, K.K., Torn, M.S. & Masiello, C.A. (2006). An ecosystem-scale radiocarbon tracer to test use of litter carbon by ectomycorrhizal fungi. *Soil Biol. Biochem.*, 38, 1077–1082.

vandenEnden, L., Frey, S.D., Nadelhoffer, K.J., LeMoine, J.M., Lajtha, K. & Simpson, M.J. (2018). Molecular-level changes in soil organic matter composition after 10 years of litter, root and nitrogen manipulation in a temperate forest. *Biogeochemistry*, 141, 183–197.

Vilgalys, R. & Hester, M. (1990). Rapid genetic identification and mapping of enzymatically amplified ribosomal DNA from several Cryptococcus species. *J. Bacteriol.*, 172, 4238–4246.

Vitousek, P.M., Gosz, J.R., Grier, C.C., Melillo, J.M. & Reiners, W.A. (1982). A comparative analysis of potential nitrification and nitrate mobility in forest ecosystems. *Ecol. Monogr.*, 52, 155–177.

Vitousek, P.M. & Howarth, R.W. (1991). Nitrogen limitation on land and in the sea: How can it occur? *Biogeochemistry*, 13, 87–115.

Voříšková, J. & Baldrian, P. (2013). Fungal community on decomposing leaf litter undergoes rapid successional changes. *ISME J.*, 7, 477–486.

Waldrop, M.P., Zak, D.R., Sinsabaugh, R.L., Gallo, M. & Lauber, C. (2004). Nitrogen deposition modifies soil carbon storage through changes in microbial enzymatic activity. *Ecol. Appl.*, 14, 1172–1177.

Walker, A.P., De Kauwe, M.G., Bastos, A., Belmecheri, S., Georgiou, K., Keeling, R.F., *et al.* (2021). Integrating the evidence for a terrestrial carbon sink caused by increasing atmospheric CO2. *New Phytol.*, 229, 2413–2445.

Wambsganss, J., Freschet, G.T., Beyer, F., Bauhus, J. & Scherer-Lorenzen, M. (2021). Tree Diversity, Initial Litter Quality, and Site Conditions Drive Early-Stage Fine-Root Decomposition in European Forests. *Ecosystems*.

Wang, J.-J., Bowden, R.D., Lajtha, K., Washko, S.E., Wurzbacher, S.J. & Simpson, M.J. (2019). Long-term nitrogen addition suppresses microbial degradation, enhances soil carbon storage, and alters the molecular composition of soil organic matter. *Biogeochemistry*, 142, 299–313.

Wang, Q., Garrity, G.M., Tiedje, J.M. & Cole, J.R. (2007). Naïve Bayesian Classifier for Rapid Assignment of rRNA Sequences into the New Bacterial Taxonomy. *Appl. Environ. Microbiol.*, 73, 5261–5267.

Whalen, E.D., Smith, R.G., Grandy, A.S. & Frey, S.D. (2018). Manganese limitation as a mechanism for reduced decomposition in soils under atmospheric nitrogen deposition. *Soil Biol. Biochem.*, 127, 252–263.

Wickham, H. (2017). *tidyverse: Easily Install and Load the "Tidyverse."*

Wickham, H., Averick, M., Bryan, J., Chang, W., McGowan, L., François, R., *et al.* (2019). Welcome to the tidyverse. *J. Open Source Softw.*, 4, 1686.

Wickings, K., Stuart Grandy, A., Reed, S. & Cleveland, C. (2011). Management intensity alters decomposition via biological pathways. *Biogeochemistry*, 104, 365–379.

Wieder, W.R., Allison, S.D., Davidson, E.A., Georgiou, K., Hararuk, O., He, Y., *et al.* (2015). Explicitly representing soil microbial processes in Earth system models. *Global Biogeochem. Cycles*, 29, 1782–1800.

Wieder, W.R., Hartman, M.D., Sulman, B.N., Wang, Y.-P., Koven, C.D. & Bonan, G.B. (2018). Carbon cycle confidence and uncertainty: Exploring variation among soil biogeochemical models. *Glob. Chang. Biol.*, 24, 1563–1579.

Wilhelm, R.C., Singh, R., Eltis, L.D. & Mohn, W.W. (2019). Bacterial contributions to delignification and lignocellulose degradation in forest soils with metagenomic and quantitative stable isotope probing. *ISME J.*, 13, 413–429.

Wood, S.N. (2011). Fast stable restricted maximum likelihood and marginal likelihood estimation of semiparametric generalized linear models. *J. R. Stat. Soc. Series B Stat. Methodol.*, 73, 3–36.

Xia, M., Guo, D. & Pregitzer, K.S. (2010). Ephemeral root modules in Fraxinus mandshurica. *New Phytol.*, 188, 1065–1074.

Xia, M., Talhelm, A.F. & Pregitzer, K.S. (2015). Fine roots are the dominant source of recalcitrant plant litter in sugar maple-dominated northern hardwood forests. *New Phytol.*, 208, 715–726.

Xia, M., Talhelm, A.F. & Pregitzer, K.S. (2017). Chronic nitrogen deposition influences the chemical dynamics of leaf litter and fine roots during decomposition. *Soil Biol. Biochem.*, 112, 24–34.

Xia, M., Talhelm, A.F. & Pregitzer, K.S. (2018). Long-Term Simulated Atmospheric Nitrogen Deposition Alters Leaf and Fine Root Decomposition. *Ecosystems*, 21, 1–14.

Zak, D.R., Argiroff, W.A., Freedman, Z.B., Upchurch, R.A., Entwistle, E.M. & Romanowicz, K.J. (2019a). Anthropogenic N deposition, fungal gene expression, and an increasing soil carbon sink in the Northern Hemisphere. *Ecology*, 100, e02804.

Zak, D.R., Blackwood, C.B. & Waldrop, M.P. (2006). A molecular dawn for biogeochemistry. *Trends Ecol. Evol.*, 21, 288–295.

Zak, D.R., Freedman, Z.B., Upchurch, R.A., Steffens, M. & Kögel-Knabner, I. (2017). Anthropogenic N deposition increases soil organic matter accumulation without altering its biochemical composition. *Glob. Chang. Biol.*, 23, 933–944.

Zak, D.R., Holmes, W.E., Burton, A.J., Pregitzer, K.S. & Talhelm, A.F. (2008). Simulated atmospheric NO3- deposition increases soil organic matter by slowing decomposition. *Ecol. Appl.*, 18, 2016–2027.

Zak, D.R., Holmes, W.E., MacDonald, N.W. & Pregitzer, K.S. (1999). Soil temperature, matric potential, and the kinetics of microbial respiration and nitrogen mineralization. *Soil Sci. Soc. Am. J.*, 63, 575–584.

Zak, D.R., Host, G.E. & Pregitzer, K.S. (1989). Regional variability in nitrogen mineralization, nitrification, and overstory biomass in northern Lower Michigan. *Can. J. For. Res.*, 19, 1521–1526.

Zak, D.R., Pellitier, P.T., Argiroff, W., Castillo, B., James, T.Y., Nave, L.E., *et al.* (2019b). Exploring the role of ectomycorrhizal fungi in soil carbon dynamics. *New Phytol.*, 223, 33–39.

Zak, D.R. & Pregitzer, K.S. (1990). Spatial and Temporal Variability of Nitrogen Cycling in Northern Lower Michigan. *For. Sci.*, 36, 367–380.

Zanne, A.E., Abarenkov, K., Afkhami, M.E., Aguilar-Trigueros, C.A., Bates, S., Bhatnagar, J.M., *et al.* (2020). Fungal functional ecology: bringing a trait-based approach to plant-associated fungi. *Biol. Rev. Camb. Philos. Soc.*, 95, 409–433.